New York Harbor Current Survey 2017-2019

Including adjacent waters of New York and New Jersey

Silver Spring, Maryland
October 2021

noaa National Oceanic and Atmospheric Administration

U.S. DEPARTMENT OF COMMERCE
National Ocean Service
Center for Operational Oceanographic Products and Services

Center for Operational Oceanographic Products and Services
National Ocean Service
National Oceanic and Atmospheric Administration
U.S. Department of Commerce

The National Ocean Service (NOS) Center for Operational Oceanographic Products and Services (CO-OPS) provides the National infrastructure, science, and technical expertise to collect and distribute observations and predictions of water levels and currents to ensure safe, efficient and environmentally sound maritime commerce. The Center provides the set of water level and tidal current products required to support NOS' Strategic Plan mission requirements, and to assist in providing operational oceanographic data/products required by NOAA's other strategic plan themes. For example, CO-OPS provides data and products required by the National Weather Service to meet its flood and tsunami warning responsibilities. The Center manages the National Water Level Observation Network (NWLON), a national network of Physical Oceanographic Real-Time Systems (PORTS®) in major U. S. harbors, and the National Current Observation Program consisting of current surveys in near shore and coastal areas utilizing bottom mounted platforms, subsurface buoys, horizontal sensors and quick response real time buoys. The Center establishes standards for the collection and processing of water level and current data; collects and documents user requirements, which serve as the foundation for all resulting program activities; designs new or improved oceanographic observing systems; designs software to improve CO-OPS' data processing capabilities; maintains and operates oceanographic observing systems; performs operational data analysis/quality control; and produces/disseminates oceanographic products.

New York Harbor Current Survey 2017-2019

Including adjacent waters of New York and New Jersey

Carl Kammerer
Katie Kirk
Christopher Paternostro
Lorraine Heilman

October 2021

U.S. DEPARTMENT OF COMMERCE
Gina M. Raimondo, Secretary

National Oceanic and Atmospheric Administration
Richard Spinrad, Ph.D., Under Secretary of Commerce for Oceans and Atmosphere

National Ocean Service
Nicole LeBoeuf, Assistant Administrator

Center for Operational Oceanographic Products and Services
Richard Edwing, Director

NOTICE

Mention of a commercial company or product does not constitute an endorsement by NOAA. Use of information from this publication for publicity or advertising purposes concerning proprietary products or the tests of such products is not authorized.

TABLE OF CONTENTS

LIST OF FIGURES

LIST OF TABLES

APPENDICES

EXECUTIVE SUMMARY

The National Oceanic and Atmospheric Administration (NOAA) National Ocean Service (NOS) Center for Operational Oceanographic Products and Services (CO-OPS) works to promote safe navigation throughout the U.S. Waterways. As part of this effort, the CO-OPS National Current Observation Program (NCOP) acquires, archives, and disseminates information on tidal currents in the coastal U.S., which is used to update the NOAA tidal current predictions. NCOP conducts internal assessments of locations in need of new tidal current predictions. The New York Harbor (NYH) region, which includes adjacent waters in New Jersey (NJ), such as Newark Bay and smaller tributaries, was identified through this process. Tidal current data are collected at new locations to help increase spatial coverage in tidal current observations and predictions and also through reoccupations of historical stations to update the observations and predictions with increased quality and accuracy. The data products generated are utilized by NOAA and the user community to help ensure safe navigation, make informed coastal zone management decisions, and support the protection of life and property. Furthermore, data collected can be used to inform the development of new hydrodynamic models or provide validation to existing ones.

This report summarizes the data collection and analysis completed by NCOP in the 2019 New York Harbor Current Survey. A total of 33 stations were successfully deployed for at least 1lunar month (29 days). One additional station (NYH1925 [Middle Ground]) was deployed but surfaced within an hour and was not reoccupied due to equipment limitations. Currents were measured at each station with an acoustic Doppler current profiler (ADCP) moored with a configuration determined by factors such as station depth, seafloor composition, expected maritime activities, anticipated currents, and available inventory. Concurrent with each deployment and recovery of an ADCP, a vertical conductivity-temperature-depth (CTD) profile was taken to ascertain the physical properties of the seawater at the approximate location of each station.

Each ADCP was configured to collect data in evenly spaced ensembles of averaged velocity observations. These ensembles were typically 6 minutes. Of the 33 stations, 1 was not recovered, data from 2 stations were unusable due to a corrupted compass matrix, and 2 stations used longer or newer data from the NY/NJ Physical Oceanographic Real-Time System (PORTS®) in lieu of the data from the short-term survey stations. The remaining 28 stations collected data of sufficient quality to be analyzed. These data include vertical or horizontal current profiles (speed and direction), water temperature, pressure, and additional quality control variables. Currents were analyzed for tidal constituents using harmonic analysis of the velocity time series data collected by the ADCP. Tidal current predictions for each station were made available online via the CO-OPS Tides and Currents website (NOAA Current Predictions).

1. INTRODUCTION

The National Ocean Service (NOS) Center for Operational Oceanographic Products and Services (CO-OPS) manages the National Current Observation Program (NCOP). The program's primary goal is to improve the quality and accuracy of tidal current predictions. Improving this information is a critical part of NOS' efforts toward promoting safe navigation in our nation's waterways. Mariners require accurate and dependable information on the movement of the waters in which they navigate. As increasingly larger ships use our ports and as seagoing commerce continues to increase, there is an increased risk to safe navigation in the nation's ports (NOAA 2018). CO-OPS acquires, archives, and disseminates information on tides and tidal currents in U.S. ports and estuaries, a vital NOS function since the 1840s. The main sources of this information for the public is the CO-OPS Tides and Currents website (NOAA Current Predictions). National Oceanic and Atmospheric Administration (NOAA) previously published Tidal Current Tables annually as required by the Navigation and Safety Regulations section of the U.S. Code of Federal Regulations (Charts…2022) until 2020. NOAA discontinued the production of these tables due to changes in paper carriage requirements as set forth by the U.S. Coast Guard (2016), and the predictions are now digitally available and accessible by NOAA. Both the collection and analysis of current observations, as well as the dissemination of the data, fall under the authority of the Navigation and Navigable Waters title of the U.S. Code (Surveys…2012; Dissemination…2021).

The flow dynamics of an estuary or tidal river can be modified by changes in natural factors, such as land motion and other morphologic changes, or through man-made alterations, such as the deepening of channels by dredging, harbor construction, bridge construction, the deposition of dredge materials, and the diversion of river flow. Changes in water flow and tidal dynamics can affect the accuracy of tidal current predictions; therefore, new data must be collected periodically to ensure that predictions remain reliable and are adjusted when necessary.

CO-OPS has developed expertise in deploying current profilers throughout the nation's coastal waters via the NCOP program. These data are used for a number of products. In addition to updating existing tidal current predictions and establishing new tidal current prediction locations (Fanelli et al. 2014), data collected through this program are utilized by NOAA and the user community in the production and refinement of other products, such as the validation of hydrodynamic forecast systems (Lanerolle et al. 2011) and integration into commercial navigation software. These products are used to ensure safe navigation, make informed coastal zone management decisions, and protect life and property.

The data described in this report were collected by NCOP during a survey in 2019 (Figure 1-1). A total of 33 stations were occupied for at least 1 lunar month (29 days). Of the 33 stations, 1 was not recovered (NYH1929 [Grant's Tomb]), and data from 2 stations (NYH1907 [Arthur Kill Port Socony] and NYH1923 [East River "B" buoy]) were unusable due to a corrupted compass matrix discovered during analysis. Analysis and generation of tidal current harmonics from 2 stations (NYH1912 [Port Richmond] and NYH1916 [Claremont Terminal Channel Entrance]) were supplemented by analyses from 2 nearby NY/NJ Physical Oceanographic Real-Time System (PORTS®) stations—n06010 (Kill Van Kull LB 14) and n05010 (Gowanus Flats LBB 32), respectively—and for these locations, the PORTS® station analyses were used. Station NYH1912 (Port Richmond) collected data for 40 days, but there was a possible compass calibration issue that led to increased noise in the flood direction velocity data. Station n06010 (Kill Van Kull LB 14) was installed in May 2020 on the same aid to navigation (ATON) as NYH1912, and the first 30-day analysis for the PORTS® station was compared with station NYH1912. These velocities were about 15% faster than those of NYH1912 with much less noise. For this reason, the PORTS® analysis was used in place of the survey station analysis. Station NYH1916 (Claremont Terminal

Entrance) collected only 14 days of data before its batteries died, which was not enough data for a reliable harmonic analysis. Data from a nearby, previously occupied PORTS® station (n05010 [Gowanus Flats LBB 32]) were analyzed and found to be an acceptable replacement; station n05010 is located about 1 km east of NYH1916 on the other side of the shipping channel and showed similar velocity trends to NYH1916 for a similar 14-day time frame. The remaining 28 stations collected data of sufficient quality to be analyzed. These data include vertical or horizontal current profiles (speed and direction), water temperature, pressure, and additional quality control variables. Currents were analyzed for tidal constituents using harmonic analysis of the velocity time series data collected by the acoustic Doppler current profiler (ADCP). All data and analysis reports presented herein are available on the Tides and Currents website (NOAA Current Predictions) or by contacting CO-OPS Stakeholder Services Branch (Contact Information).

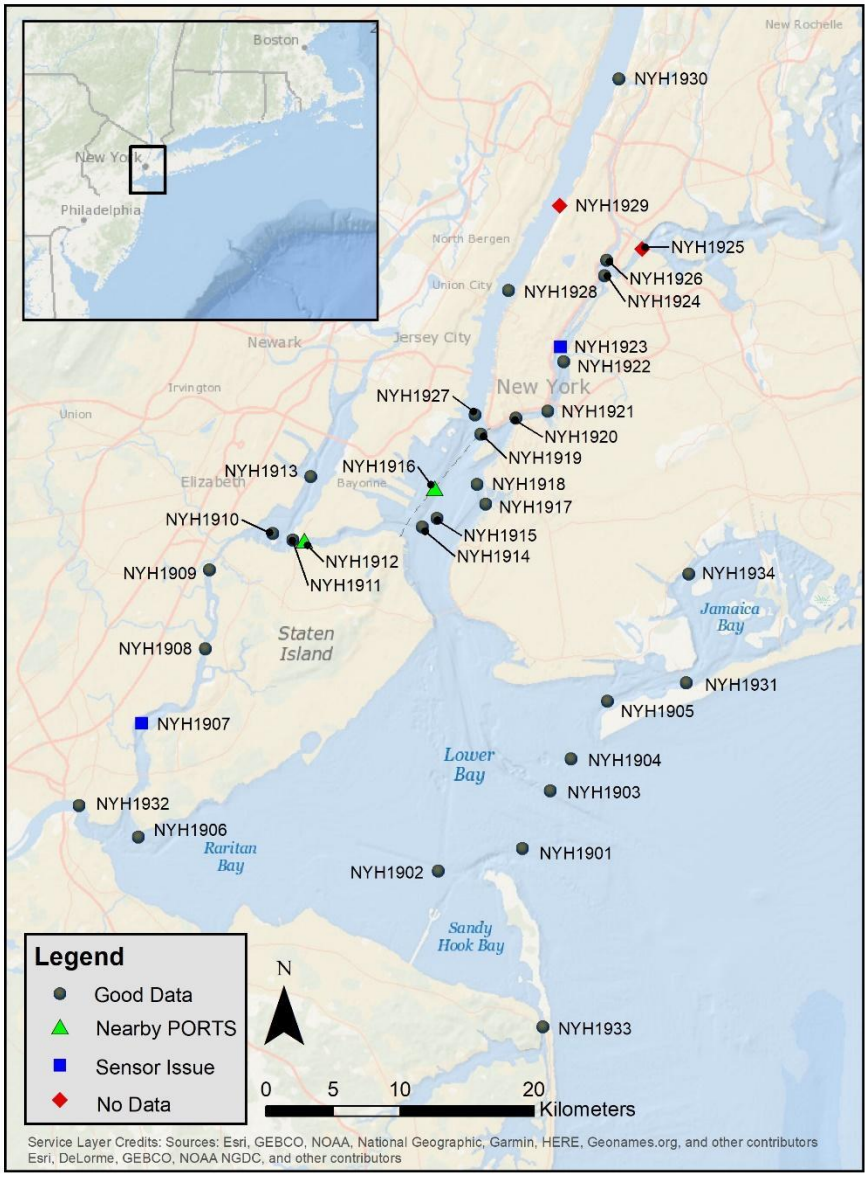

Figure 1-1. All stations deployed for the NYH survey of 2019. Stations where no data were collected are indicated by a red diamond. Stations where data were collected but there was an issue with the compass matrix are indicated by a blue square. Stations where a nearby PORTS® station was used in lieu of survey data are indicated by a green triangle. All other stations collected good data and are indicated by a gray dot.

2. PROJECT DESCRIPTION

New York Harbor was identified by an internal assessment (Fanelli et al. 2014) as the region in most need of updating predictions with an NCOP project using modern oceanographic equipment. While surveys have been conducted in adjacent regions—in the Hudson River from the George Washington Bridge to Albany (2005-2006) and Long Island Sound (2010)—the last large-scale current observation project of New York Harbor was conducted from August 1980 to June 1981 using mechanical Grundy current meters moored at discrete depths (Browne and Dingle 1983). The 2019 survey collected data in a similar geographic scope as the survey from the 1980s. Additionally, there was a large survey conducted in the 1930s with NOAA current prediction stations derived from those data. There is an active PORTS® system (New York/New Jersey Harbor…) in the region, as well as the New York operational forecast system (NYOFS; New York and New Jersey Operational…).

Initial site locations were proposed based upon the internal needs and capabilities of NOAA. Additional station recommendations were provided through meetings and correspondence with users, including professional mariners; federal, state and local partners; as well as academics and researchers. The final survey study was conducted by incorporating oceanographic needs, engineering restrictions, and criteria set forth by the International Hydrographic Organization (IHO 2008). As an example of the type of criteria used for site selection, Figure 2-1 shows a map of ship traffic density from automatic identification system (AIS) ship tracks. Traffic density is a key determination of current meter placement.

In 2018, a reconnaissance was conducted to gather information about the physical characteristics of proposed sites. This reconnaissance provided the necessary information for exact locations, platform engineering, and instrument frequencies for the proposed stations. All proposed sites were visited to gather data about their physical characteristics such as depth, bottom type, and vertical profiles of water temperature and salinity. This information was then used to plan the platform and sensor configurations for each current observation station. During reconnaissance operations, each site was visited using a vessel equipped with a fathometer to determine the depth of the site, a conductivity-temperature-depth (CTD) sensor to determine salinity and water temperature, and a Ponar-style bottom sampler to determine the nature of the seabed at the site (e.g., mud, silt, sand). Based upon the reconnaissance, 34 deployment locations were identified, which were occupied using methods described in section 3. This technical report focuses on the results of these ADCP current meter deployments.

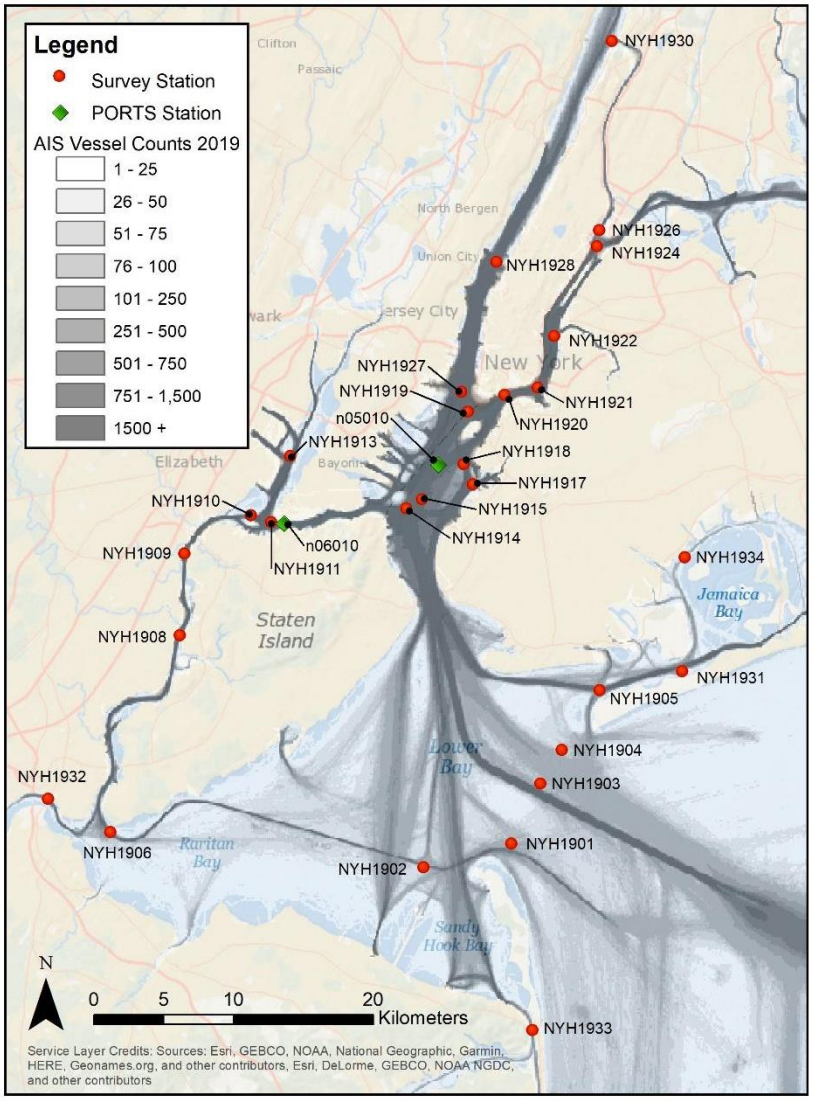

Figure 2-1. 2019 AIS tracks for all vessels in New York Harbor and vicinity. AIS data from Vessel Traffic Data.

2.1 Geographic scope

The project region is highly urbanized with a population estimate of about 19.2 million during the summer of 2019 (Metropolitan and Micropolitan…2021) containing the cities of New York and Newark.

Located at the center of the Mid-Atlantic Bight, the greater oceanographic region in this study is formally known as the New York-New Jersey Harbor Estuary. For the purpose of this project, the term "New York Harbor" is used generally to include the waters of the Hudson River in the New York City vicinity, south to the Verrazano Narrows where it enters the Lower Bay, as well as the East River, Newark Bay, Arthur Kill, and Kill Van Kull. This project also included New York Harbor's interconnected greater regional waterways of Raritan Bay, Sandy Hook Bay, Rockaway Inlet, and Jamaica Bay.

Current measurements were collected at locations from Spuyten Duyvil on the Hudson River and Middle Ground on the East River to Ambrose Channel at the terminus of Lower Bay to the New York Bight. The lateral bounds included the Marine Parkway Bridge in Jamaica Bay, the Highlands Bridge on the Shrewsbury River, the Raritan River Entrance, and the middle reach of Newark Bay (Figure 2-2).

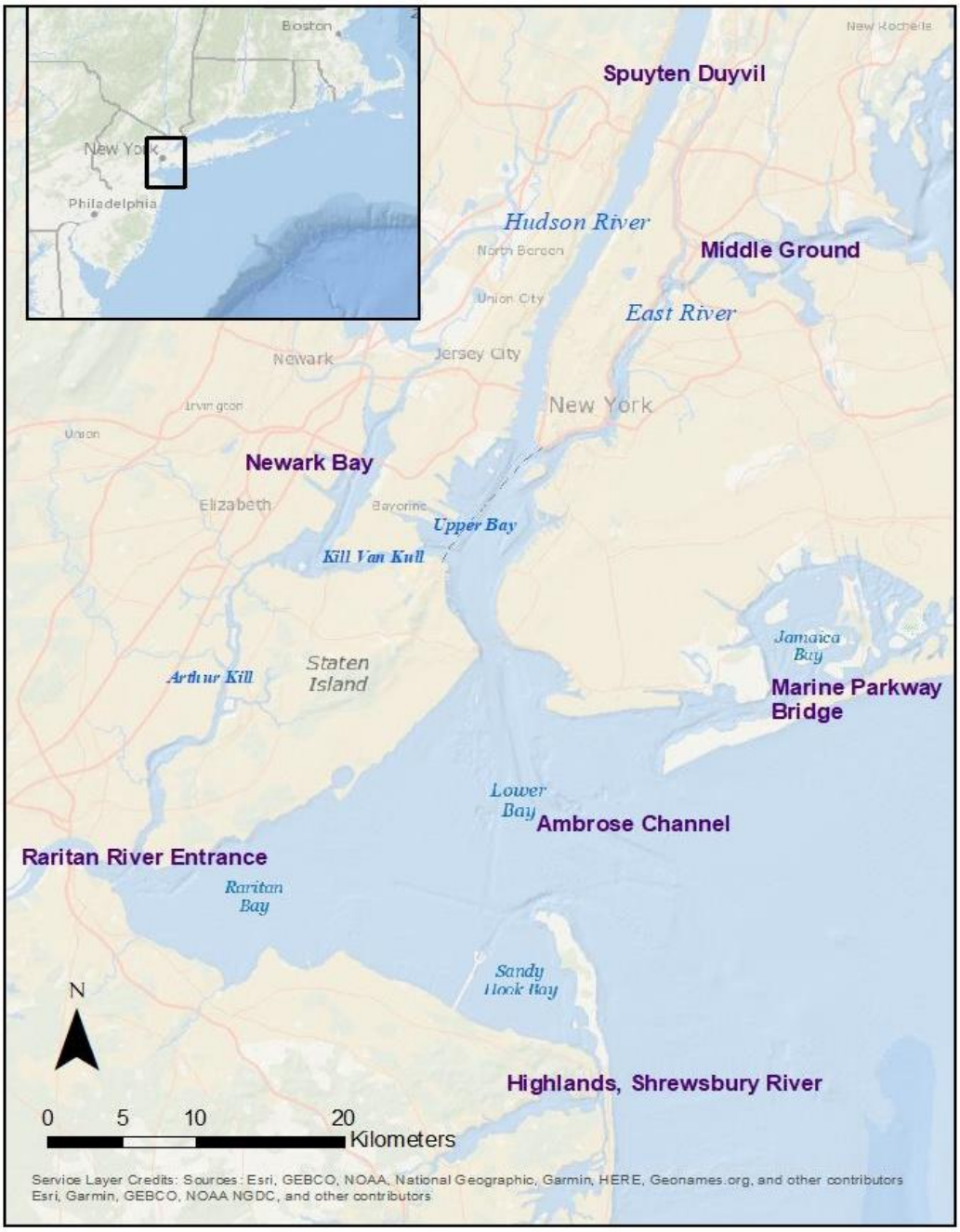

Figure 2-2. The survey region with extents labeled in magenta.

2.2 Physical oceanographic overview

The greater New York Harbor region is comprised of numerous interconnected rivers, kills (Hudson, Raritan, Kill Van Kull, Arthur Kill, etc.), and bays (Upper, Lower, Raritan, etc.), and it forms one of the most intricate natural harbors in the world (Restoring New York…). However, much of the region can be discussed as 2 systems: The Hudson Raritan Estuary (HRE) and the East River. The East River is generally included in the HRE; however, there is enough of a physical oceanographic difference between the 2 to describe them as distinct systems.

2.2.1 Hudson Raritan Estuary

Situated at the northwestern apex of the New York Bight, bound by the East River and lower reaches of the Hudson and Raritan rivers, the HRE continues seaward until it encounters the Atlantic Ocean along a transect between Sandy Hook and Rockaway Point, and it includes the connected bays. The HRE is partially mixed and primarily composed of flooded river valleys, with the Hudson providing an order of magnitude more freshwater than any other source (Oey et al. 1985). Seawater enters from the Atlantic Ocean, as well as the East River's connection to Long Island Sound, and its reach varies throughout the year, depending upon river flows and tidal cycles (Bowen and Geyer 2003). The estuary has been greatly altered through dredging, the hardening of shoreline, and the infilling of marshlands (Ralston et al. 2018). Tides are semidiurnal, as determined by their Defant ratio (Table 2-1), which is defined as: $(K_1 + O_1) / (M_2 + S_2)$. This ratio is used to define the nature of the tide as it changes from strict semidiurnal to strict diurnal: For a Defant ratio less than 0.25, the tides are semidiurnal; for a Defant ratio between 0.25 and 1.5, the tides are mixed, primarily semidiurnal; for a ratio between 1.5 and 3.0, the tides are mixed but mostly diurnal; and for a ratio greater than 3, the tides are diurnal (Defant 1958). As will be shown in sections 5 and 6, tidal currents are also mainly semidiurnal with some slightly mixed, mainly semidiurnal signals in the lower Hudson River. HRE's tides have great diurnal ranges (GT) of 1.542 m to 1.681 m.

Table 2-1. Great Diurnal Ranges (GT) for the project area.

Name	ID	GT	Defant
Kings Point	8516945	2.377	0.13
The Battery	8518750	1.542	0.19
Bergen Point West Reach	8519483	1.681	0.18
Sandy Hook, NJ	8531680	1.593	0.19

2.2.2 East River

Connecting Long Island Sound to the Hudson Raritan Estuary, the East River is a 26 kilometer (km), hydraulically driven strait. It lies between the Bronx/Manhattan and Long Island and starts between Throgs Neck and Willets Point running westerly to Hell Gate, then southwesterly to the Battery. There are only minimal influences from the many tributaries along its path, including the Bronx and Harlem Rivers, and Westchester, Flushing, and Newtown Creeks.

Hydraulic straits are created when large differences in timing of tides on either side of the strait create a pressure gradient. For the East River, the water levels at The Battery (NOAA tide station number 8518750) on the southern end of Manhattan are about 3 hours out of phase from Kings Point (8519645) on Long Island Sound.

3. METHODS

On-water operations were conducted with a mix of NOAA-owned and contracted vessels. The NOAA-owned research vessel (R/V) Tornado (Figure 3-3), a 7.6-meter (m) (25 feet [ft]) pilothouse-style boat manufactured by Parker, was used for operations where lifting in excess of 135 kg was not needed. For larger platforms (those greater than 135 kg), operations were contracted to Goodwin Marine, who provided 2 vessels. The first contracted vessel was the R/V James K Goodwin (Figure 3-1), a 33.5 m (110 ft) 1981 Graham with a 10-ton A-Frame with 144 m^2 (1550 ft^2) of deck space, which was used for deployment operations in August 2019. The second contracted vessel was the R/V Jamie Hanna (Figure 3-2), a 16.8 m (55 ft) custom build with a 2268 kg (2.5-ton) A-frame with 45 m^2 (480 ft^2) of deck space, which was used during recovery operations in October 2019.

Figure 3-1. R/V James K Goodwin deploying a trawl-resistant bottom mount (TRBM) in the East River.

Figure 3-2. R/V Jamie Hanna offloading an Eddie Shih (ES2) bottom mount platform at the U.S. Army Corps of Engineers' (USACE) Caven Point Marine Terminal in Jersey City, N.J.

Figure 3-3. The NOAA R/V Tornado at the U.S. Army Corps of Engineers' (USACE) Caven Point Marine Terminal.

On-water operations consisted of deploying a calibrated ADCP in an appropriate platform at each station location and recovering it after the planned station occupation period (Table A-1). For each station deployment and recovery, the water depth from the vessel's fathometer was recorded, and a CTD vertical profile was taken using a YSI CastAway®-CTD to ascertain the physical properties of the seawater at the approximate location of each station. All station metadata were recorded on station log sheets. For each station, the ADCP instrument's internal compass was calibrated after the batteries were installed. Calibrations were performed to manufacturers' specifications before the deployment for bottom mounted ADCPs, or after the instrument was mounted to the side of an ATON for mounted ADCPs. No compass calibration was conducted on the side-looking ADCP, as it collects data relative to the direction of the instrument (X-Axis,Y-Axis, Z-Axis, [XYZ]) and not in Earth-coordinates (East, North, Up [ENU]). However, detailed directional measurements were made to determine the orientation of the side-looking ADCP relative to the Earth.

3.1 Description of instrumentation and platforms

At each station, the ADCP was mounted in either a bottom-mounted platform for upward-facing measurements, on a floating ATON for downward-facing measurements, or attached to a fixed structure for side-looking (horizontal) measurements (Table B-1).

Currents were measured at each station using an ADCP with a platform configuration determined by factors such as station depth, seafloor composition, expected maritime activities, anticipated currents, and available instrument and platform inventory. All stations were equipped with one of the following: a Teledyne RD Instruments (TRDI) Workhorse Sentinel with frequencies of 300 kilohertz (kHz), 600 kHz, or 1200 kHz, or a Nortek Aquadopp (AqD) with frequencies of 600 kHz, 1000 kHz, or 2000 kHz. The maximum distance of an ADCP profile is a function of the instrument frequency, with lower frequency instruments capable of longer profiles. The instrument frequency for each station was therefore determined primarily by calculating the distance within the water in which current measurements were desired. For vertical profiling (bottom mounts and ATON), this distance is the depth of the water column below the mean higher high water (MHHW) tidal datum plus an added range buffer to account for uncertainties in depth and potential significant events (Table B-1). For side-looking profiles, this distance is intended to reach at least the center of the navigational channel when possible.

3.1.1 Bottom mounts

Bottom mounts are designed to rest on the seafloor and provide a stable platform for an upward-facing ADCP during station occupation. Gimbals are used to keep ADCPs vertical on all bottom mounts except for fiberglass grates. All bottom-mounted platforms were positioned on the seafloor with no surface presence. Stations were recovered by either activating an acoustic release or by a ground dragline. In the event that an equipped acoustic release failed to work properly, a secondary means of recovery (such as dragging) was employed. Bottom-mount platforms used during this project were either manufactured by Mooring Systems, Inc. (MSI) or DeepWater® Buoyancy (DWB, previously Flotation Technologies), or they were purpose-built by engineers at NOAA (Table 3-1).

Table 3-1. Bottom-Mount Platforms

Platform and Manufacturer	Specifications	Deployment and Recovery Method	Picture of Platform
MTRBM MSI	Base: 2.5 cm fiberglass grate Shell: Fiberglass or urethane cover with Length: 178 cm Width: 122 cm Height: 48 cm Weight in water (without ballast): 23 kg Weight in air: 60 kg	Platform is lowered to place and released. Recovery is by acoustically releasing a float to the surface with a line tethered to the base. A ground line is attached between the platform and a small anchor. If the release fails to operate as intended, a backup recovery via the ground line is performed by dragging a grapnel to snag the line.	
Tri-Pod MSI	Aluminum with molded urethane gimbals, lead ballast, and stainless-steel hardware. Diameter: 150 cm Height: 50 cm Ballasted weight in: Air: 31 kg Water: 25 kg	Platform is lowered to place and released with a slip line. A ground line is attached between the platform and a small anchor or to a fixed structure. Recovery is with a grapnel to snag the ground line.	
Fiberglass Grate NOAA	2.5 cm grid size fiberglass with lead weights as feet and for ballast 45 × 55 cm Strong back is used to hold instrument. No gimbal is present.	Platform is lowered to place and released with a slip line. A ground line is attached between the platform and a small anchor or to a fixed structure. Recovery is with a grapnel to snag the ground line.	

Platform and Manufacturer	Specifications	Deployment and Recovery Method	Picture of Platform
ES-2 NOAA	Fiberglass shell with stainless-steel hardware 224 × 178 × 84 cm Weight in air: 363 kg	Platform is lowered to the bottom. Acoustically released pop-up buoy to the surface. Entire platform is pulled from the bottom.	
TRBM DWB	185 × 178 × 51 cm Weight in water: 109 kg Weight in air: 454 kg Float buoyancy: 91 kg	Platform is lowered to place and released with a slip line. Recovery is performed by activating an acoustic release on the foam pod. The foam pod is attached to the base with a line. The entire platform is recovered. A ground line is attached between the platform and a small anchor. If the release fails to operate as intended, a backup recovery via the ground line is performed by dragging a grapnel to snag the line.	
H-TRBM (Formerly GP35) MSI	Diameter: 89 cm Height: 43 cm 27 kg ballast is used. Weight in seawater: 5 kg (empty) 31 kg (ballasted) Weight in air: 18 kg (empty) 45 kg (ballasted):	Platform is lowered to place and released with a slip line. A ground line is attached between the platform and a small anchor or to a fixed structure. Recovery is with a grapnel to snag the ground line.	

3.1.2 Horizontal mount

One station (NYH1933 [Shrewsbury River Highlands Bridge]) was occupied using a side-looking ADCP mounted to the bridge structure using clamps and a pole (Figure 3-4). This mount was designed and built by NOAA. The ADCP is held in the mount by a clamp and oriented to collect data across the channel.

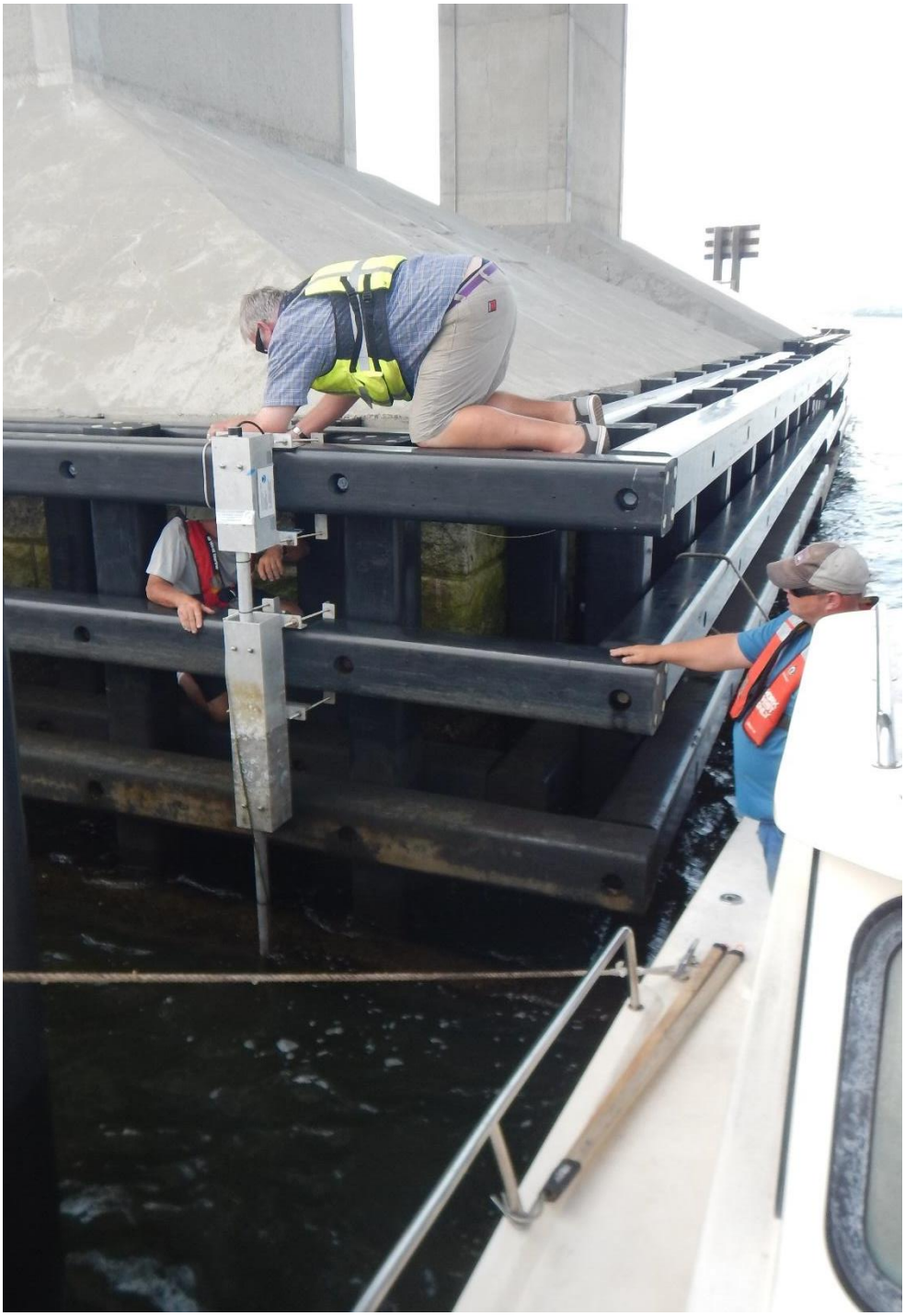

Figure 3-4. Horizontal crib mount being installed. ADCP is held at the bottom of the pole, below the surface.

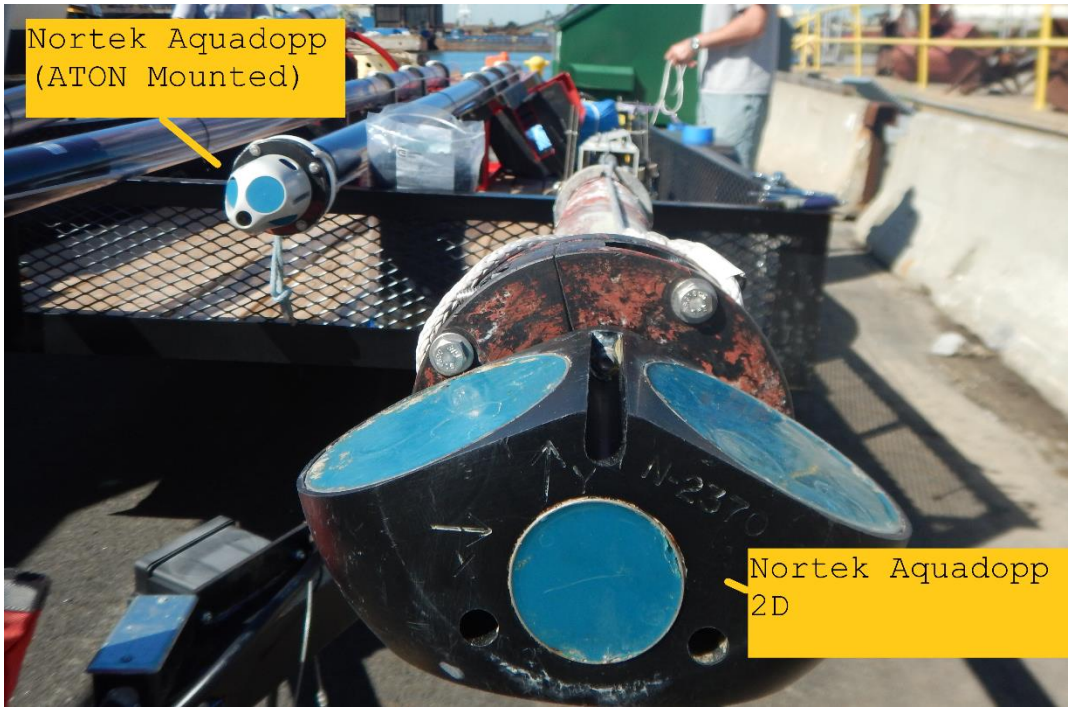

Figure 3-5. Bottom of side-looking Nortek AqD 2D ready for installation. View is looking up the pole to the mount. ATON-mounted, downward-facing Aquadopp is pictured to the left of the side-looker, mounted in a tube attached to a Clamparatus and ready for installation.

3.1.3 ATON mounted

ATON-mounted ADCPs can observe currents in or adjacent to navigational channels where bottom mounts are impractical or not allowed. For NCOP operations, an Oceanscience Clamparatus (Bosley et al. 2005) without a topside electronics enclosure (Figure 3-6) was mounted to the U.S. Coast Guard buoy through an eye bolt, which held a downward-facing ADCP in a tube about 2 m below the surface (Figure 3-5). A communications cable was attached to the ADCP and fed through the Clamparatus tube for calibration and programming. The cable was left attached and tucked into the tube during the deployment. The ADCP was calibrated on the ATON during deployment to ensure the metal buoy did not interfere with the ADCP compass and magnetic variation. Instruments were configured to collect data internally.

Figure 3-6. Clamparatus before adding tube and instrument.

3.2 ADCP setup and data collection

ADCPs compute water velocity by sending out a series of acoustic pulses, or pings, and measuring each acoustic ping's return signal for Doppler shift. Unlike single-point current meters, ADCPs are generally configured to measure a profile of the water column. Profiles are created from many discrete bins of data collected in the water directly away from the acoustic heads of the ADCP. Bins are determined from the timing of acoustic returns of the unique signal ("ping") sent from the instrument transducer using the speed of sound in water to calculate the two-way travel time over the distance traveled. Water velocity is calculated by measuring the Doppler shift of each ping after reflection off microscopic bubbles or particulate matter suspended in the water; these measurements are then averaged across each bin of the profile.

Bins therefore represent spatially averaged subdivisions along the profile. Optimal bin size is a compromise between higher spatial resolution along the profile (i.e., smaller bins) and lower standard deviation of the velocity ensemble (i.e., larger bin size increases the number of returning pings to calculate the spatial average). Bin size, like profile distance, is also a function of ADCP frequency. Higher frequency instruments measure smaller bins than lower frequency instruments with the same standard deviation; however, lower frequency instruments can measure longer profiles and thus are used at deeper stations.

Velocity profiles can be collected either vertically (upward- and downward-facing ADCPs) or horizontally (side-looking ADCPs). Because the ADCP is measuring either a three-dimensional (bottom and ATON platforms) or two-dimensional (side-looking) flow field, the acoustic transducer heads are set at an angle with respect to the instrument's measurement profile. For the upward-facing ADCPs used in this survey, the angle is either 20 degrees or 25 degrees. For three-dimensional flow measurements, a minimum of 3 acoustic transducers are necessary. The Doppler-

shifted velocities along each beam can then be transformed mathematically into any orthogonal coordinate system, such as an east-north-up orientation (with the help of a compass).

Each ADCP was configured to collect profiles of data in 6-minute averages (called "ensembles") of acoustic pulses ("pings"). The pings per ensemble (the number of transmitted acoustic pulses whose returns as described above are averaged in time to form a single velocity measurement for each bin) should minimize the theoretical standard deviation of expected velocity within an ensemble with respect to the engineering constraints of the system. NCOP uses manufacturer-supplied software which calculates the ensemble's standard deviation, battery usage, and memory usage for the anticipated duration of the deployment for a specified number of pings per ensemble, number of bins, and bin size. All these factors affect battery life.

The optimal number of pings is a compromise between reducing the ensemble standard deviation and choosing an appropriate bin size and number of bins to ensure sufficient battery life and data storage for the expected conditions at each station. TRDI Workhorses are self-contained ADCPs with internal data storage and battery packs. For this project, stations were configured to minimize standard deviation by maximizing pings per ensemble while still ensuring sufficient battery life to complete the planned deployment duration.

There are some additional constraints on velocity profiles from ADCPs. Because of the angled beams, a portion of the water column near the water surface (or bottom) will be lost to side-lobe interference (approximately 5-10 percent of the profile depth depending upon beam angle). Transducer ringing, the result of the noise of the transmit pulse on the co-located transducer and receiver, leads to the loss of part of the profile nearest the ADCP head. Blanking distance accounts for this and varies as a function of ADCP frequency and transducer properties. The manufacturer's recommended default settings for blanking distance were used on both TRDI and Nortek instruments.

In bottom-mounted platforms, the ADCPs have an upward orientation; thus, bin 1 is the bin closest to the ADCP near the seafloor, and the profile extends to the surface. Conversely, in ATON mounts, the ADCP has a downward orientation where bin 1 is near the surface and increases in number toward the bottom.

The following ancillary measurements were collected and used as data quality assurance parameters: water temperature, pressure (depth), and instrument tilt collected at the sensor. Beam echo intensity and correlation magnitude were also collected (for TRDI ADCPs only) for each transducer head at each bin of the profile.

ADCPs were calibrated and tested for proper operation using built-in internal testing algorithms. Upon completion of these procedures, a unique configuration file was uploaded to each instrument based upon settings derived from the manufacturers' software. A unique, 5-character deployment name and the time to start pinging were also programmed. For all instruments that were redeployed for the second half of the survey, an examination of the ADCP's performance was conducted, and new settings were configured based upon the new location.

3.3 Description of data processing and quality control

The sampling rate for the ADCP data was 10 times per hour (centered every 6 minutes from the top of the hour through 54 minutes past the hour). Each sample was an average of up to 360 evenly timed pings based on the ADCP setup and frequency. Even though the shortest tidal constituent period is about 2 hours, 6-minute samples enable a high-resolution estimation of the maximum and minimum tidal currents with the ability to capture short duration, non-tidal events. This rate also provides a statistically sound time series in which erroneous records are less likely to influence the longer series.

Quality control measures were used to mark each record as "bad," "good," or "questionable" based on best practices implemented by CO-OPS (Paternostro et al. 2005) and based on the community-accepted QARTOD (Quality Assurance/Quality Control of Real-Time Oceanographic Data) standards and recommendations (IOOS 2019; IOOS 2020). Quality control applied to the measurements consists of threshold checks (for speed, tilt [pitch and roll], echo amplitude, and correlation magnitude) and rate of change checks (for speed, pitch, roll, and heading). An automated algorithm flagged the records that failed any of these checks. Questionable data were reviewed by an experienced analyst and marked as either "bad" or "good." Only good data are disseminated to the public and used for harmonic analysis.

The principal flow (currents) direction is calculated by maximizing the direction of variance. This calculation enables an orthogonal transformation from an east-north coordinate system to major and minor flow direction axes (generally along- and cross-channel, respectively). Representing the currents in the major and minor axes components is especially beneficial in coastal and estuarine areas, which exhibit a rectilinear reversing flow rather than a rotary flow. In these cases, a significant majority of energy is along the major axis, and we can effectively represent the tidal currents with a single variable (major axis current speed).

All ADCP data collected were analyzed to separate the harmonic or tidal part of the signal from the residual or non-tidal flow (Parker 2007). Data were extracted from the binary instrument output into columnar ASCII data and then processed further by NOAA's harmonic analysis routines (Zervas 1999). Harmonic analyses were then performed upon the current velocity time series in the major and minor flow directions.

The preferred analysis method for tidal current data is an optimization technique called "Least Squares Harmonic Analysis" (LSQHA) (Parker 2007). The least squares technique allows for the presence of data gaps and can be used on time series of varying lengths. Amplitudes and phases of a given set of tidal constituents are resolved by using this method. The frequencies and number of tidal constituents for each station are determined by the length of the time series. LSQHA was used to calculate harmonic constituents at all but 1 survey station. NOAA typically collects at least 33 days of data to ensure that most tidal energy can be adequately resolved by the least squares analysis.

Predictions provided online by CO-OPS are generated directly from harmonic constituents to meet U.S. Coast Guard vessel carriage requirements.

4. DATA ACQUIRED

Data were acquired at 32 of 33 stations occupied during the summer of 2019, with only the unrecovered station at Grant's Tomb (NYH1930) failing to provide any data. However, analysis revealed that data from 2 stations (NYH1907 [Arthur Kill Port Socony], and NYH1923 [East River "B" buoy]) were unusable due to a corrupted compass matrix. The tables in appendices A and B describe station data and metadata used in the analysis. Additionally, all stations have CTD data from vertical profile casts taken at deployment and recovery.

The estimated depth of the current profiler platform and the measurement bin depths are given in meters relative to an approximation of mean lower low water (MLLW). This estimated MLLW depth is calculated statistically from the known height of the platform above the bottom in combination with the time series from the ADCP's pressure sensor. Error in the MLLW calculated at a given current station is the result of both the length of time of observations and uncertainties in the observed station depth. Station depth uncertainty is affected by any pressure sensor errors (such as drift and offset errors) and platform instability. Swanson (1974) calculated MLLW sigma errors of ±0.4 to 0.3 m for tide observations with a time series of 30-90 days. Calculated depth is therefore a best approximation. This MLLW approximation can be compared to the station depth, which is logged using the boat's fathometer during deployment and recovery and entered into the database.

Stations in Table A-1 of the appendix are listed with position, depth as recorded at deployment, and station occupation start and end dates.

5. STATION RESULTS

A brief, quantitative description of a subset of survey stations is provided in this section. These include stations that exhibit characteristics of different flow regimes. A map of the stations described in this section is shown in Figure 5-1.

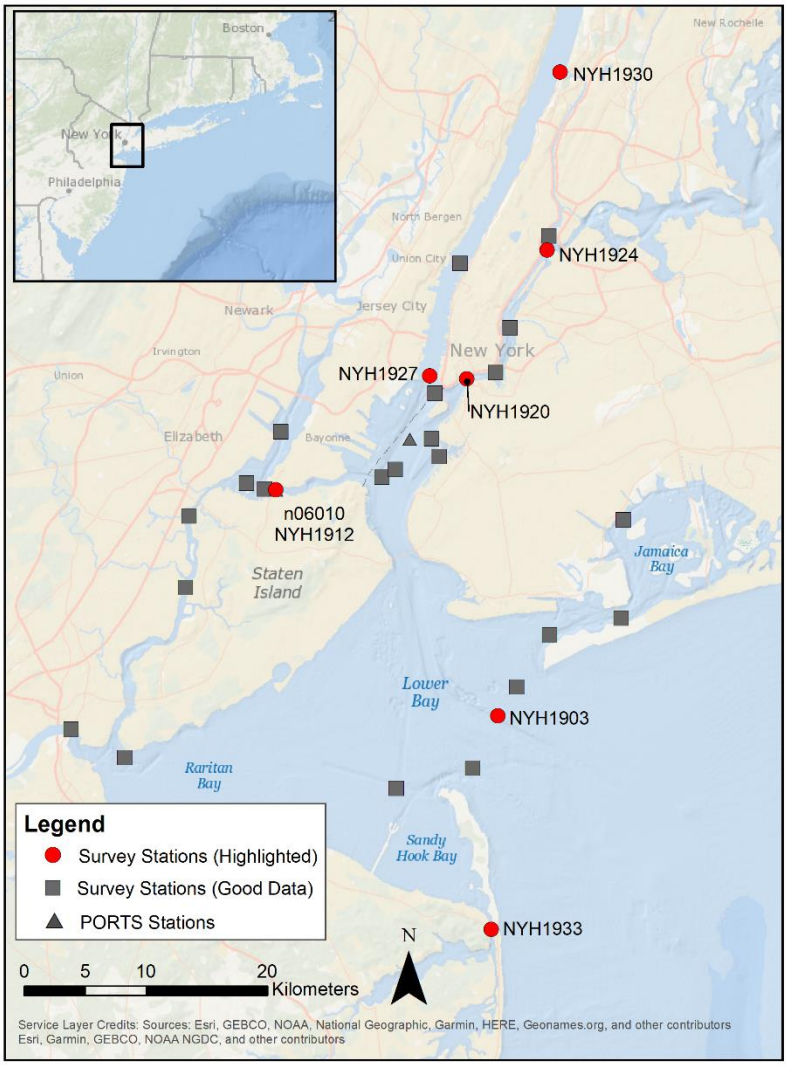

Figure 5-1. Map of all stations. Stations labeled with red circles are highlighted in this section.

For each station in this section, a description of the mean maximum flood current (MFC) and mean maximum ebb current (MEC) is given for the station's near-surface depth bin represented in the official NOAA tidal current predictions (TCP). For some stations, up to 2 additional depths are available in TCP (NOAA Current Predictions). For ADCPs, "bin 1" refers to the depth closest to the instrument's head (bottom-most for bottom mounted, upper-most for ATON mounted, and closest to the structure for side-looking); the bin number increases with distance from the instrument. The principal flood direction is the predominant axis of flow as

described in section 3.6. Directions are provided in degrees from true north. The variance along this axis is provided to give an indication of how confined the flow is along the axis; a high percentage variance implies a rectilinear flow. Seven stations are described in this section. These stations were selected based on spatial representation and/or scientific interest. The results presented below are a small subset of the full analyses conducted on the data sets. Defant ratios for the uppermost bin in the water column or the bin closest to the ship channel are provided to indicate tide type. For each of the 7 stations described, there are 5 figures that include the following:

1. A scatter plot of the north versus east velocity component of the entire data set at the near-surface depth bin.
2. Two plots of a subset of the velocity time series at the near-surface depth bin. The upper plot shows a comparison of observed (green dots) major-axis velocity and calculated (red line) tidal predicted velocity; the lower plot shows the residual flow (the difference between observed and predicted velocity).
3. A vertical profile of the mean velocity along the major (red "×") and minor (blue "+") axis of the water column. This represents the approximate mean residual (non-tidal) circulation throughout the water column. The surface level is estimated (shown as a blue wavy line).
4. A vertical profile plot showing the timing and speed of the MFC throughout the water column.
5. A vertical profile plot showing the timing and speed of the MEC throughout the water column.

5.1 NYH1903 - Ambrose Channel

This station was deployed for 69 days (August 12, 2019-October 20, 2019) in 9.6 m (31.5 ft) of water. A TRDI Workhorse 1200 kHz ADCP mounted in a TRBM collected 30 half-meter bins of data, 16 of which met quality control criteria for full analysis. Bins 1, 9, and 15 are available on TCP, representing approximate depths of 8.5 m, 4.5 m, and 1.5 m (28.0 ft, 14.9 ft, and 5.1 ft, respectively) below MLLW, respectively.

Ambrose Channel is the principal navigation channel entering the Lower Bay, inbound to New York Harbor. This station was deployed just north of the channel. Observed currents are rectilinear (Figure 5-2), with major axis variance between 96.2% and 98.7%. This station is very tidal, which is indicated by the low residuals, as seen in Figure 5-3. LSQHA resolved 25 constituents and accounted for 93-96% of the total energy in the velocity data. A mean southeasterly (ebb) flow is greatest near the surface and decreases with depth (Figure 5-4). Mean MFC and MEC currents range between 52 cm/s and 100 cm/s (1.0 knot (kn) and 2.0 kn), and their timing does not vary much with depth (Figure 5-5 and 5-6). The Defant ratio in the uppermost bin was 0.143, indicating that this station is semidiurnal.

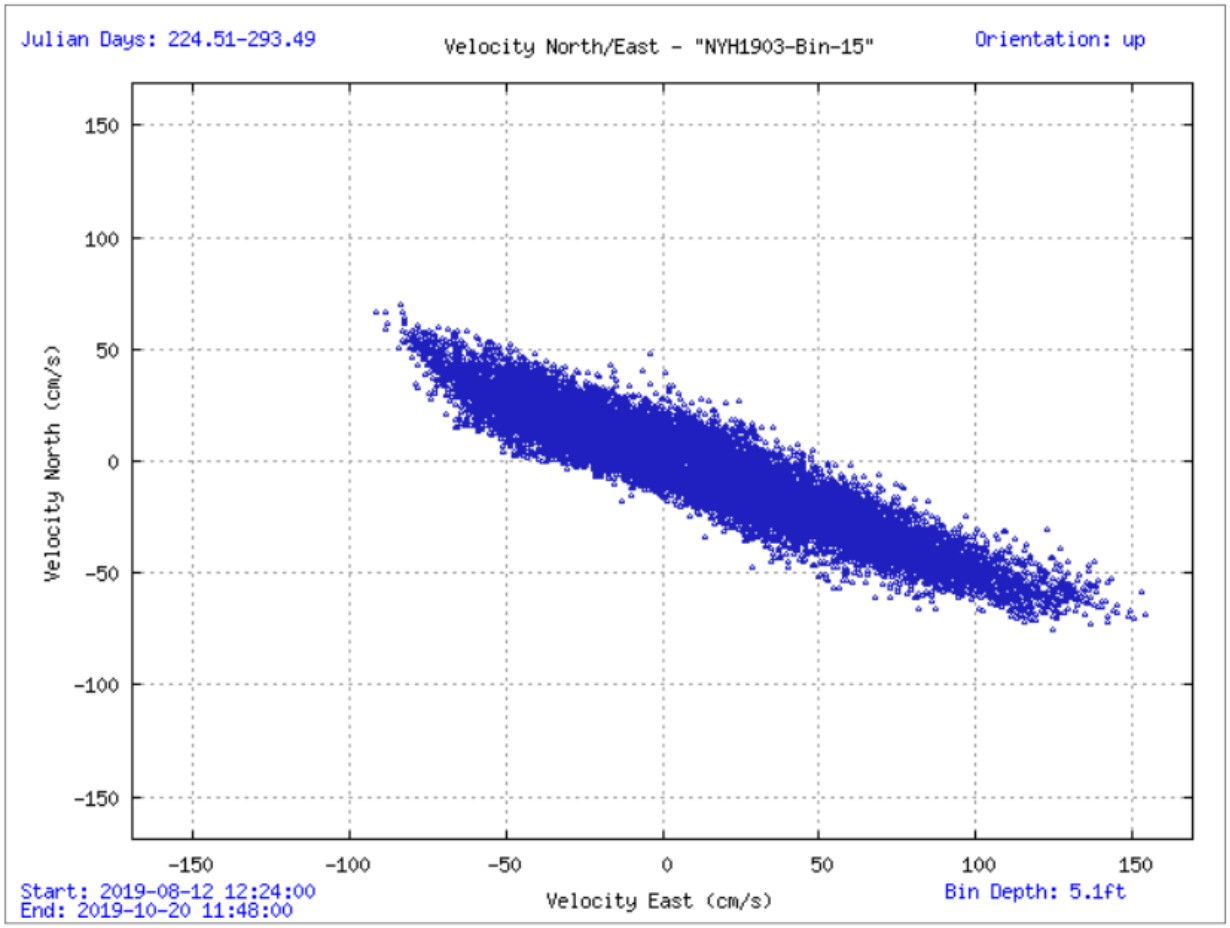

Figure 5-2. Scatter plot of north-versus-east velocity for station NYH1903 at the near-surface bin, bin 15 at 1.5 m below MLLW.

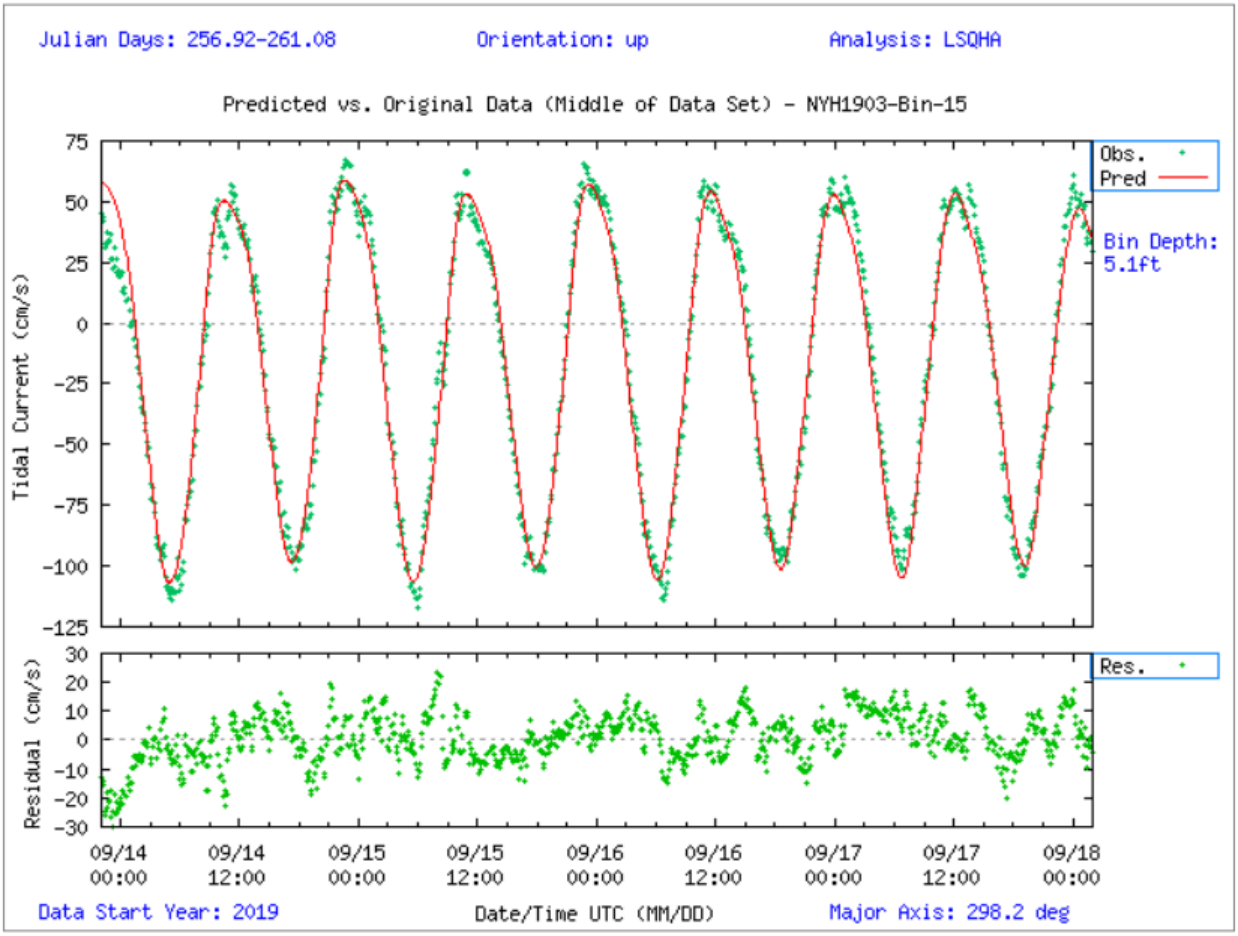

Figure 5-3. Comparison of observed major axis velocity data (green points) to predicted tidal velocity along the major axis for station NYH1903. The lower figure shows the non-tidal residual, the difference between the predicted and observed velocity from the upper prediction bin.

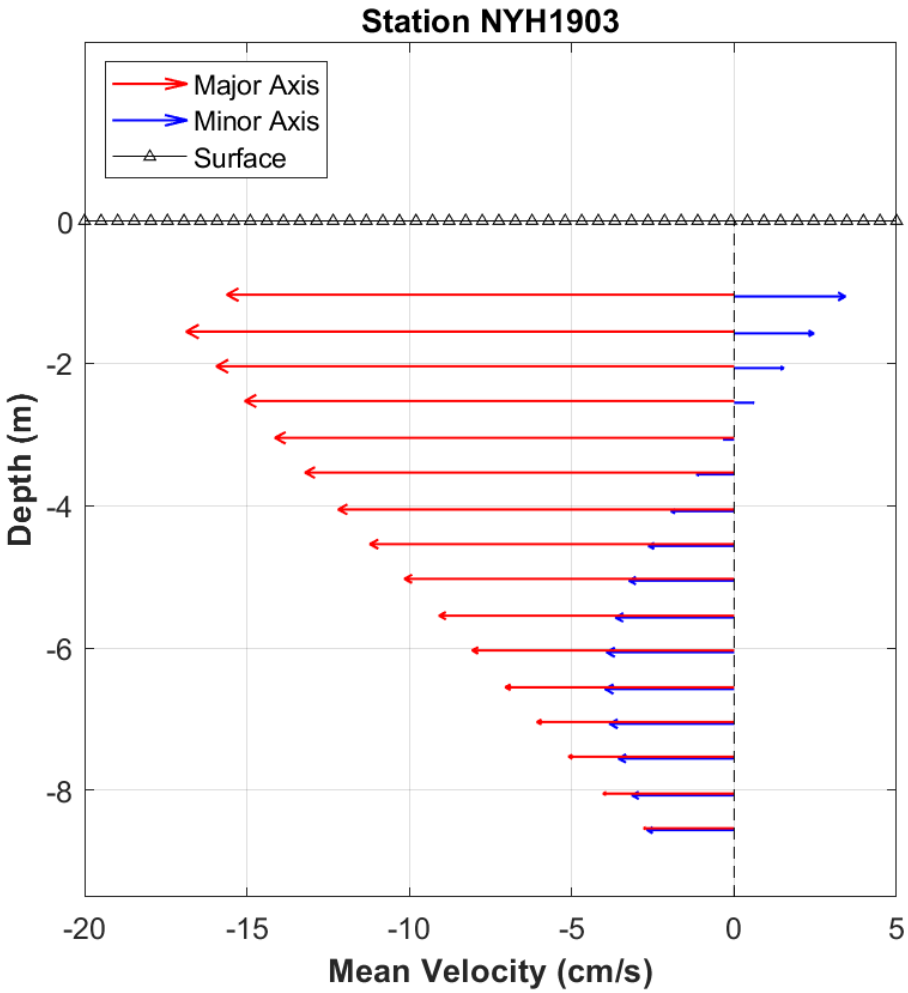

Figure 5-4. NYH1903 mean velocity profile by depth. Only depths that passed quality control criteria are shown. This station was configured to collect 0.5 m bins.

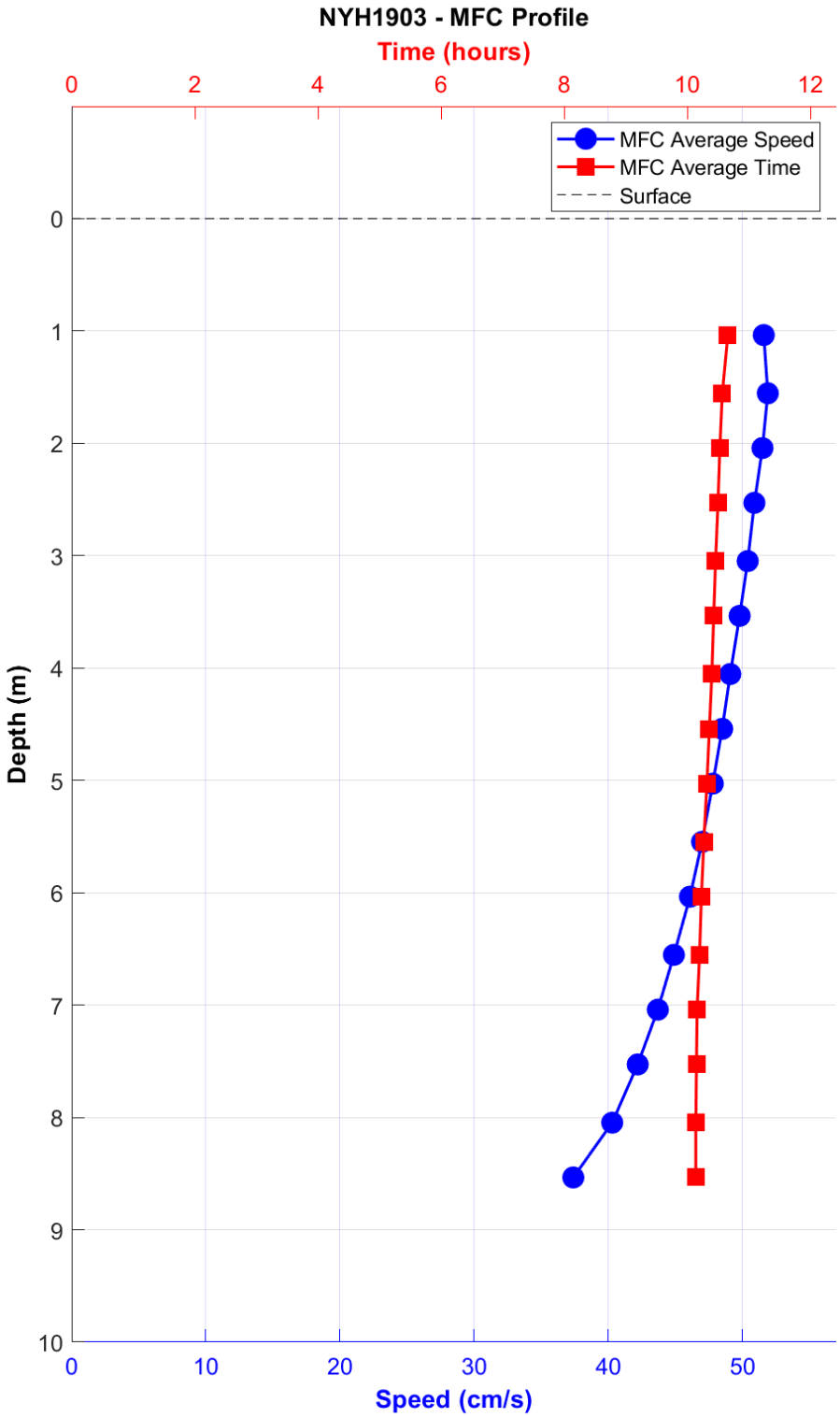

Figure 5-5. NYH1903 MFC timing (GI - in red squares) and speed (blue circles) by depth bin. Bin 1 is the deepest bin observed at approximately 8.5 m below MLLW, and the top-most good bin is bin 16 (1.5 m below MLLW).

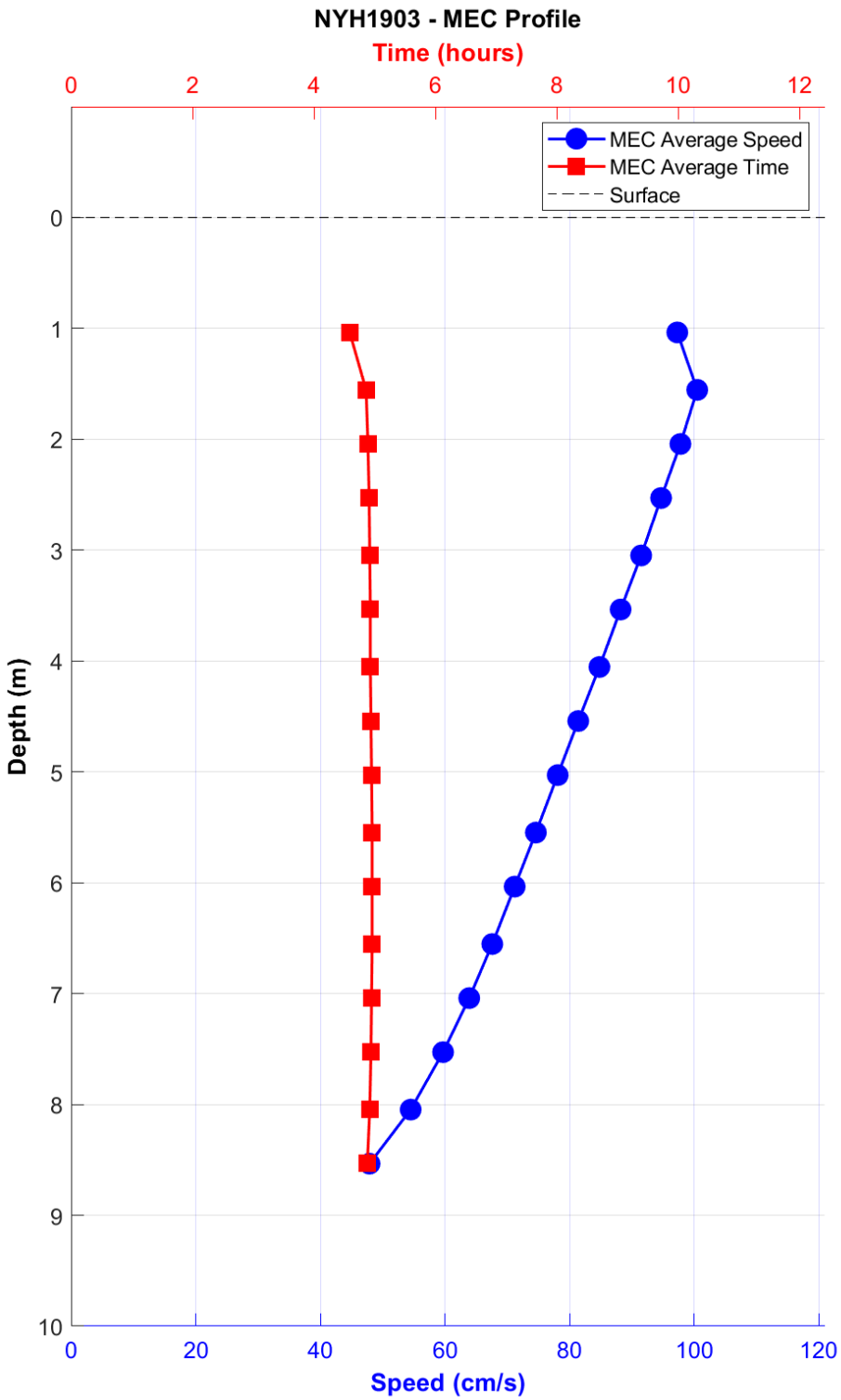

Figure 5-6 NYH1903 MEC timing (GI – red squares) and speed (blue circles) by depth bin. Bin 1 is the deepest bin observed at approximately 8.5 m below MLLW, and the top-most good bin is bin 16 (1.5 m below MLLW).

5.2 NYH1920 – Brooklyn Bridge

This station was deployed for 69 days (August 12, 2019-October 20, 2019) in 17.6 m (57.7 ft) of water. A TRDI Workhorse 600 kHz ADCP mounted in a TRBM collected 25 1.0 m bins of data, 12 of which met quality control criteria for full analysis. Bins 1, 10, and 12 are available on TCP, representing approximate depths of 13.5 m, 4.5 m, and 2.5 m (44.1 ft, 14.6 ft, and 8.0 ft) below MLLW, respectively.

Brooklyn Bridge is at the southwestern end of the East River near the confluence of the Hudson River and Upper Bay. This station was deployed in the northern third of the channel. Observed currents are extremely rectilinear (Figure 5-7), with major axis variance of 99.3-99.8%. This station is very tidal, as seen in Figure 5-8. LSQHA resolved 25 constituents and accounted for 98% of the total energy in the velocity data. A mean southwesterly (ebb) flow is seen throughout the water column (Figure 5-9). Mean MFC and MEC currents peak at 140 cm/s and 154 cm/s (2.7 kn and 3.0 kn) respectively, and their timing does not vary much with depth (Figures 5-10 and 5-11). The Defant ratio in the upper good bin was 0.037, indicating that this station is semidiurnal.

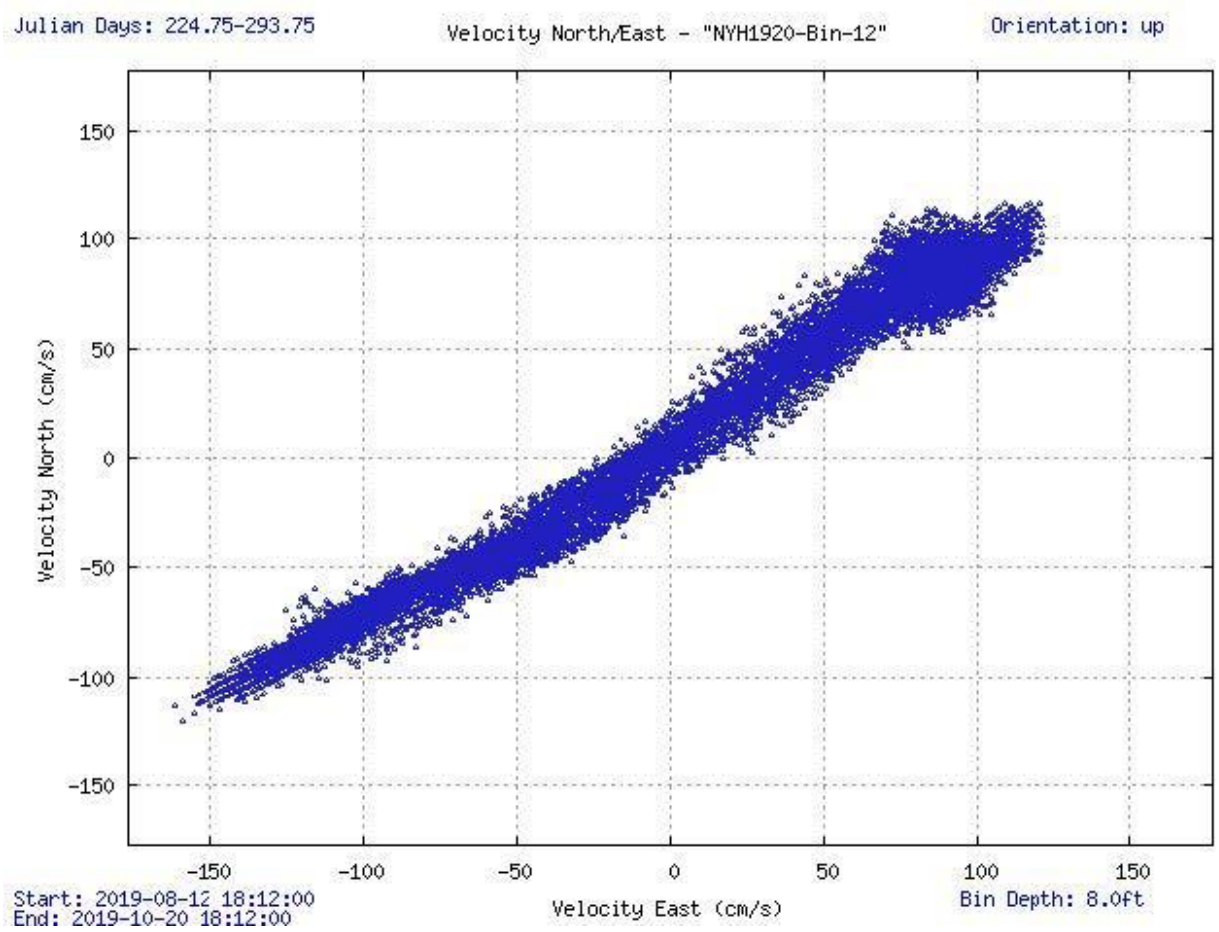

Figure 5-7. Scatter plot of north-versus-east velocity for station NYH1920 at the near-surface bin, bin 12 at 2.5 m below MLLW.

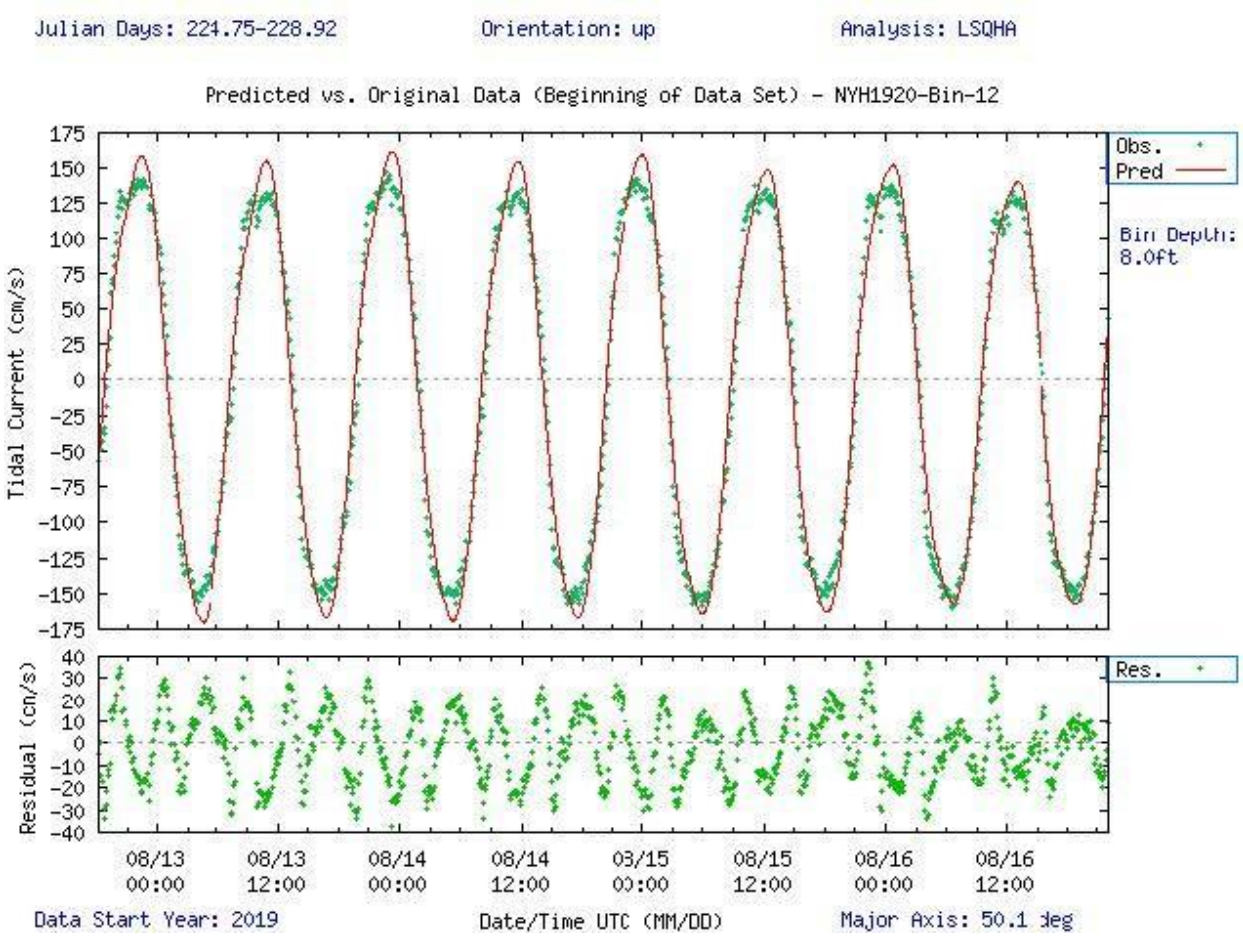

Figure 5-8. Comparison of observed major axis velocity data (green points) to predicted tidal velocity along the major axis for station NYH1920. The lower figure shows the non-tidal residual, the difference between the predicted and observed velocity from the upper panel.

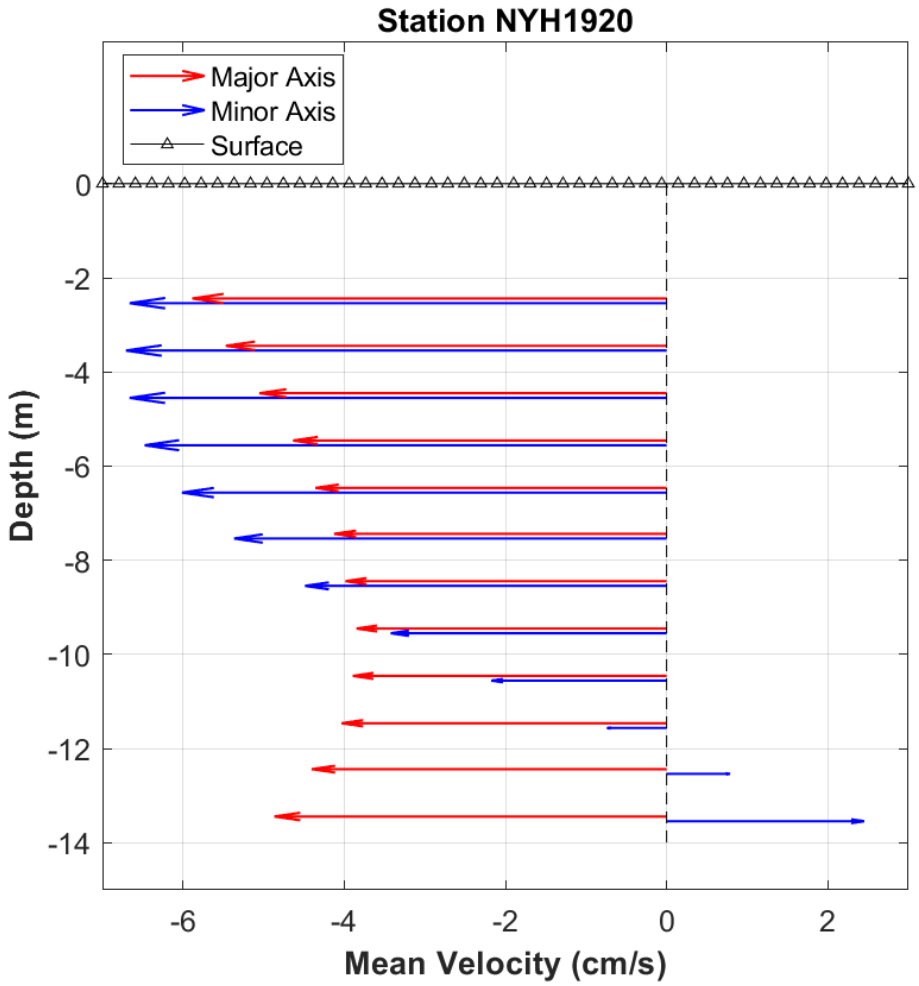

Figure 5-9. NYH1920 mean velocity profile by depth. Only depths that passed quality control criteria are shown. This station was configured to collect 1.0 m bins.

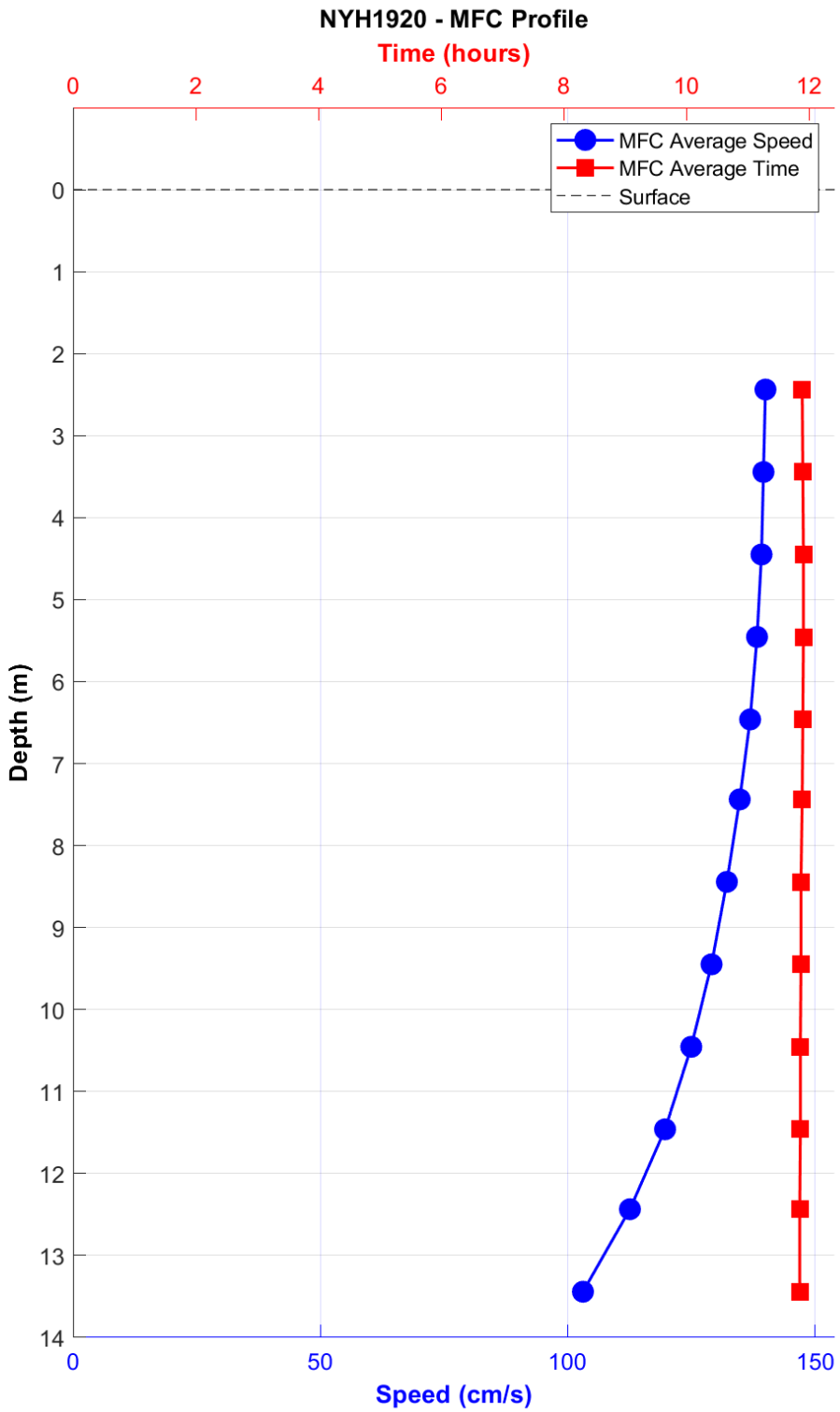

Figure 5-10. NYH1920 MFC timing (GI - in red squares) and speed (blue circles) by depth bin. Bin 1 is the deepest bin observed at approximately 13.5 m below MLLW, and the top-most good bin is bin 12 (2.5 m below MLLW).

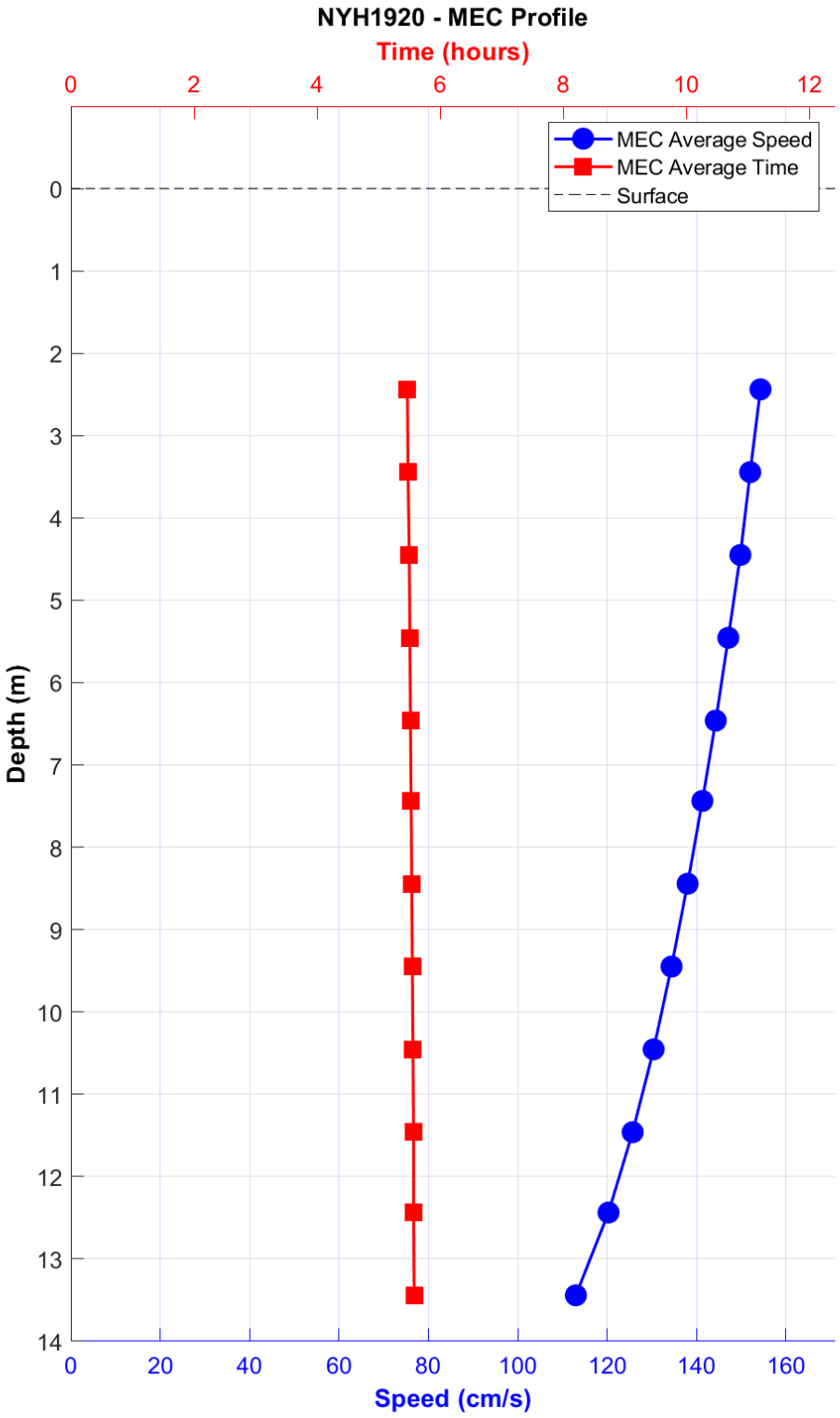

Figure 5-11. NYH1920 MEC timing (GI – red squares) and speed (blue circles) by depth bin. Bin 1 is the deepest bin observed at approximately 13.5 m below MLLW, and the top-most good bin is bin 12 (2.5 m below MLLW).

5.3 NYH1924 – Hell Gate

This station was deployed for 68 days (August 13, 2019-October 20, 2019) in 13.4 m (44.0 ft) of water. A TRDI Workhorse 600 kHz ADCP mounted in a TRBM collected 20 1.0 m bins of data, 9 of which met quality control criteria for full analysis. Bins 1, 6, and 9 are available on TCP, representing approximate depths of 9.8 m, 4.8 m, and 1.8 m (32.0 ft, 15.6 ft, and 5.8 ft) below MLLW, respectively.

The station Hell Gate is a reoccupation of the historical, hydraulically derived prediction location. Logistical constraints prevented a deployment at the narrowest constriction, which would likely have measured stronger currents. This location is to the south of Mill Rock at the confluence of the East and Harlem Rivers. Observed currents are extremely rectilinear (Figure 5-12), with major axis variance of 99.4-99.6%. This station is almost entirely tidal, as seen in Figure 5-13. LSQHA resolved 25 constituents and accounted for 99% of the total energy in the velocity data. A mean southwesterly (ebb) flow is seen throughout the water column (Figure 5-14). Mean MFC and MEC currents have a range of 182-228 cm/s (3.5-4.4 kn), and their timing does not vary much with depth (Figures 5-15 and 5-16). The Defant ratio in the upper good bin was 0.028, indicating that this station is semidiurnal.

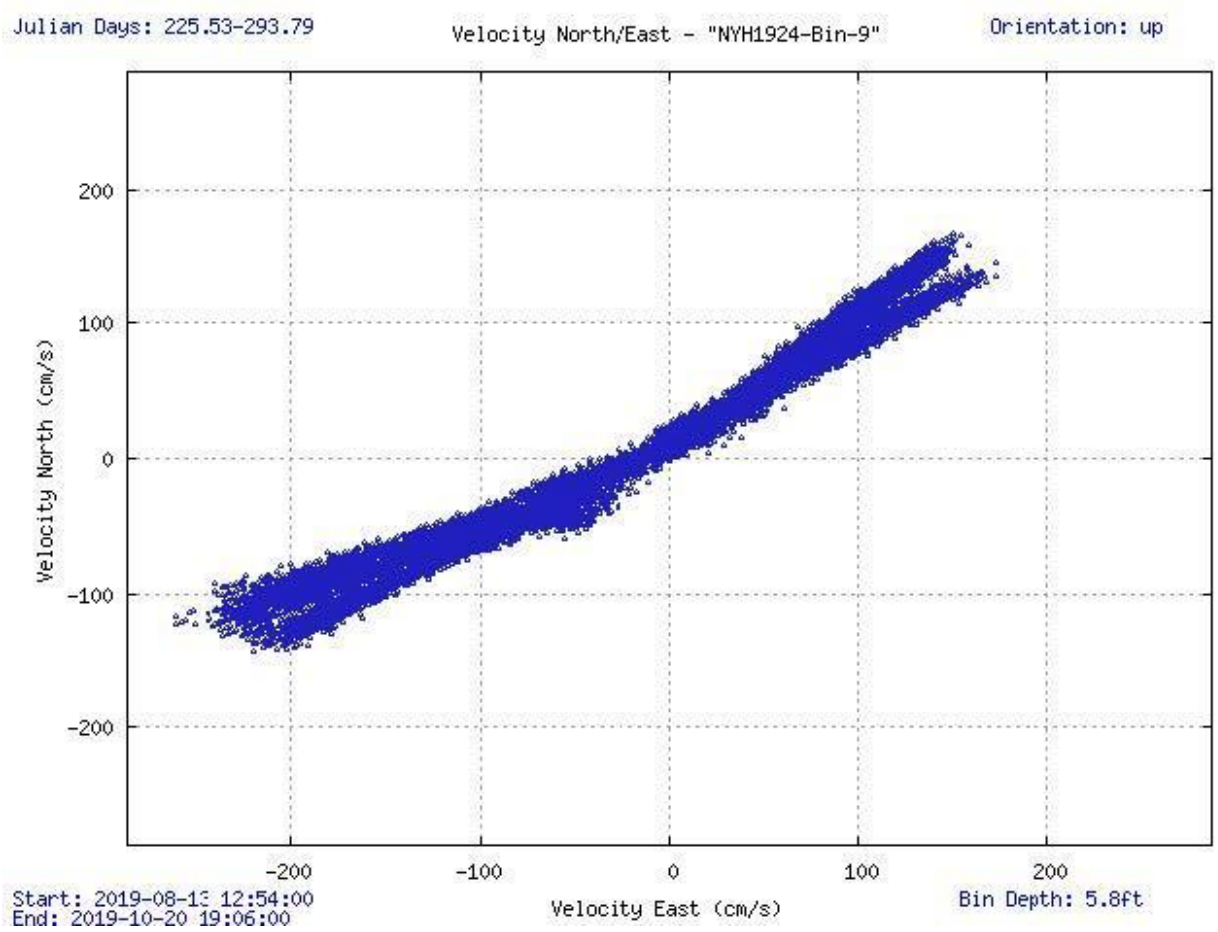

Figure 5-12. Scatter plot of north-versus-east velocity for station NYH1924 at the near-surface bin, bin 9, at 1.8 m below MLLW.

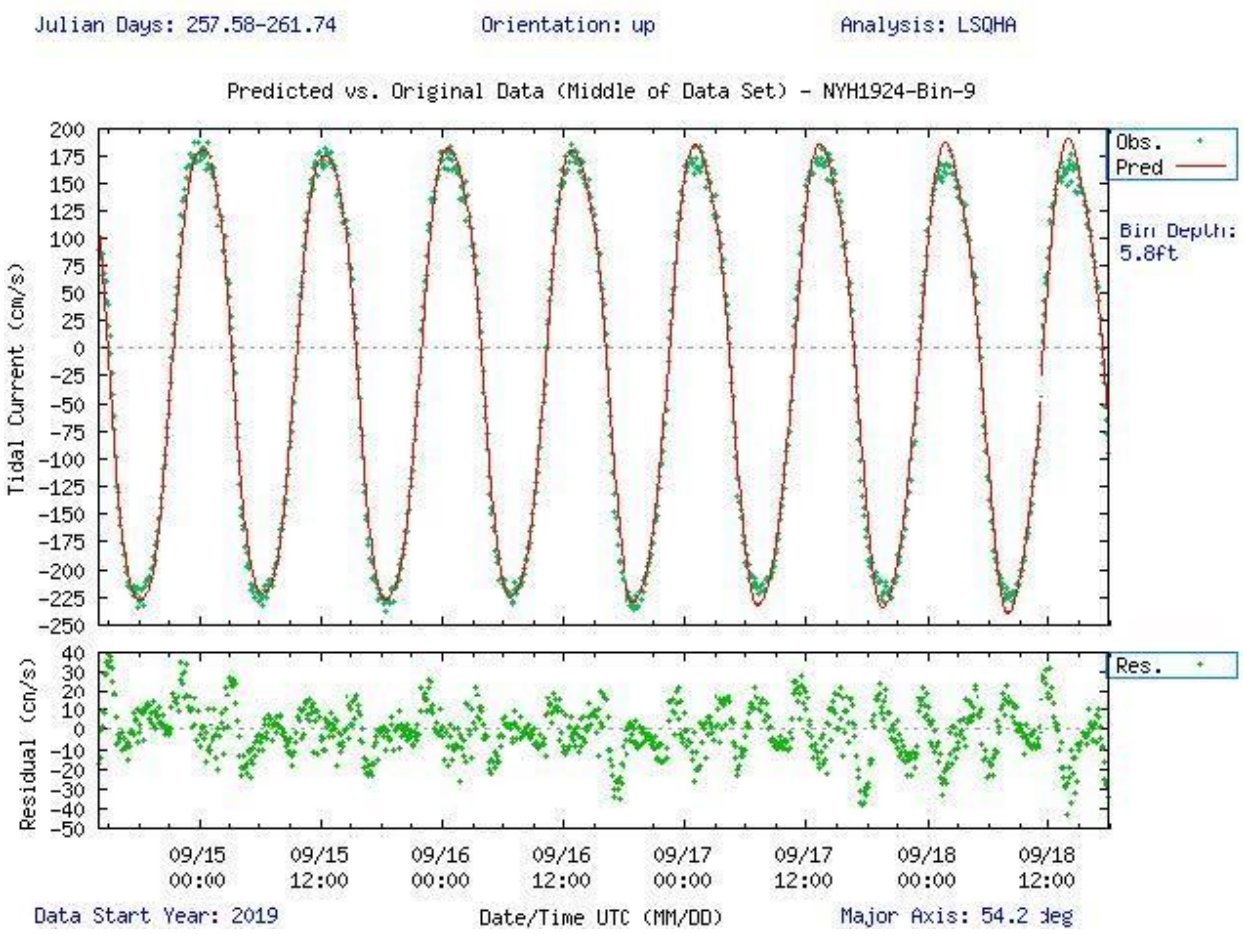

Figure 5-13. Comparison of observed major axis velocity data (green points) to predicted tidal velocity along the major axis for station NYH1924. The lower figure shows the non-tidal residual, the difference between the predicted and observed velocity from the upper panel.

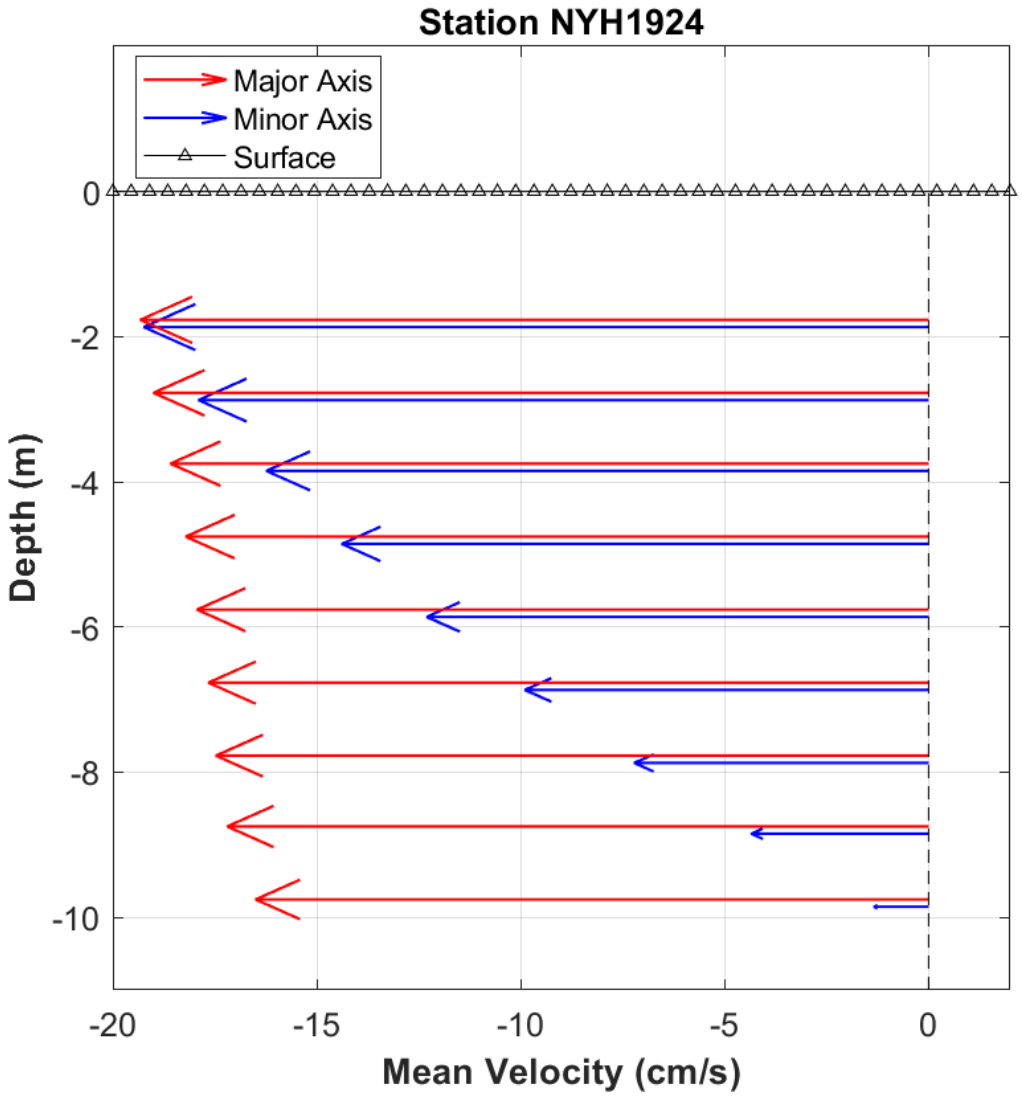

Figure 5-14. NYH 1924 mean velocity profile by depth. Only depths that passed quality control criteria are shown. This station was configured to collect 1.0 m bins

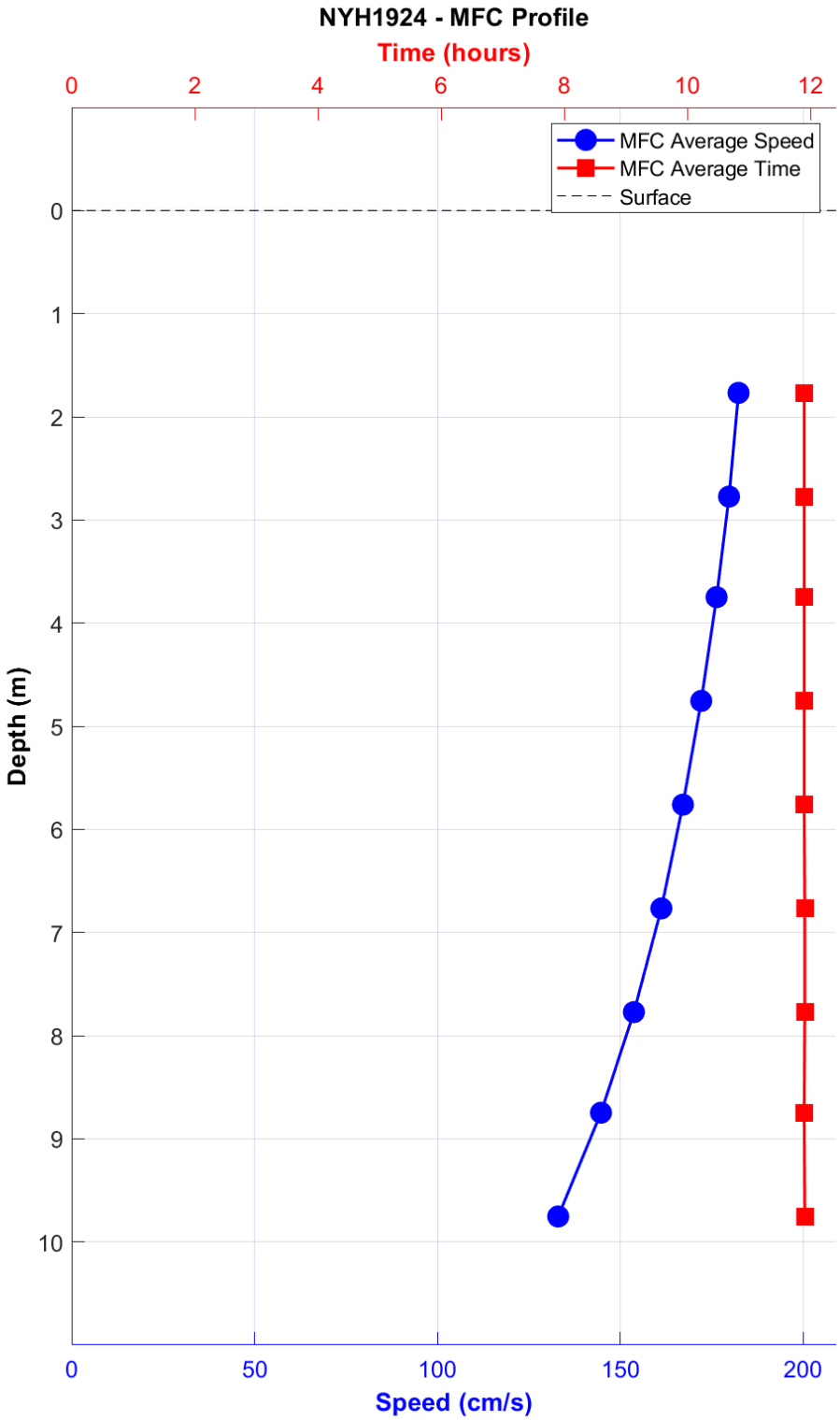

Figure 5-15. NYH1924 MFC timing (GI - in red squares) and speed (blue circles) by depth bin. Bin 1 is the deepest bin observed at approximately 9.8 m below MLLW, and the top-most good bin is bin 9 (1.8 m below MLLW).

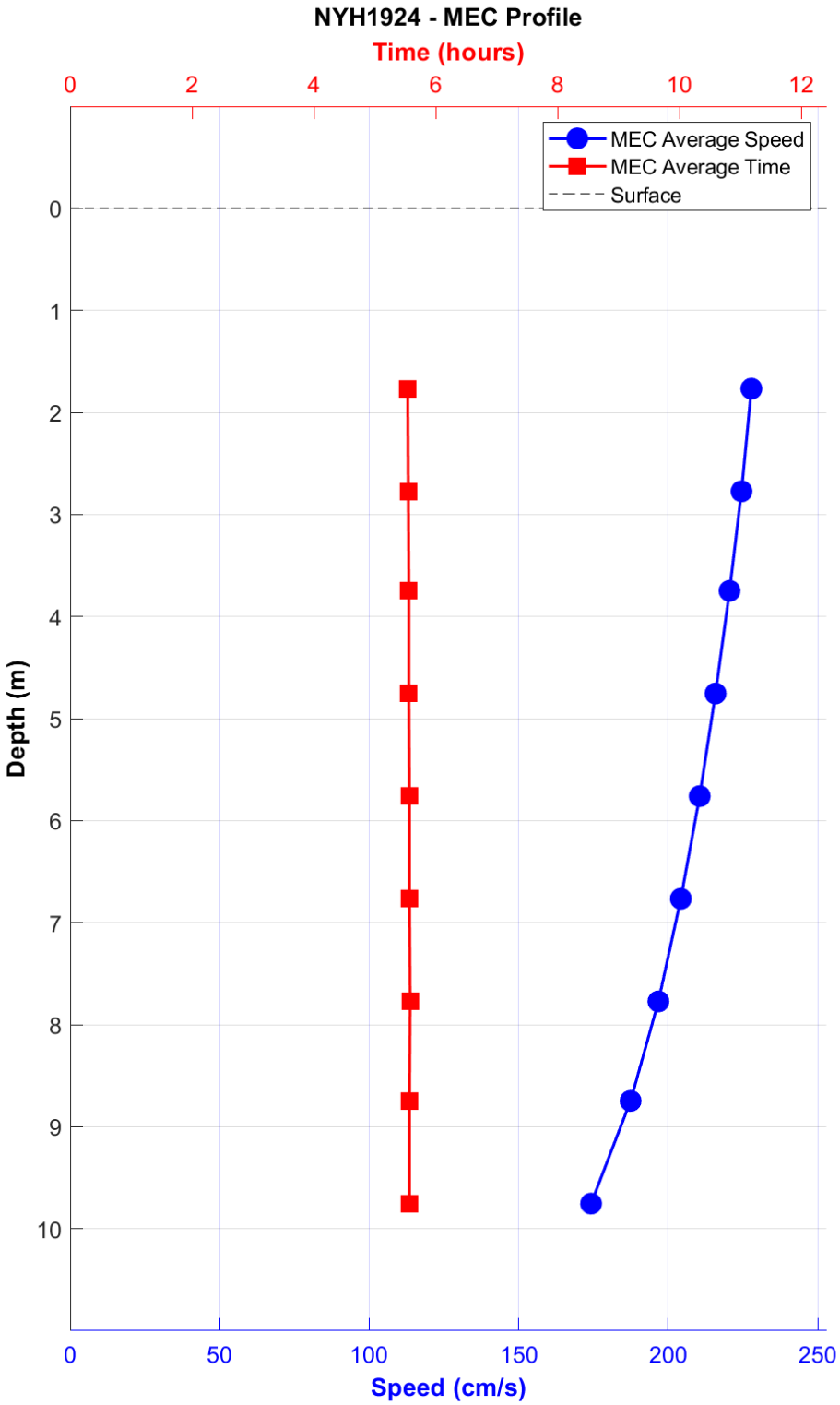

Figure 5-16. NYH1924 MEC timing (GI – red squares) and speed (blue circles) by depth bin. Bin 1 is the deepest bin observed at approximately 9.8 m below MLLW, and the top-most good bin is bin 9 (1.8 m below MLLW).

5.4 NYH1927 – Hudson River Entrance

This station was deployed for 69 days (August 12, 2019-October 20, 2019) in 17.6 m (57.7 ft) of water. A TRDI Workhorse 600 kHz ADCP mounted in an ES-2 collected 25 1.0 m bins of data, 14 of which met quality control criteria for full analysis. Bins 2, 8, and 13 are available on TCP, representing approximate depths of 13.0 m, 7.0 m, and 2.0 m (28.0 ft, 14.9 ft, and 5.1 ft) below MLLW, respectively.

This station was deployed near the southern end of the Hudson River where it merges with the greater Hudson Raritan Estuary at Upper Bay. Observed currents are rectilinear, with major axis variance of 96.8-99.0% (Figure 5-17). This station is tidal, which is indicated by the low residuals, as seen in Figure 5-18. LSQHA resolved 25 constituents and accounted for 91-96% of the total energy in the velocity data. Mean flow stratification is observed at this station, where a mean southerly (ebb) flow is seen at the surface, which changes to a mean northerly (flood) flow at depth (Figure 5-19). Mean MFC and MEC currents have a range of 82-113 cm/s (1.6-2.2 kn), and their timing does not vary much with depth (Figures 5-20 and 5-21). The Defant ratio in the upper good bin was 0.291, indicating that this station is mixed, mainly semidiurnal.

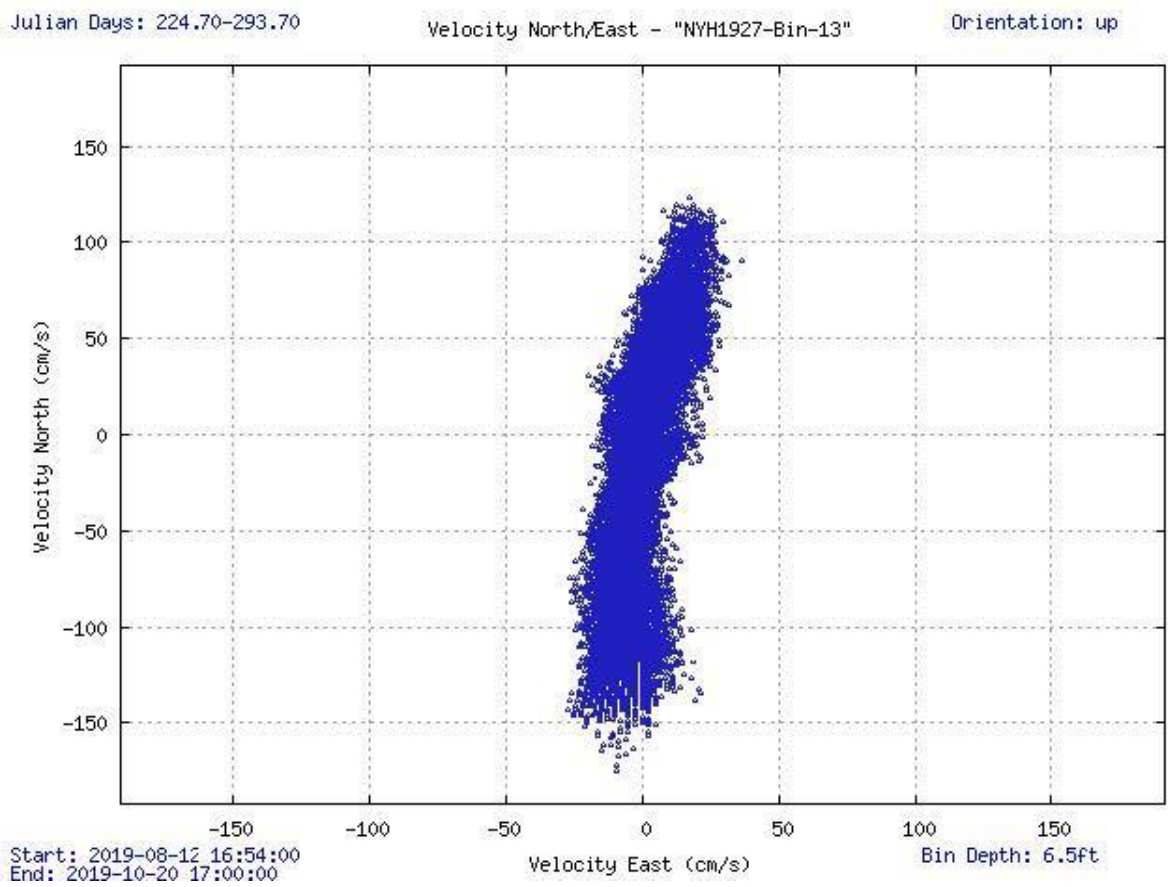

Figure 5-17. Scatter plot of north-versus-east velocity for station NYH1927 at the near-surface bin, bin 13 at 2.0 m below MLLW.

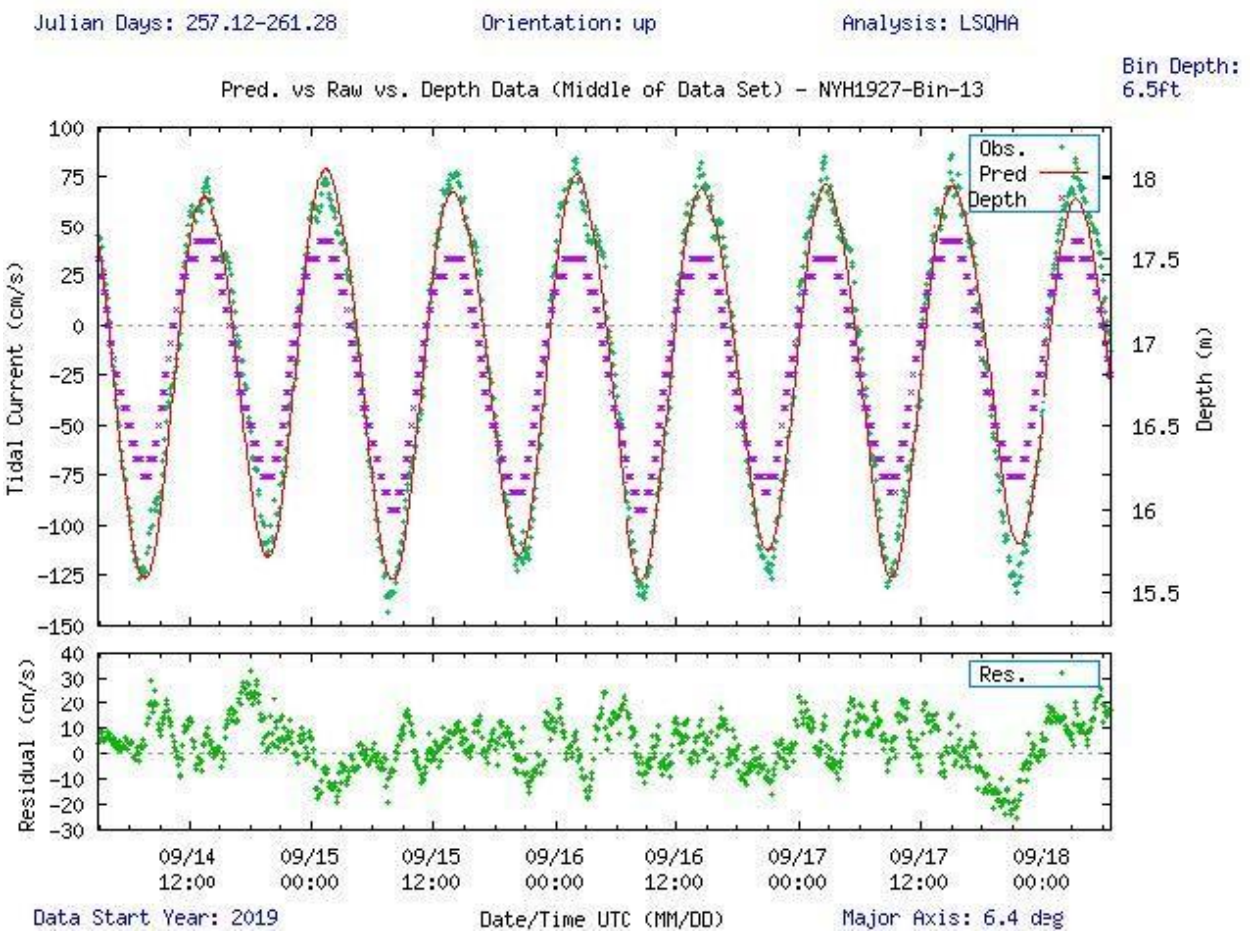

Figure 5-18. Comparison of observed major axis velocity data (green points) to predicted tidal velocity along the major axis for station NYH1927. Pressure sensor data is included to show the phase alignment of the tide and current for this location. The lower figure shows the non-tidal residual, the difference between the predicted and observed velocity from the upper panel.

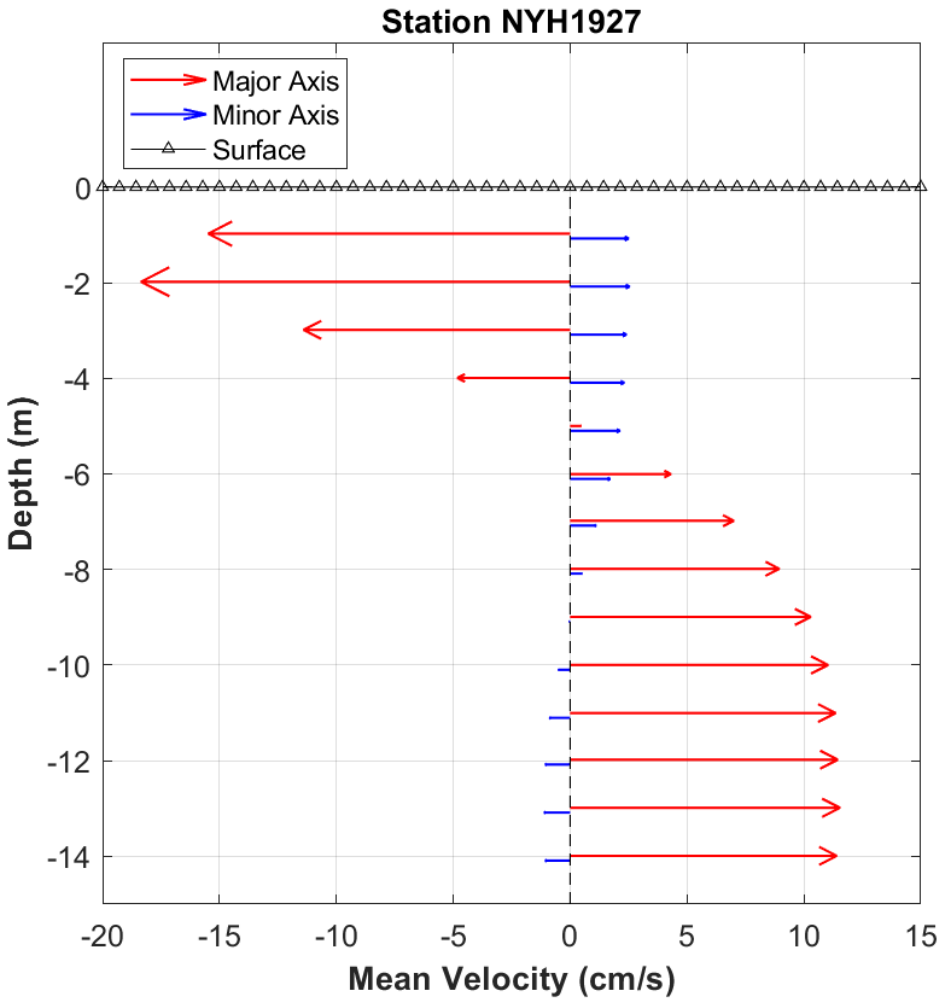

Figure 5-19. NYH1927 mean velocity profile by depth. Only depths that passed quality control criteria are shown. This station was configured to collect 1.0 m bins.

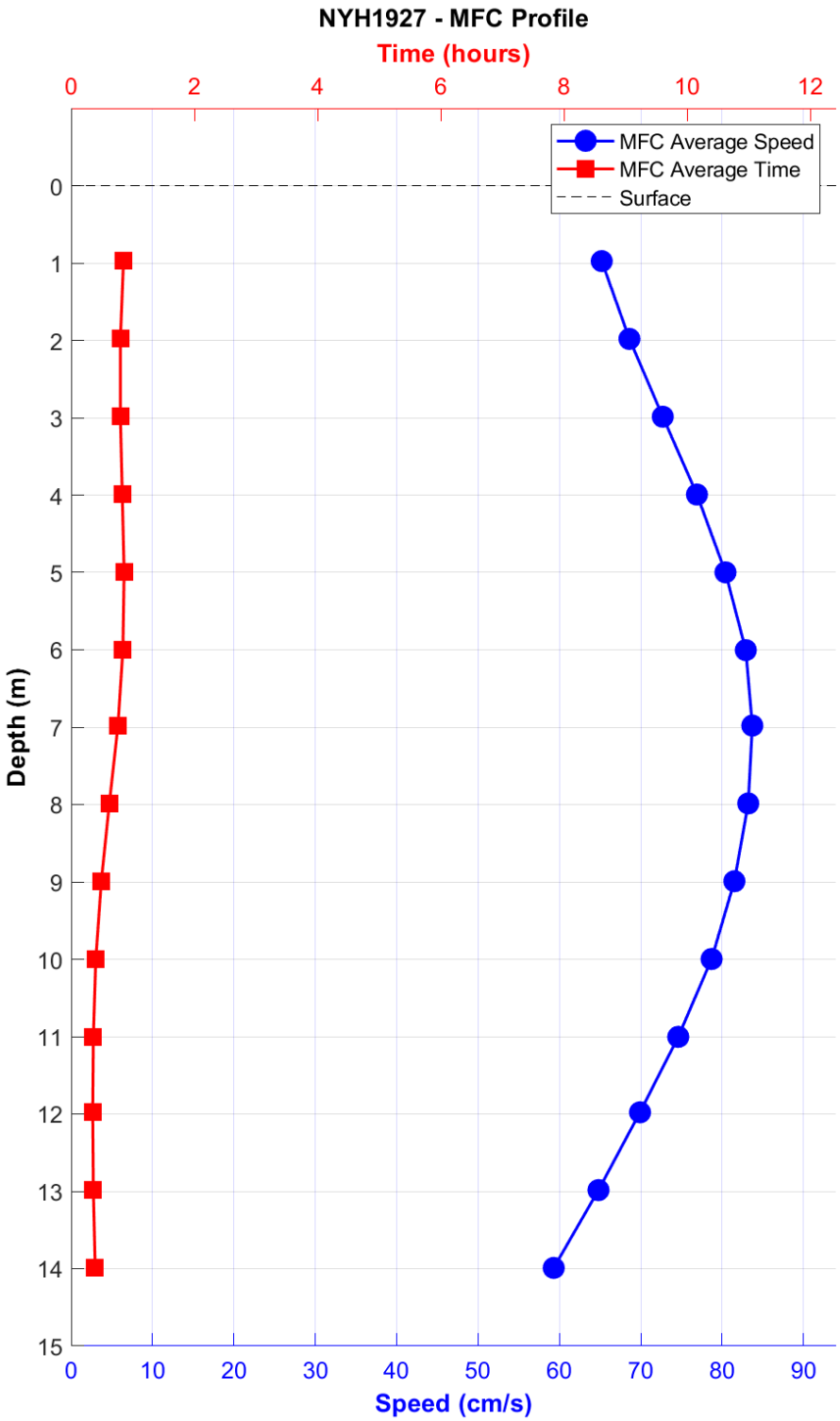

Figure 5-20. NYH1927 MFC timing (GI - in red squares) and speed (blue circles) by depth bin. Bin 1 is the deepest bin observed at approximately 13.0 m below MLLW, and the top-most good bin is bin 14 (1.0 m below MLLW).

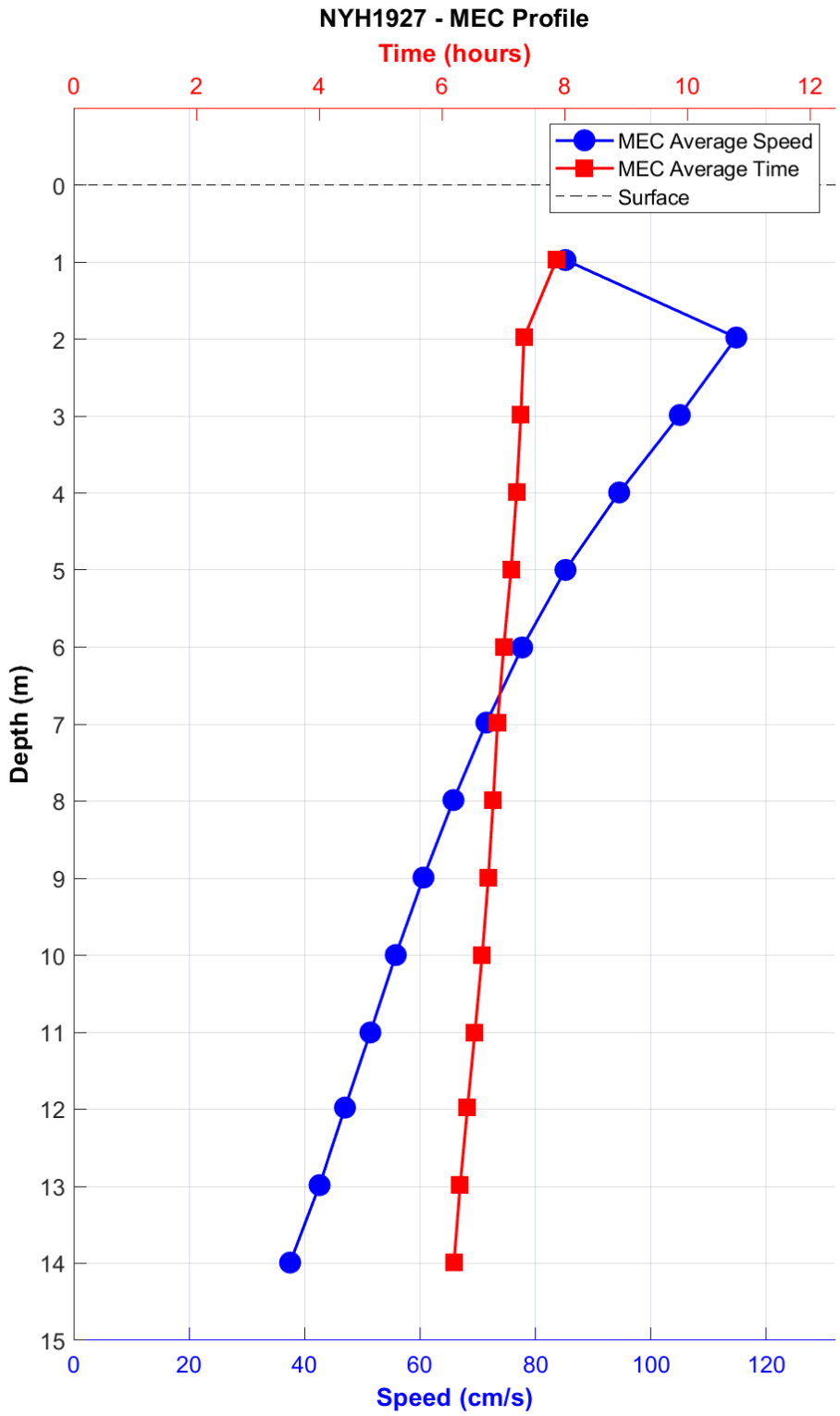

Figure 5-21. NYH1927 MEC timing (GI – red squares) and speed (blue circles) by depth bin. Bin 1 is the deepest bin observed at approximately 13.0 m below MLLW, and the top-most good bin is bin 14 (1.0 m below MLLW).

5.5 NYH1930 – Spuyten Duyvil

This station was deployed for 70 days (August 12, 2019-October 21, 2019) in 19.5 m (64.0 ft) of water. A TRDI Workhorse 600 kHz ADCP mounted in an ES-2 collected 25 1.0 m bins of data, 15 of which met quality control criteria for full analysis. Bins 3, 8, and 14 are available on TCP, representing approximate depths of 13.7 m, 8.7 m, and 2.7 m (45.1 ft, 28.7 ft, & 9.0 ft) below MLLW, respectively.

The station Spuyten Duyvil was deployed on the eastern side of the Hudson River, at the entrance to Spuyten Duyvil Creek. The creek flows into the Harlem River and connects to the East River near Hell Gate. Observed currents are mostly rectilinear with some westward deviation on the ebb influenced by the westward flow out of the Spuyten Duyvil Creek (Figure 5-22). Major axis variance had a range of 96.2-98.8% percent. This station is very tidal, as seen in Figure 5-23. LSQHA resolved 25 constituents and accounted for 93-95% of the total energy in the velocity data. A small mean southwesterly (ebb) flow was observed at the surface and becoming negligible toward the seafloor (Figure 5-24). MFC and MEC currents had a range of 93-106 cm/s (1.8–2.1 kn) (Figures 5-25 and 5-26). Both ebb and flood timings lag slightly at the surface. The Defant ratio in the upper good bin was 0.259, indicating that this station is mixed, mainly semidiurnal near the surface.

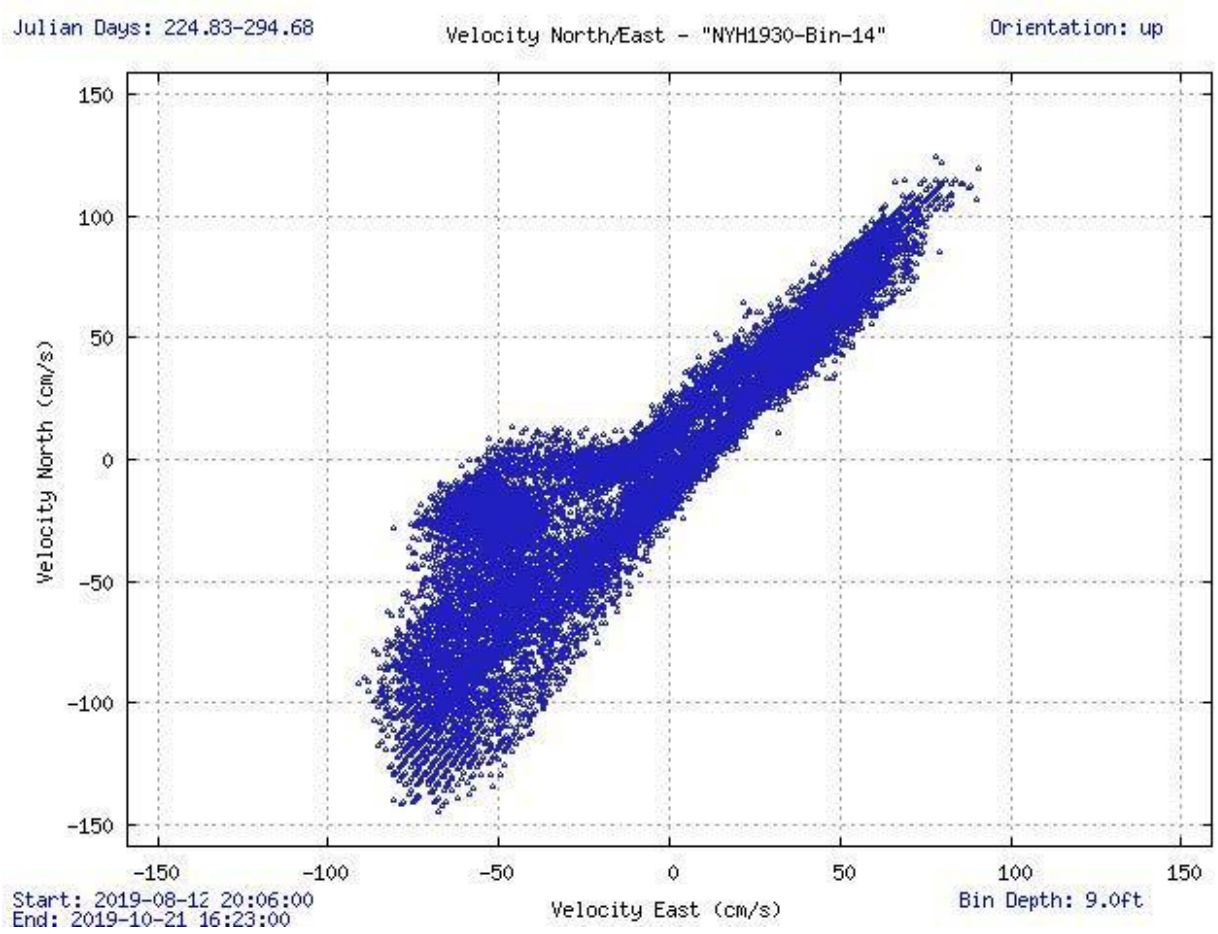

Figure 5-22 Scatter plot of north-versus-east velocity for station NYH1930 at the near-surface bin, bin 14 at 2.7 m below MLLW. The westward lobe on the ebb is likely the influence ofSpuyten Duyvil.

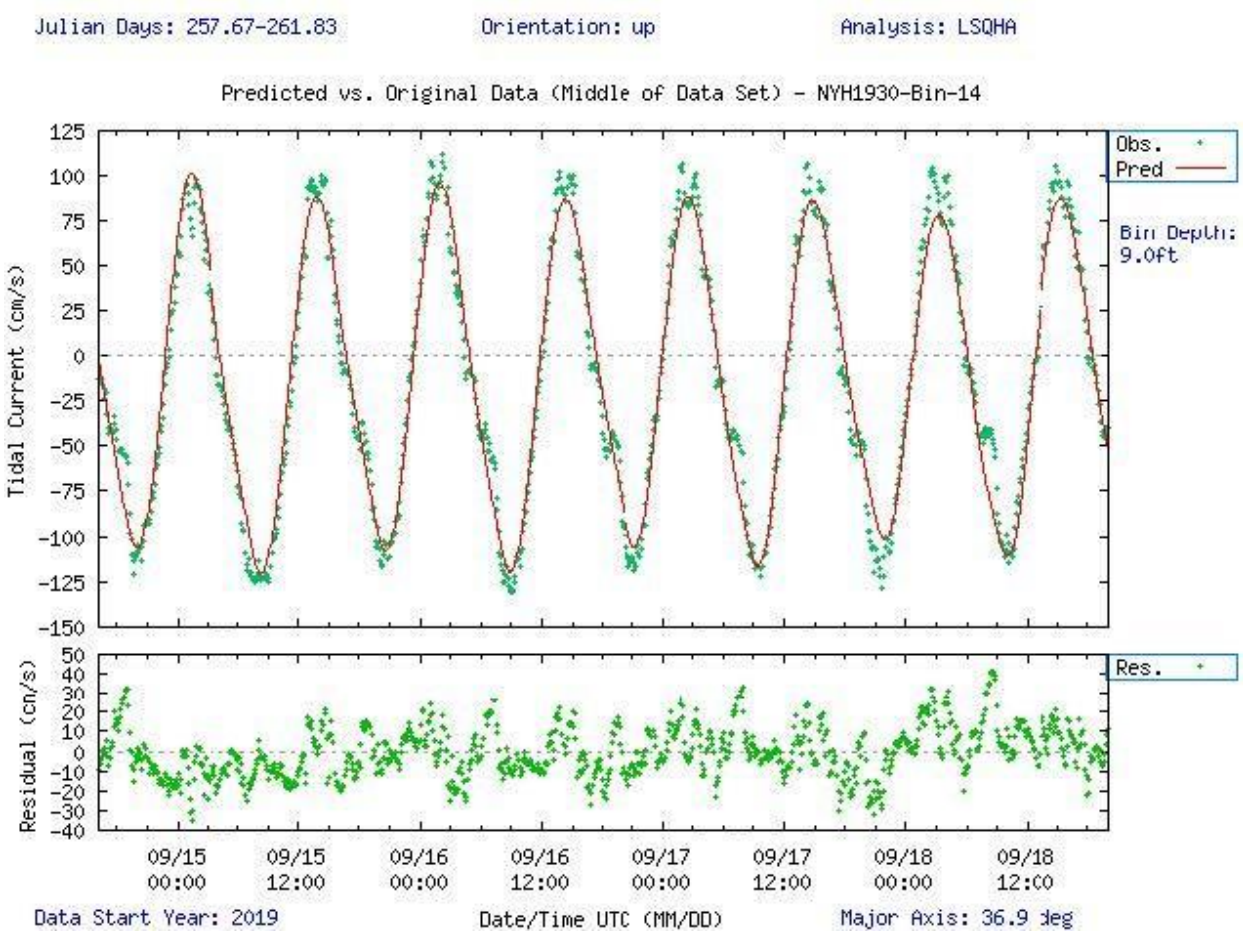

Figure 5-23. Comparison of observed major axis velocity data (green points) to predicted tidal velocity along the major axis for station NYH1930. The lower figure shows the non-tidal residual, the difference between the predicted and observed velocity from the upper panel.

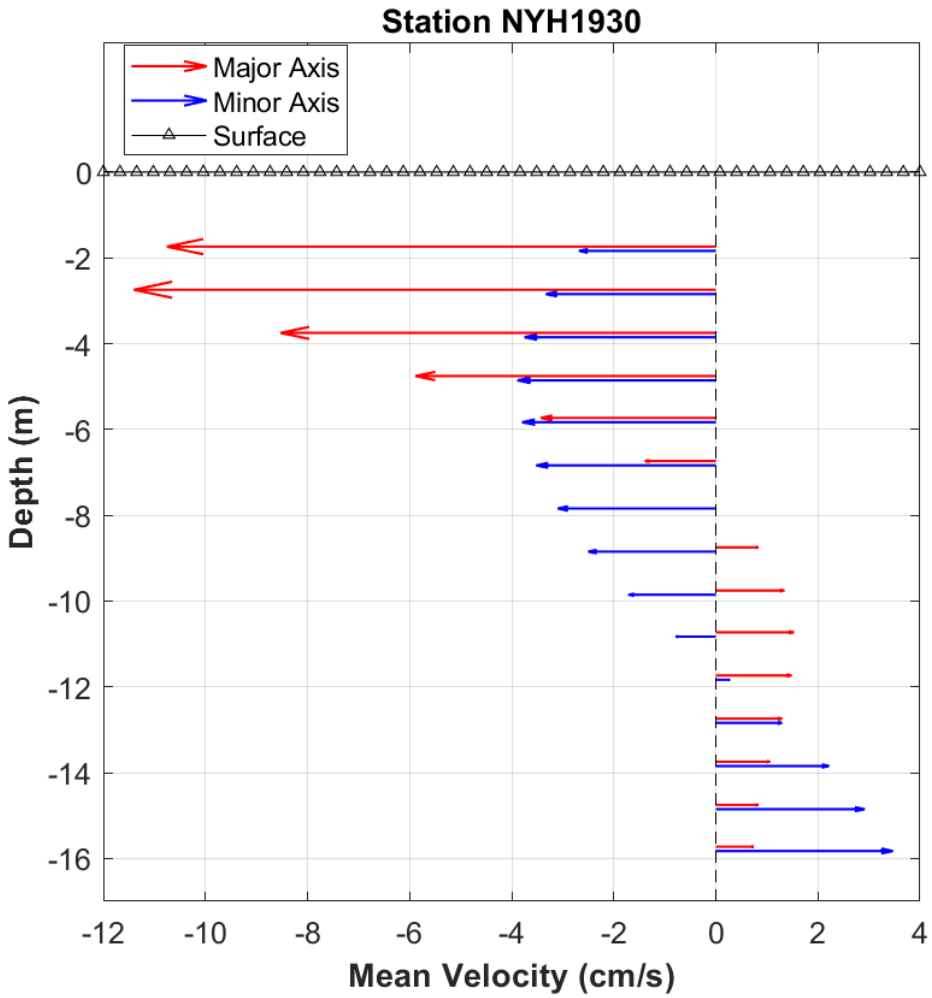

Figure 5-24. NYH1930 mean velocity profile by depth. Only depths that passed quality control criteria are shown. This station was configured to collect 1.0 m bins.

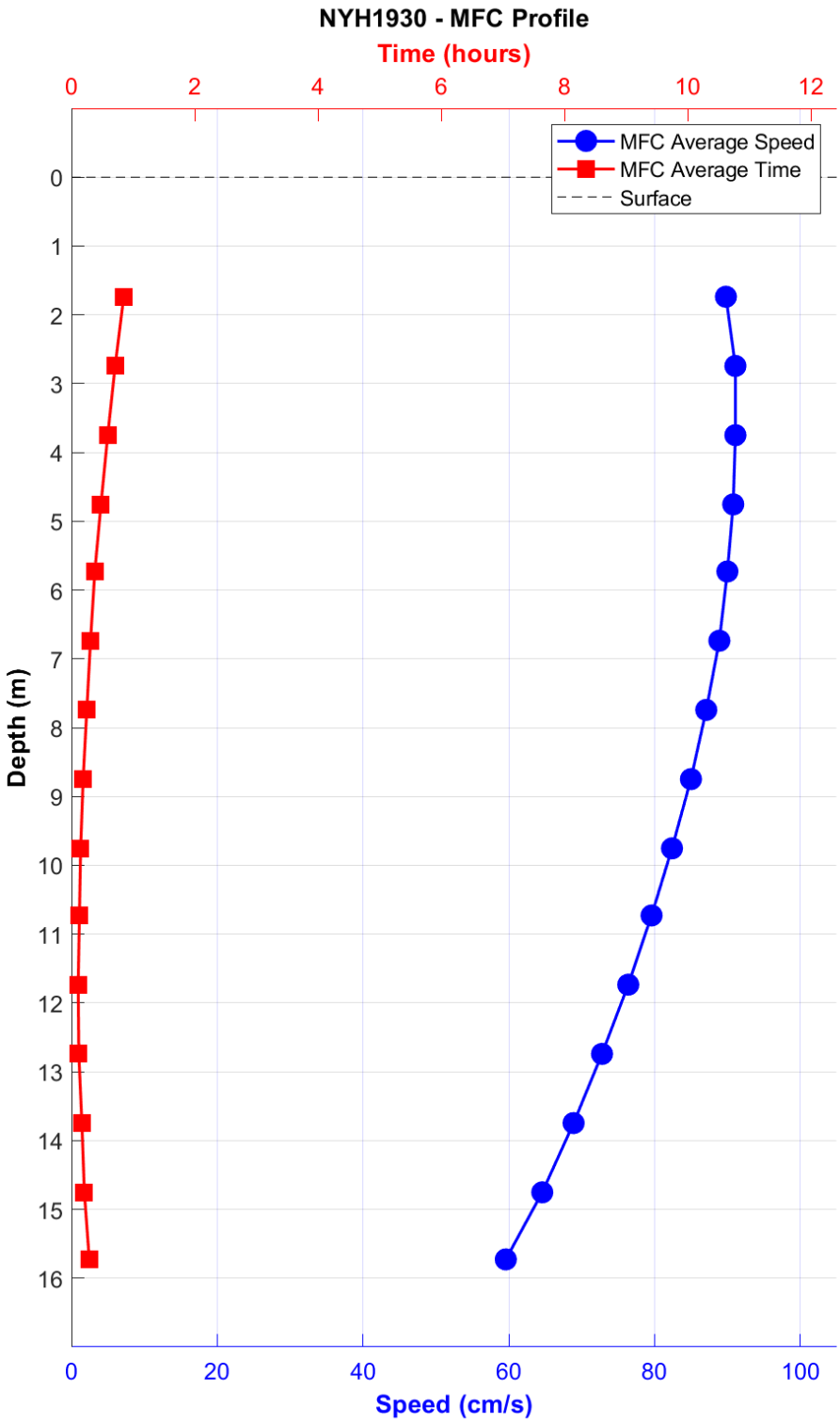

Figure 5-25. NYH1930 MFC timing (GI - in red squares) and speed (blue circles) by depth bin. Bin 1 is the deepest bin observed at approximately 15.7 m below MLLW, and the top-most good bin is bin 15 (1.7 m below MLLW).

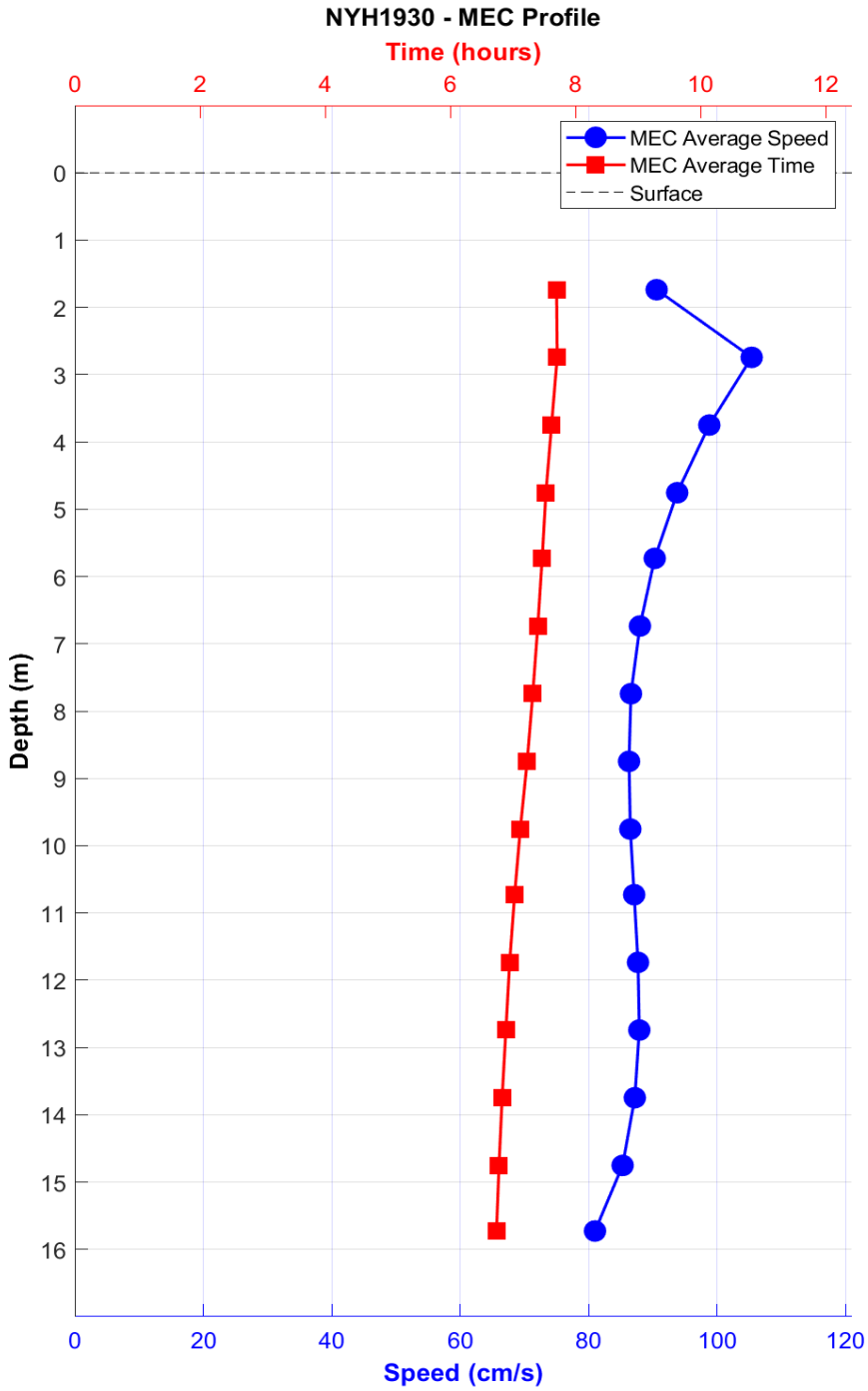

Figure 5-26. NYH1930 MEC timing (GI – red squares) and speed (blue circles) by depth bin. Bin 1 is the deepest bin observed at approximately 15.7 m below MLLW, and the top-most good bin is bin 15 (1.7 m below MLLW).

5.6 NYH1933 – Highlands, Shrewsbury River

This station was deployed for 43 days (June 26, 2019-August 08, 2019) at a depth of 3.2 m (10.3 ft) below MLLW (statistical) in 6.2 m (20.3) of total water depth. A 600 kHz Nortek Aquadopp ADCP configured for horizontal measurements was mounted on bridge cribbing using a clamp and pole as described in section 3.3. Ten 4.0-m bins were collected. Bin 5 is available on TCP representing 20.5 m (67.3 ft) from the sensor, in the center of the channel.

The Navesink River flows into the Shrewsbury River and empties into Sandy Hook Bay. This station is at a constriction where a bridge connects the northern end of New Jersey's barrier island system near Sandy Hook with the mainland. Observed currents are extremely rectilinear, with major axis variance exceeding 99% throughout all good bins (Figure 5-27). LSQHA resolved 25 constituents and accounted for 97-98% of the total energy in the velocity data. This station is very tidal, as seen in Figure 5-28. A small mean southerly (ebb) flow at mid-channel was observed, with a small northerly (flood) flow along the side of the channel near the sensor (Figure 5-29). MFC and MEC currents range between 118 cm/s and 113 cm/s (2.3 kn and 2.2 kn), and their timing does not vary much with distance (Figures 5-30 and 5-31). The Defant ratio in the upper good bin was 0.126, indicating that this station is semidiurnal.

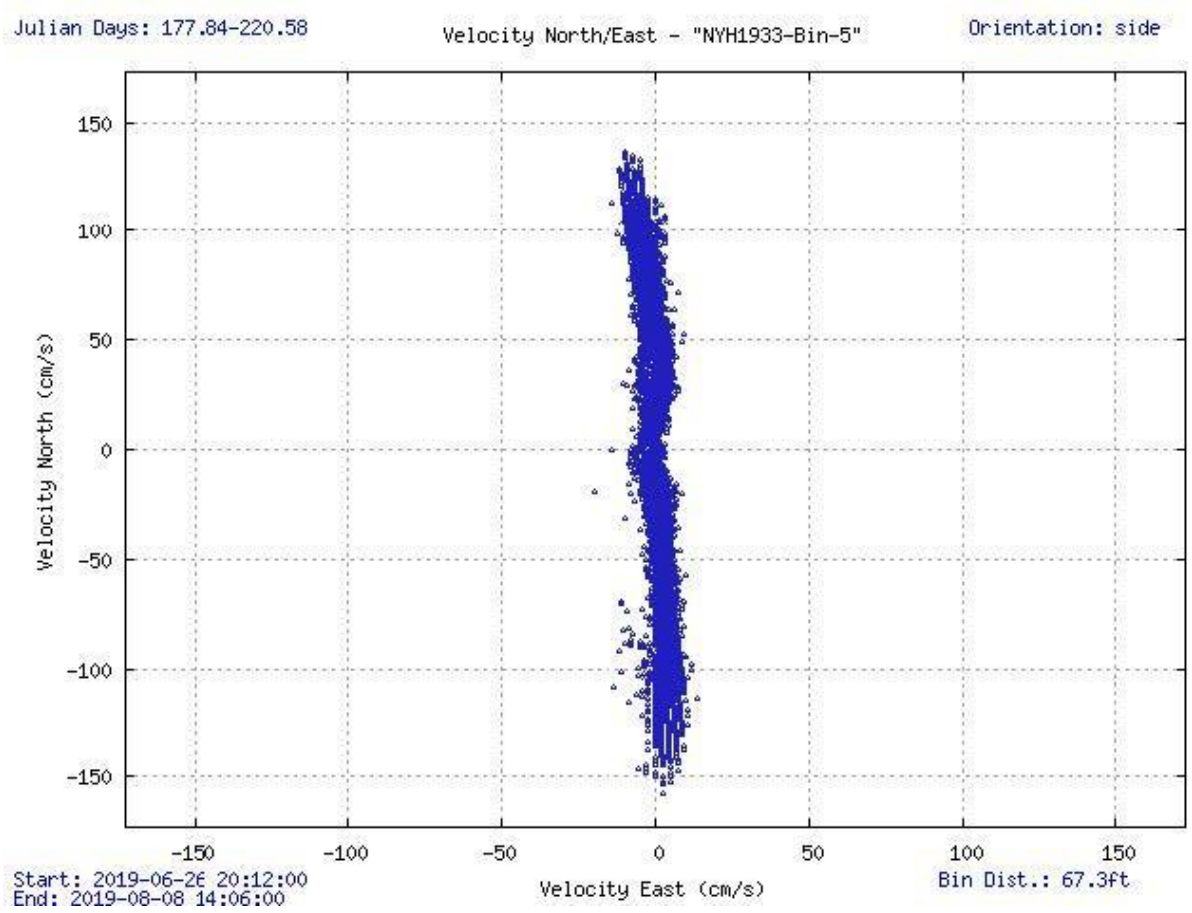

Figure 5-27. Scatter plot of north-versus-east velocity for station NYH1933 at the prediction bin, bin 5 at 20.5m from the instrument.

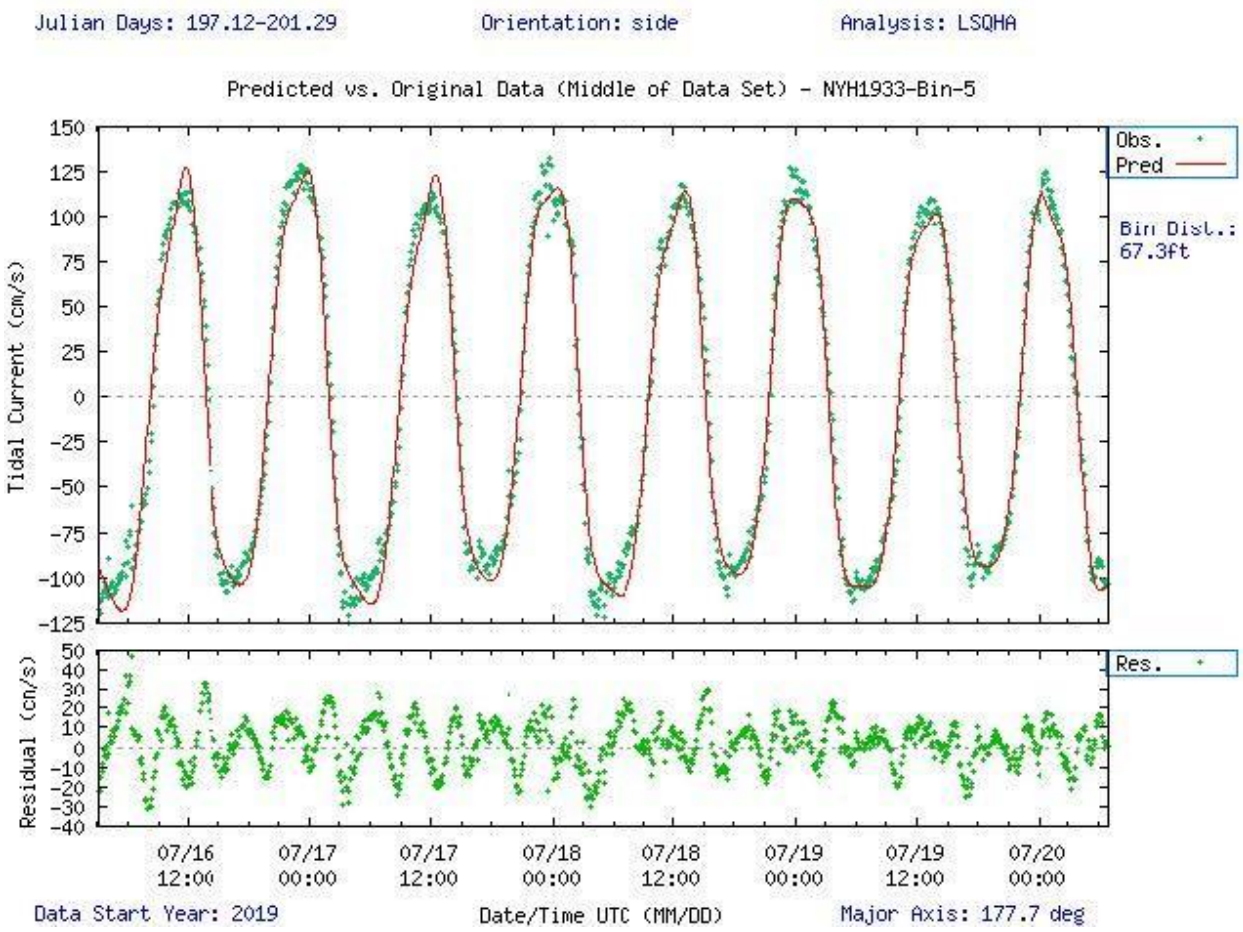

Figure 5-28. Comparison of observed major axis velocity data (green points) to predicted tidal velocity along the major axis for station NYH1933. The lower figure shows the non-tidal residual, the difference between the predicted and observed velocity from the upper panel.

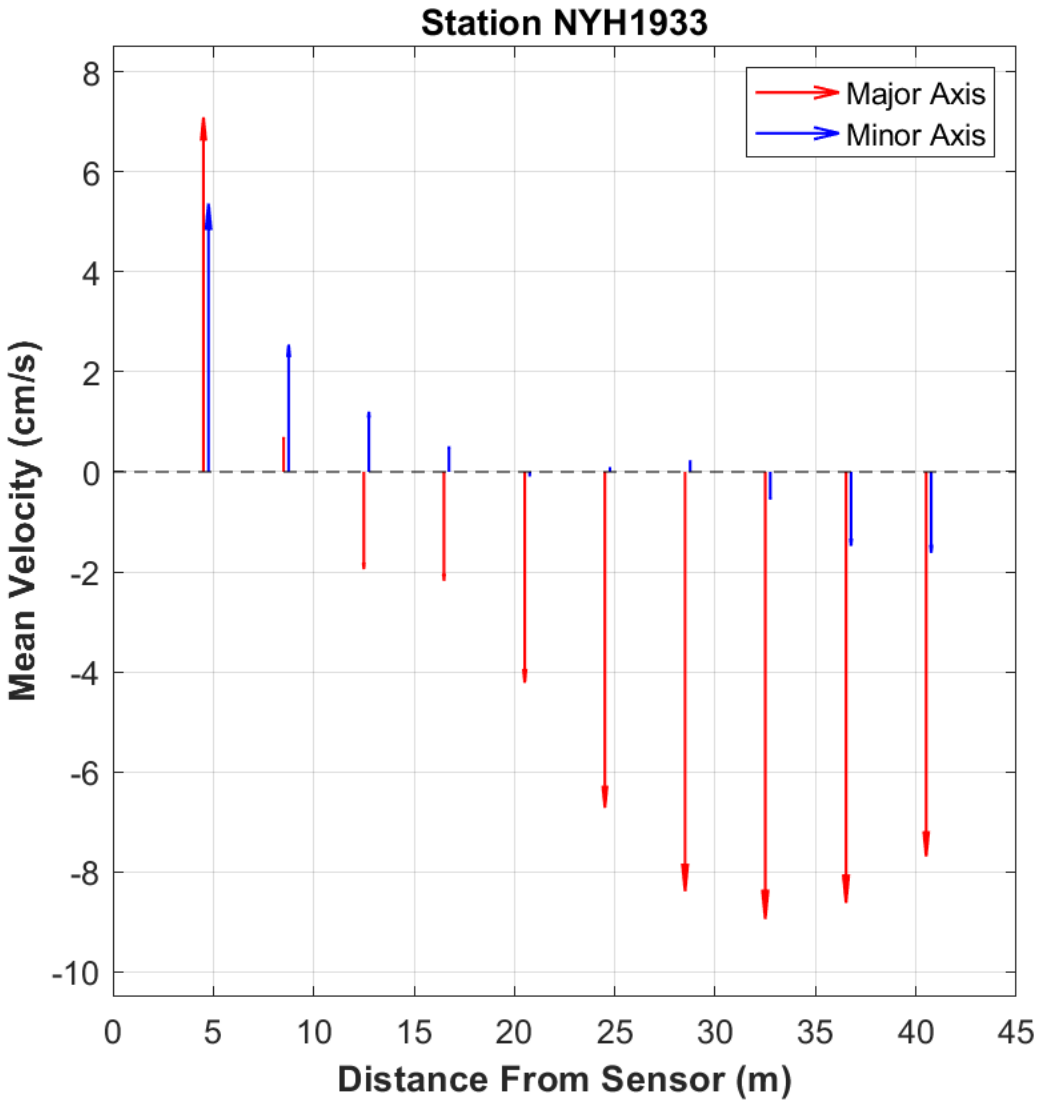

Figure 5-29. NYH1933 mean velocity profile by distance. Only bins that passed quality control criteria are shown.

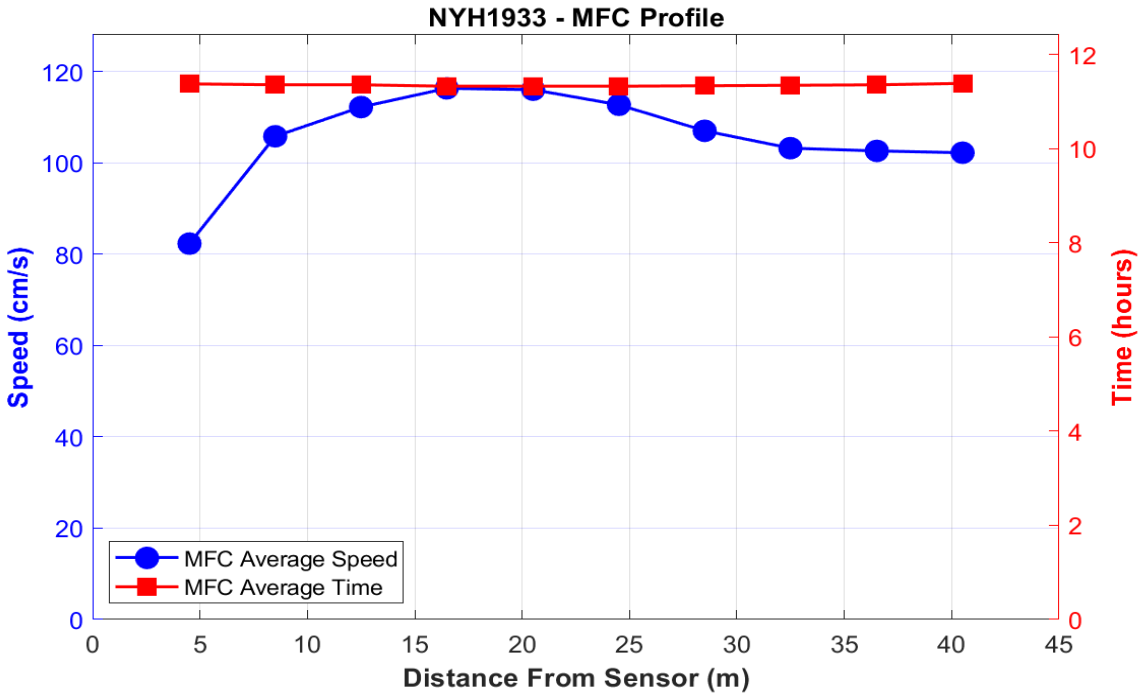

Figure 5-30. NYH1933 MFC timing (GI - in red squares) and speed (blue circles) by distance bin.

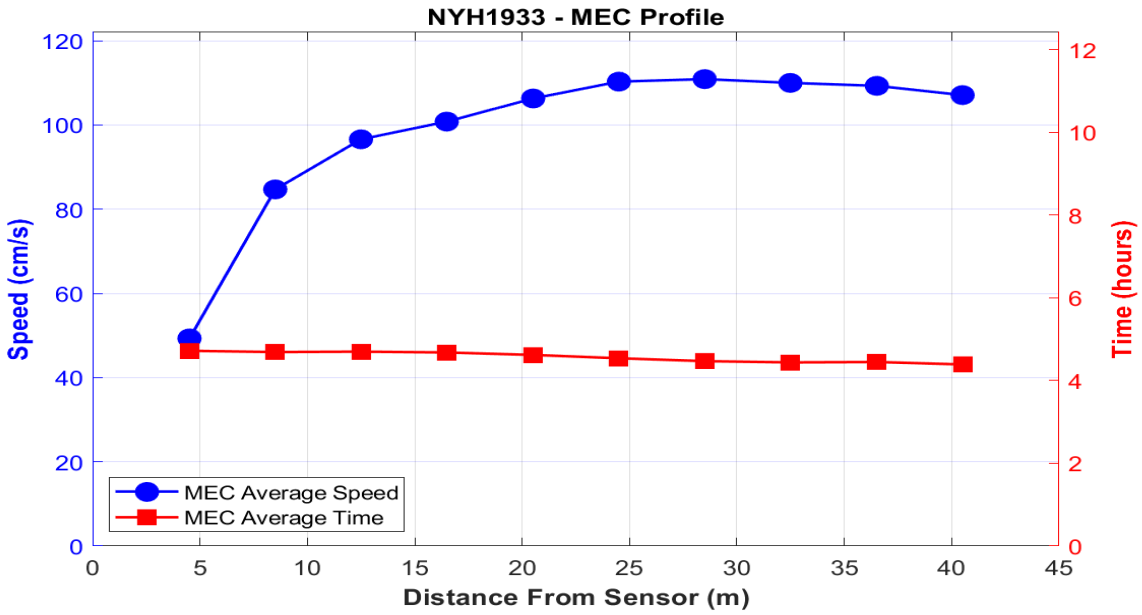

Figure 5-31. NYH1933 MEC timing (GI – red squares) and speed (blue circles) by distance bin.

5.7 NYH1912/n06010 – Port Richmond (Kill Van Kull LB 14)

The Kill Van Kull connects Upper New York Bay with Newark Bay between Bayonne, NJ, and Staten Island, NY. NYH1912 (Port Richmond) was occupied for 40 days from June 29, 2019-August 08, 2019 on USCG ATON buoy 14, approximately 0.1 nm east of where the Bayonne Bridge crosses Kill Van Kull, in 16 meters of water using a 1000 kHz Z-cell Nortek AqD. Data from NYH1912 were analyzed using LSQHA with 25 constituents and resolved 86-93% of the observed energy. PORTS® station n06010 (Kill Van Kull LB14) was subsequently installed on

buoy 14 using a 1000 kHz Nortek AqD on May 21, 2020. A 6-month (June 22, 2020-Nov 24, 2020) analysis of station n06010 was performed, resolving 29 constituents. This analysis accounted for 93% of the observed energy in all good bins and is used for the comparison in this section. Figures 5-32 and 5-33 demonstrate that the timing of both MFC and MEC were similar throughout the water column. Station NYH1912 had slightly stronger mean ebb currents (eastward) near the surface and weaker mean ebb currents at depth than n06010; however, mean flood current speeds (westward) were slightly stronger for n06010 at all depths. As opposed to survey stations, PORTS® stations are regularly maintained for longer durations which allows for longer analysis windows, resolving more constituents for updated predictions. Since the comparisons between the deployments were similar, and the PORTS® station had a longer analysis window, the PORTS® station was used for a new TCP station using bins 1, 4, and 10, representing approximate depths of 2.5 m, 6.5 m, and 12.5 m (11.6 ft, 21.5 ft, and 5.1 ft) below the surface, respectively.

Observed currents for n06010 were rectilinear and consistent throughout the water column, with major axis variances from 98.0-98.5% throughout all good bins (Figure 5-34). This station is very tidal as seen in Figure 5-35. A small mean westerly (flood) flow at mid-channel was observed, increasing slightly with depth (Figure 5-36). The Defant ratio in the upper good bin was 0.107, indicating that this station is semidiurnal.

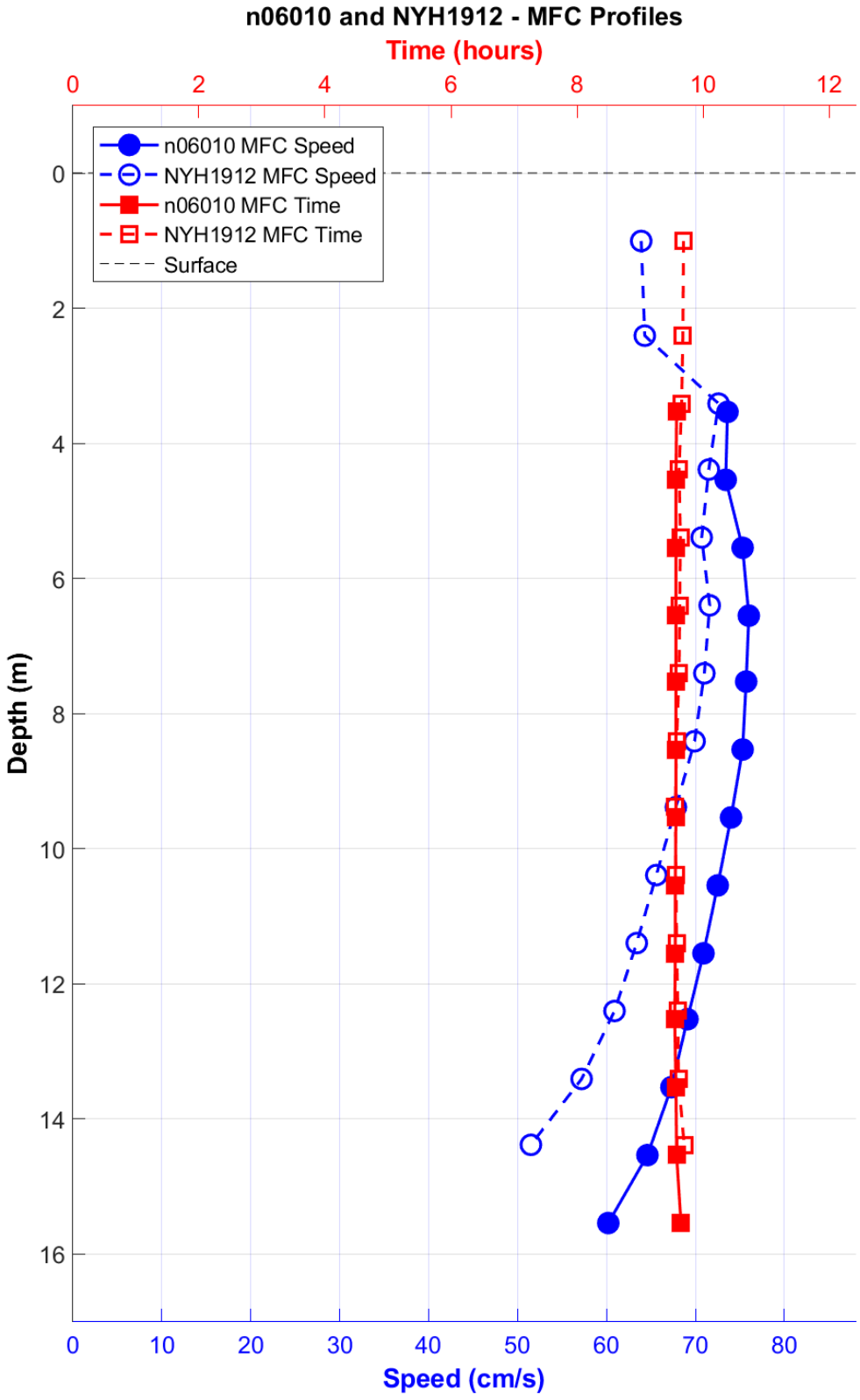

Figure 5-32. MFC comparison between NYH1912 and n06010 showing similar timing (red squares) but higher speeds (blue circles) for n06010.

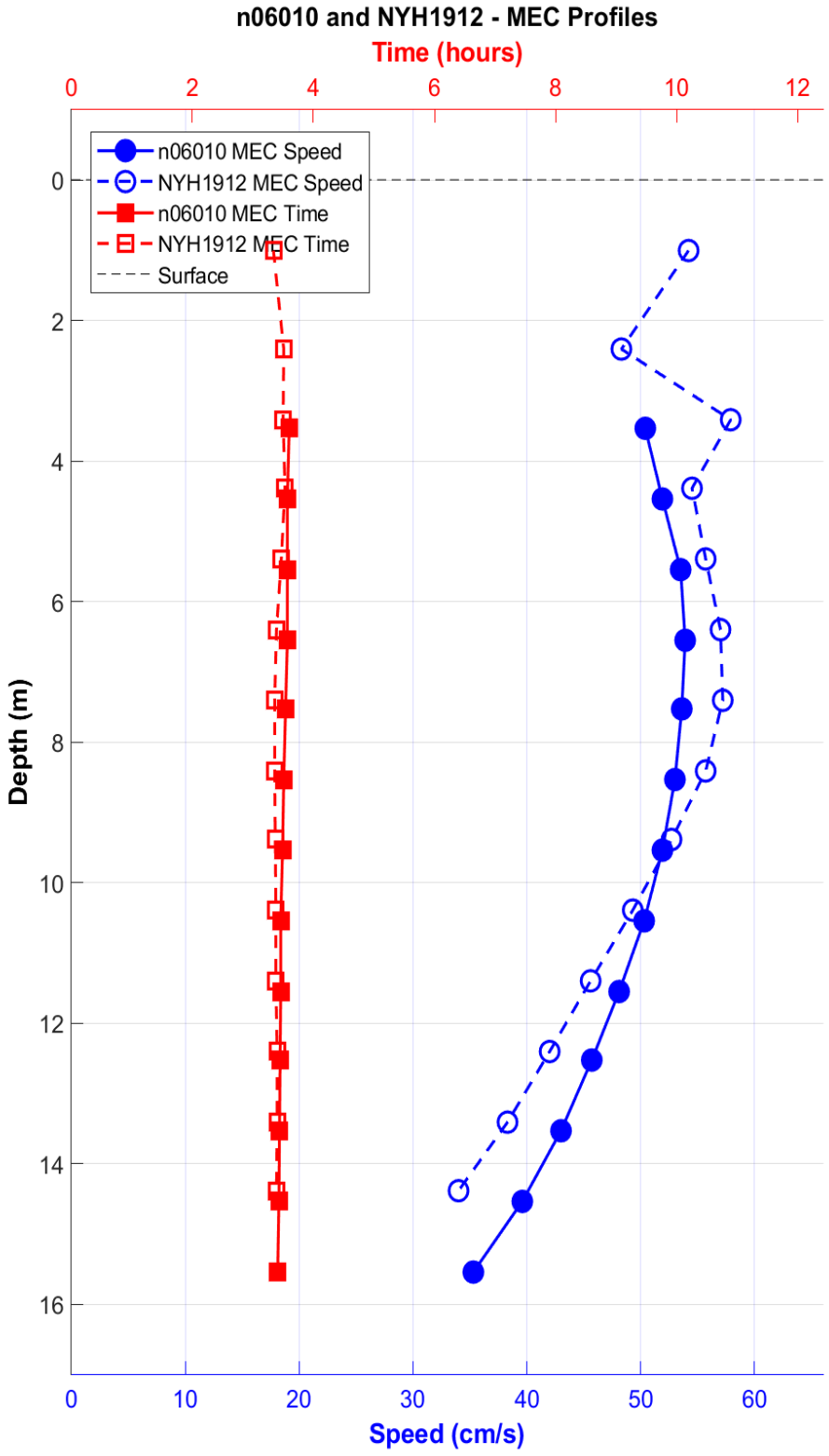

Figure 5-33. MEC comparison between stations NYH1912 and n06010 showing similar timing (red squares) but more speed shear for NYH1912.

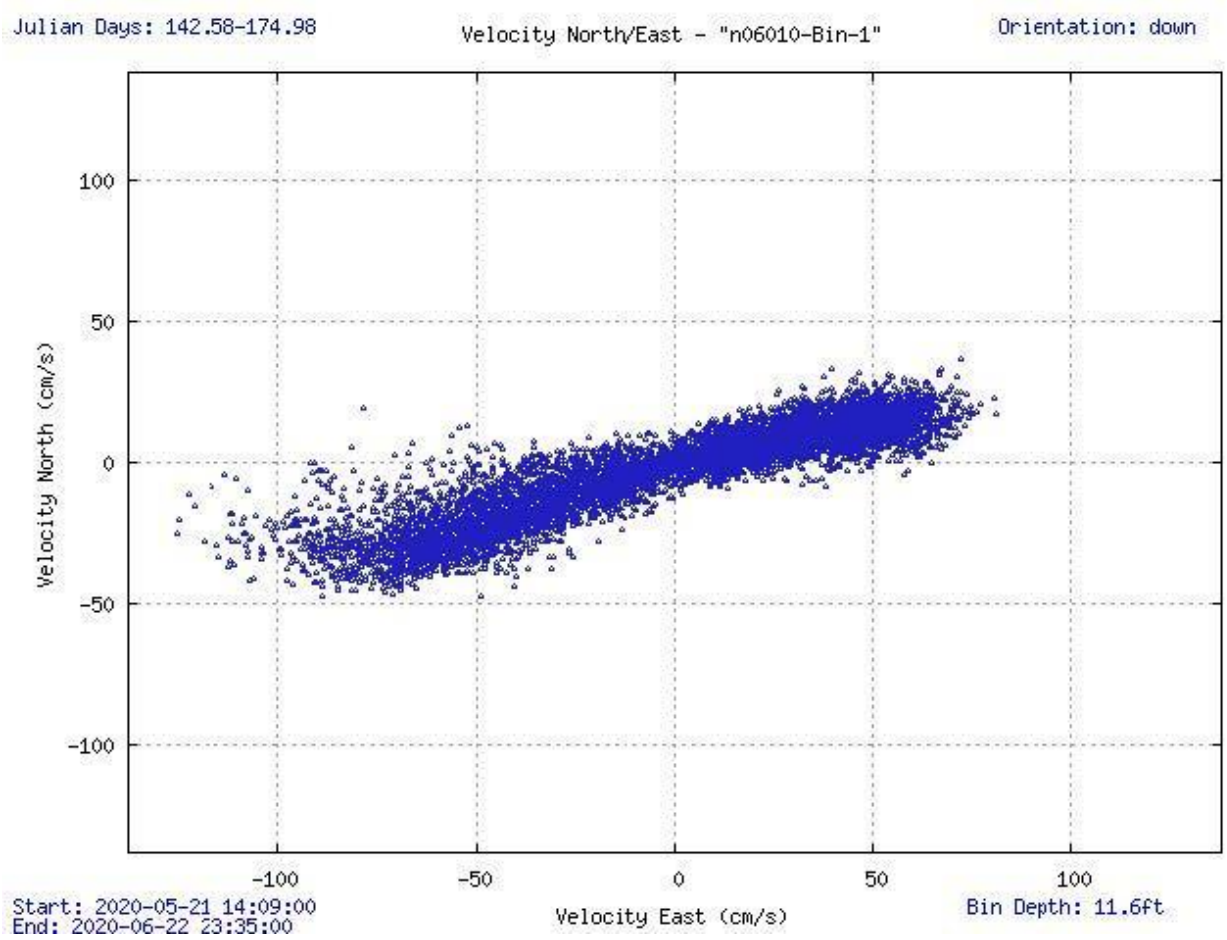

Figure 5-34. Scatter plot of north-versus-east velocity for station n06010 at the prediction bin, bin 1 at 3.5m from the instrument.

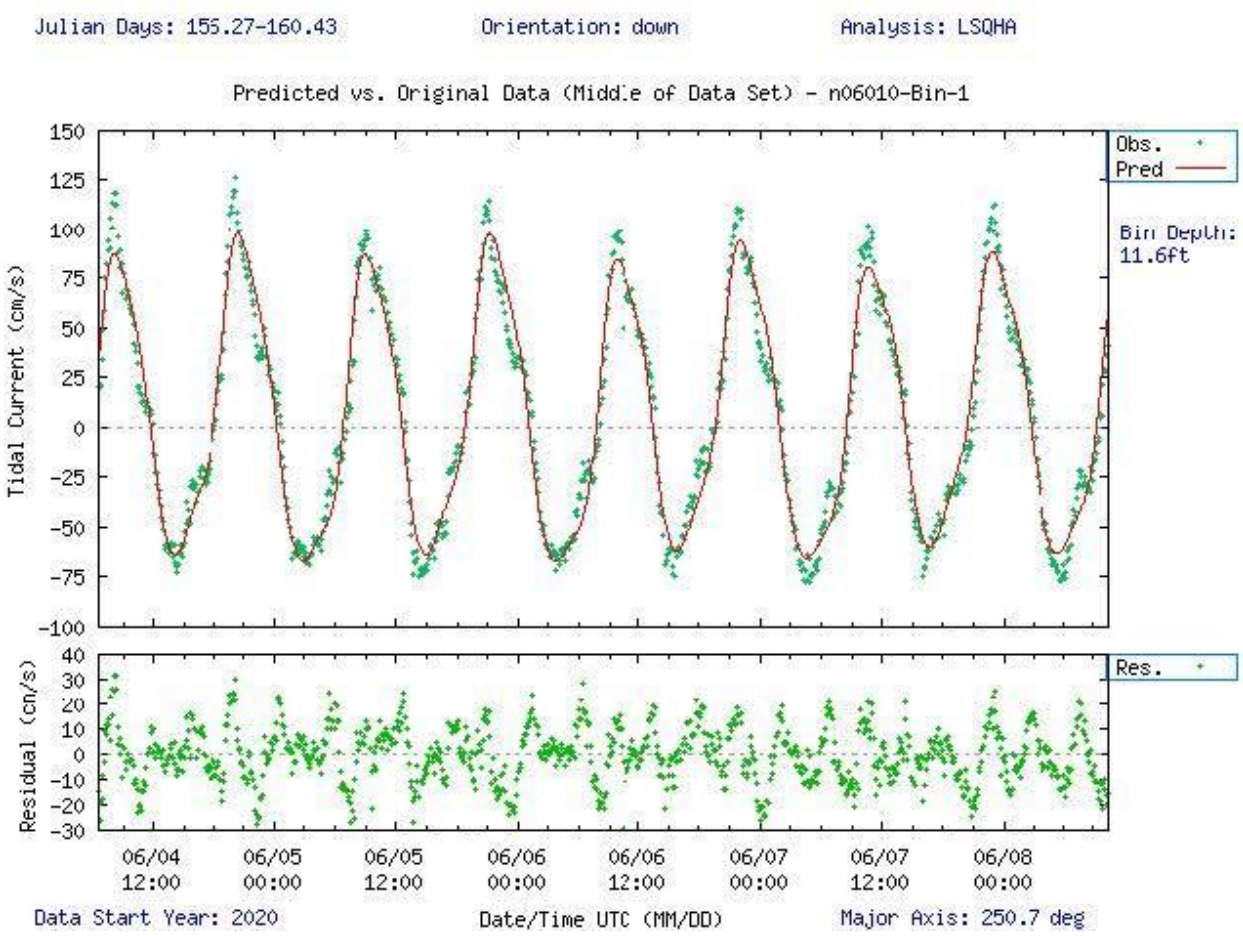

Figure 5-35. Comparison of observed major axis velocity data (green points) to predicted tidal velocity along the major axis for station n06010. The lower figure shows the non-tidal residual, the difference between the predicted and observed velocity from the upper panel.

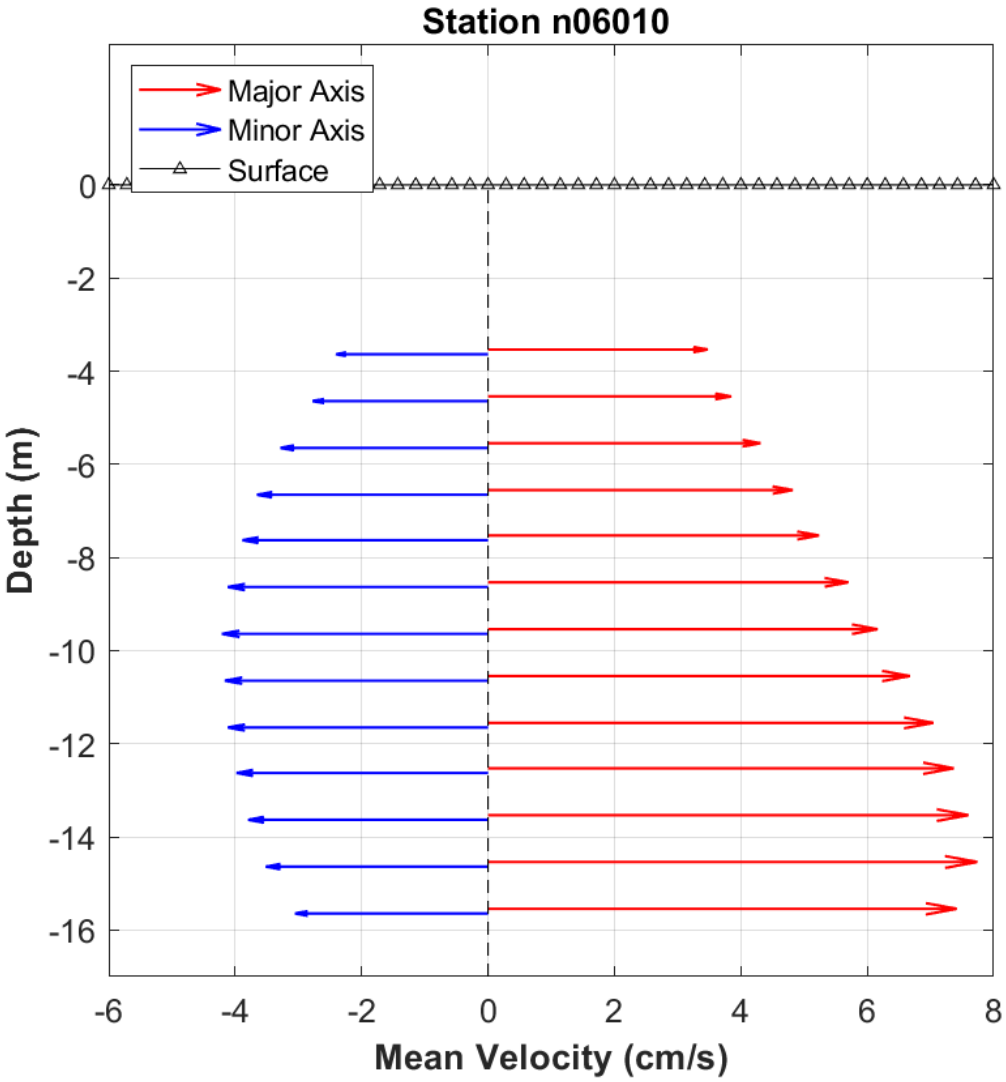

Figure 5-36. Station n06010 mean velocity profile by distance. Only bins that passed quality control criteria are shown.

6. SPATIAL VARIATION

6.1 Harmonic constituents

Harmonic constituents were generated for all stations in this study using the methods described in section 3.6. For most stations, tidal harmonic constituents show that the M_2 tidal constituent (the principal lunar semidiurnal constituent) is the dominant constituent. This means that tidal characteristics for most stations in the New York Harbor region are predominately semidiurnal. Only stations in the Hudson River and at The Battery showed mixed semidiurnal characteristics. All stations are rectilinear; they exhibit a back-and-forth tidal current motion between flood and ebb, and exhibit no or very limited rotary characteristics. For the 30 stations analyzed (including the two replaced by PORTS® stations), Figure 6-1 shows the Defant ratio, which is the ratio of the principal diurnal constituents (O_1, K_1) to the principal semidiurnal component (M_2, S_2) of the tides for the major axis.

The spatial distributions of select tidal ellipses of the principal semidiurnal and diurnal constituents are shown in Figures 6-2 to 6-5. The figures clearly show that M_2 is the dominant constituent and that bathymetry (particularly the locations of channels) is the driving force behind the relative strength and orientation of the M_2 and other constituents, as well as the degree of rectilinearity of the ellipses. For example, station NYH1924 (Hell Gate)—a narrow portion of the East River hydraulic strait discussed in section 2.1.2—is extremely rectilinear, M_2-dominated, and has the fastest tidal velocities measured in the survey.

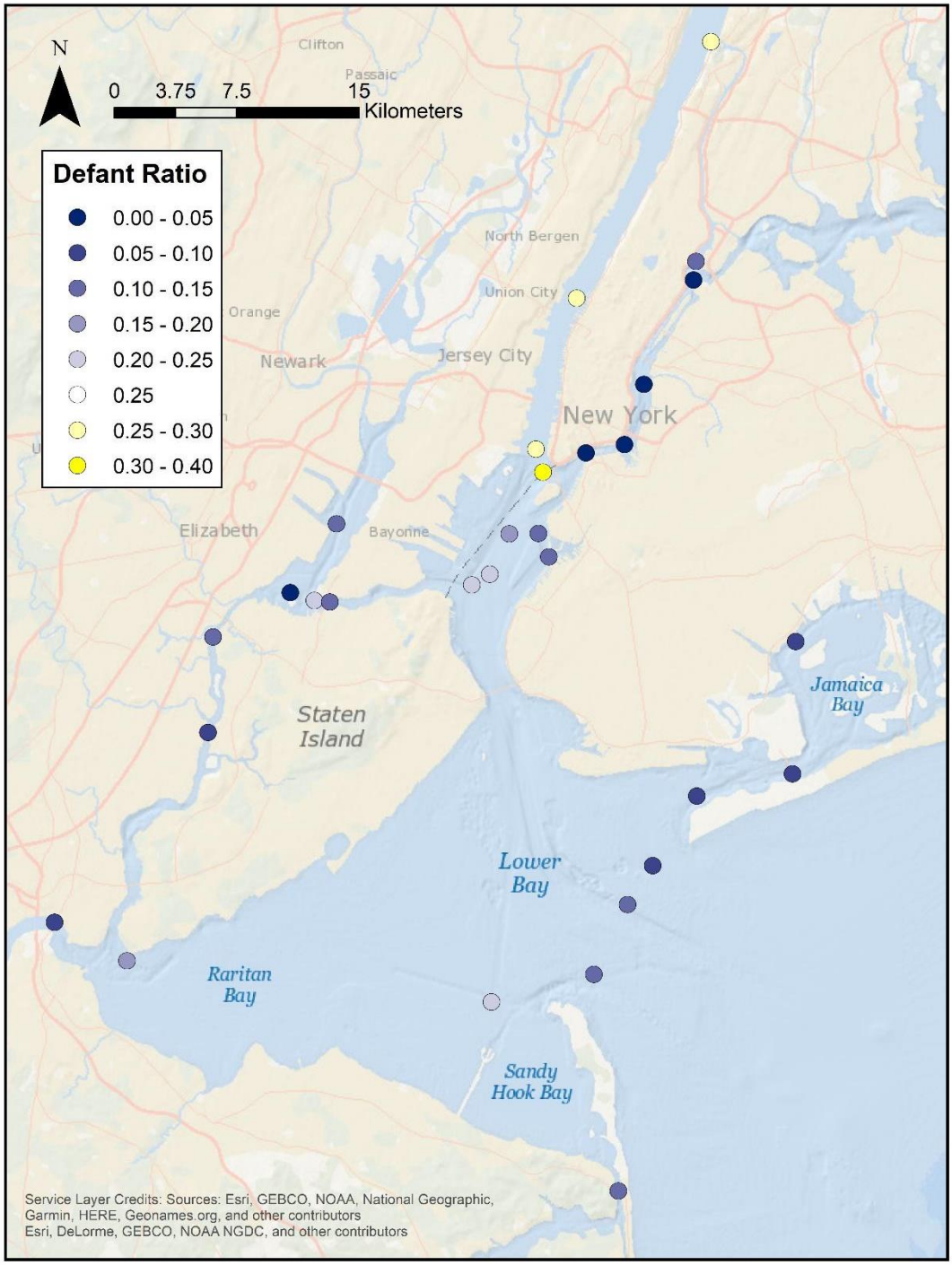

Figure 6-1. Defant ratios for upper prediction bins at survey stations. Semidiurnal tides (Defant ratio <0.25, depicted in lighter shades) are observed at most stations, excluding the Hudson River. Stations with mixed semidiurnal (0.25 to 1.5) are located in the Hudson River and at The Battery. No stations show either mixed diurnal tides (1.5-3.0) or diurnal tides (Defant ratio >3.0).

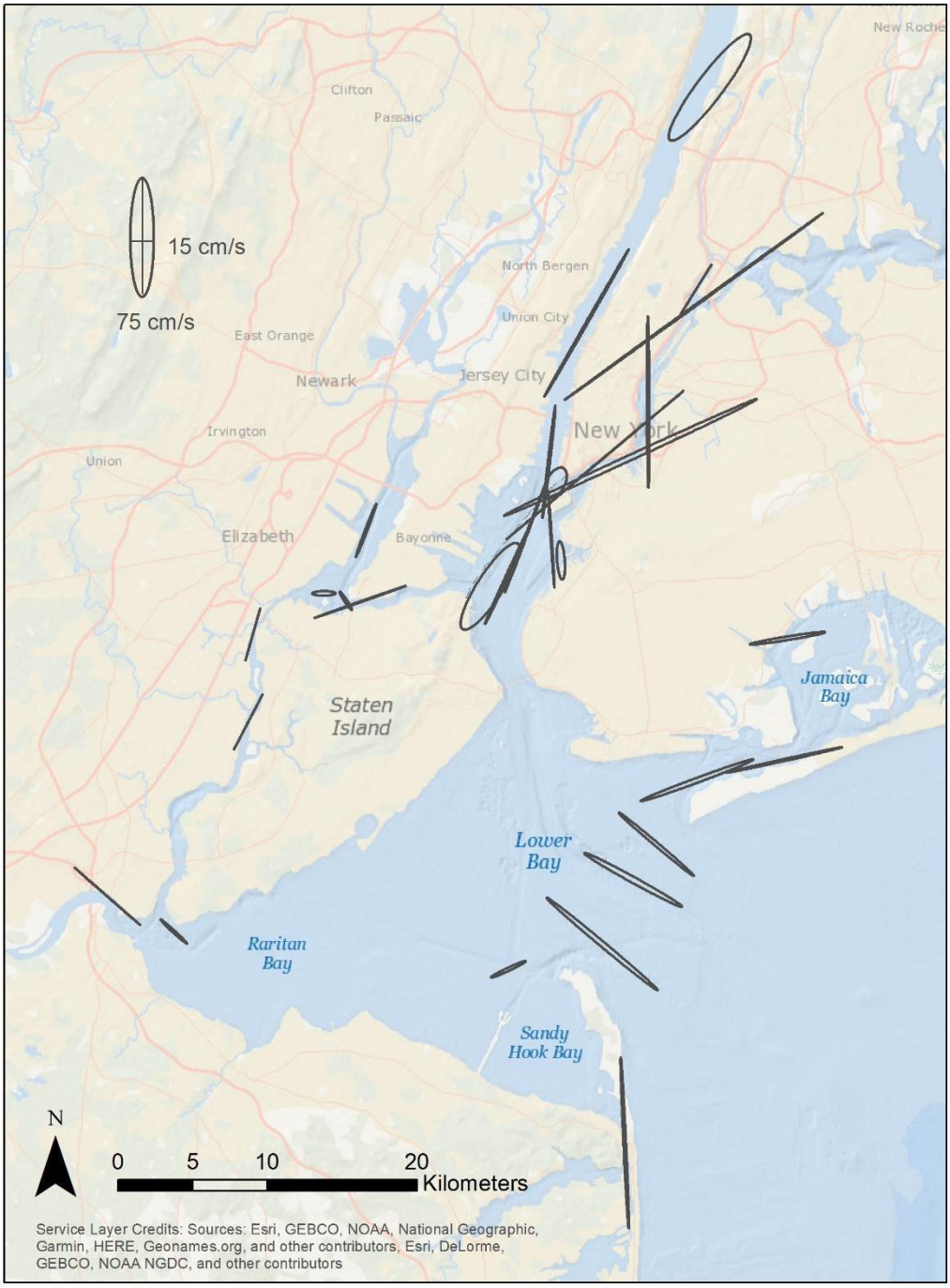

Figure 6-2. M_2 tidal ellipses for the entire study region showing the topographic steering of the ellipses.

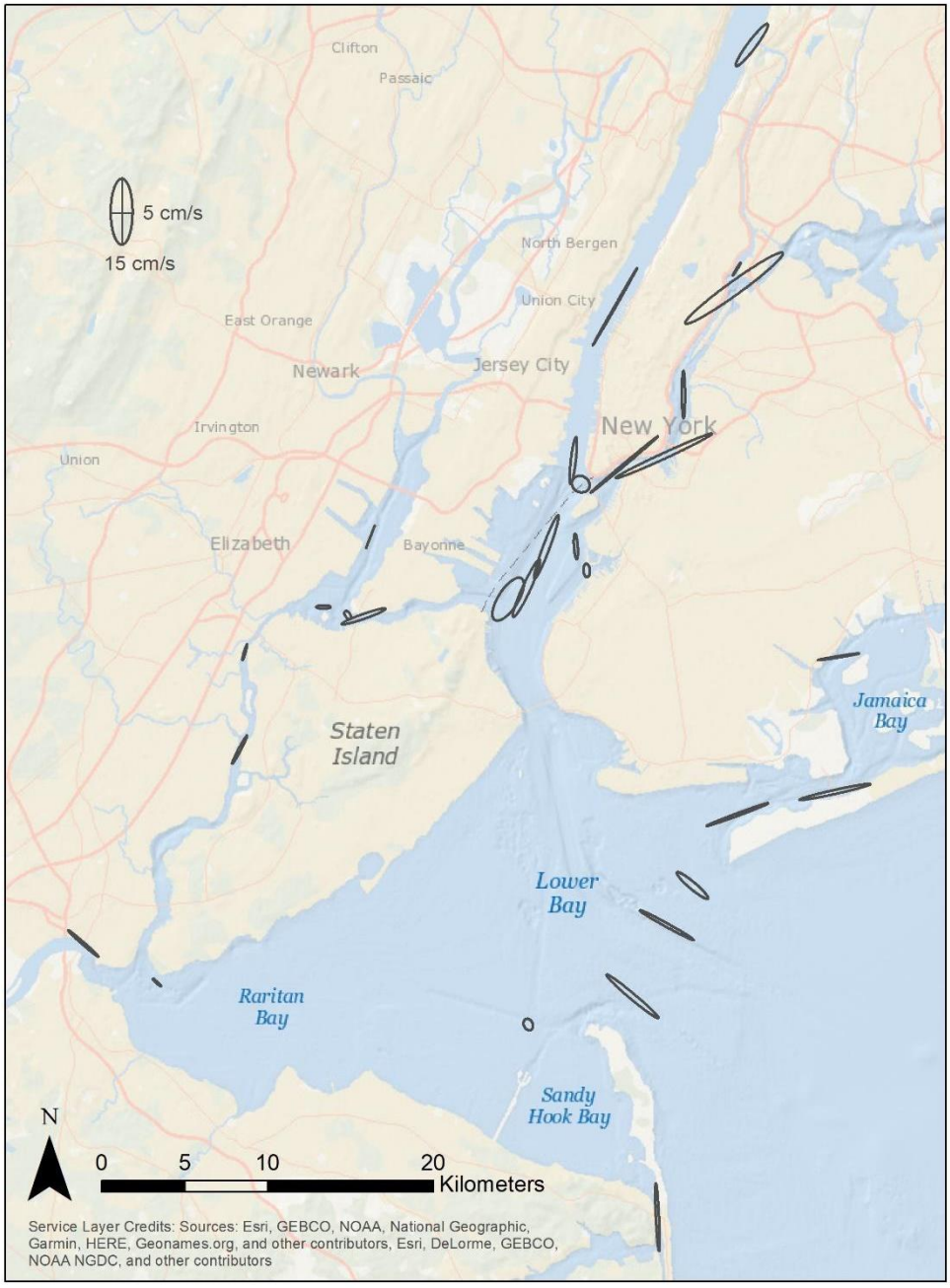

Figure 6-3. S_2 tidal ellipses for the entire study region. Note that these are on a different scale than M_2 in order to see the ellipses. These data are at about 1/5 the scale of the M_2 data.

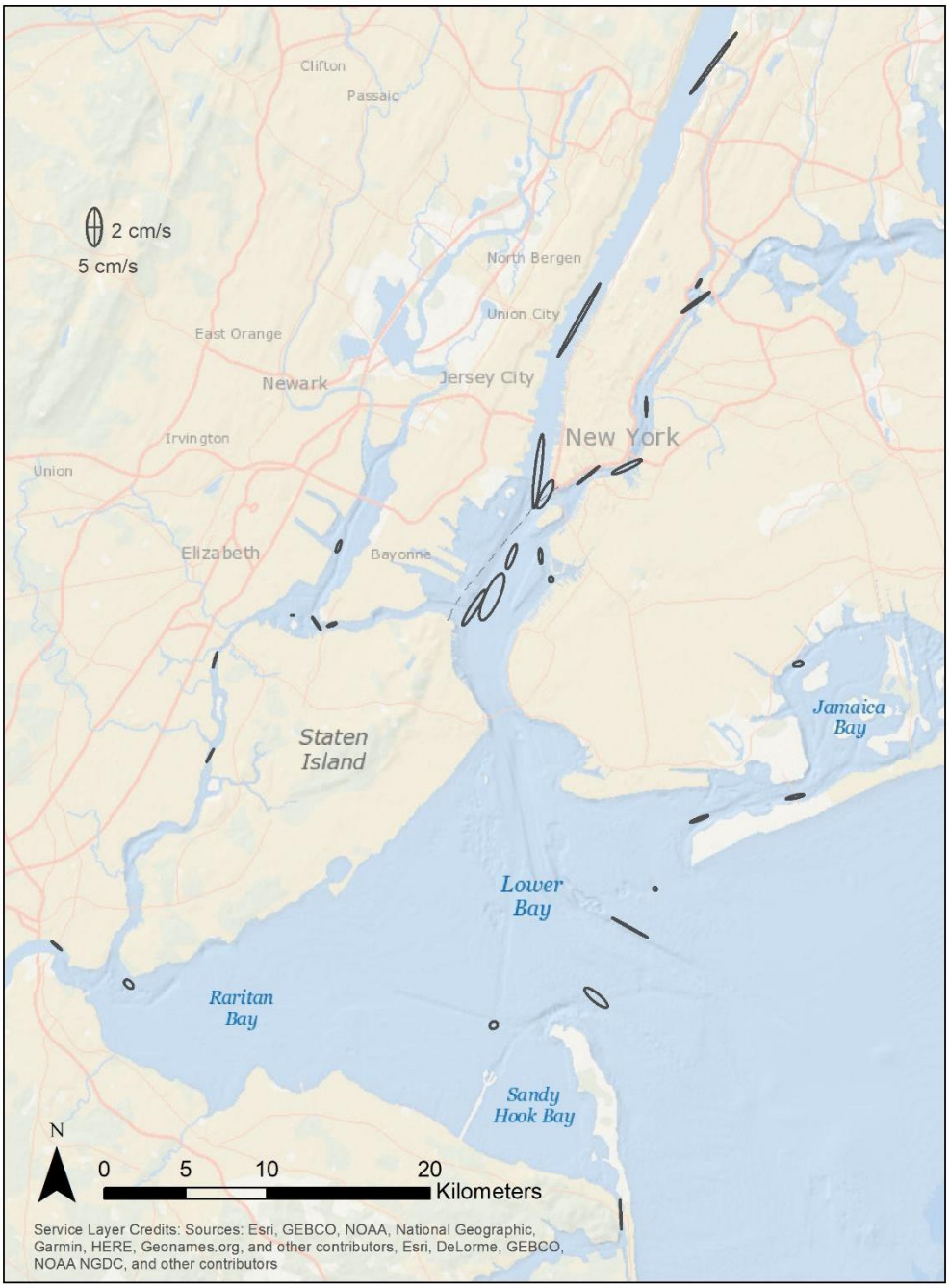

Figure 6-4. O_1 tidal ellipses for the entire study region. Note that these are on a different scale than M_2 in order to see the ellipses. These data are at about 1/15 the scale of the M_2 data.

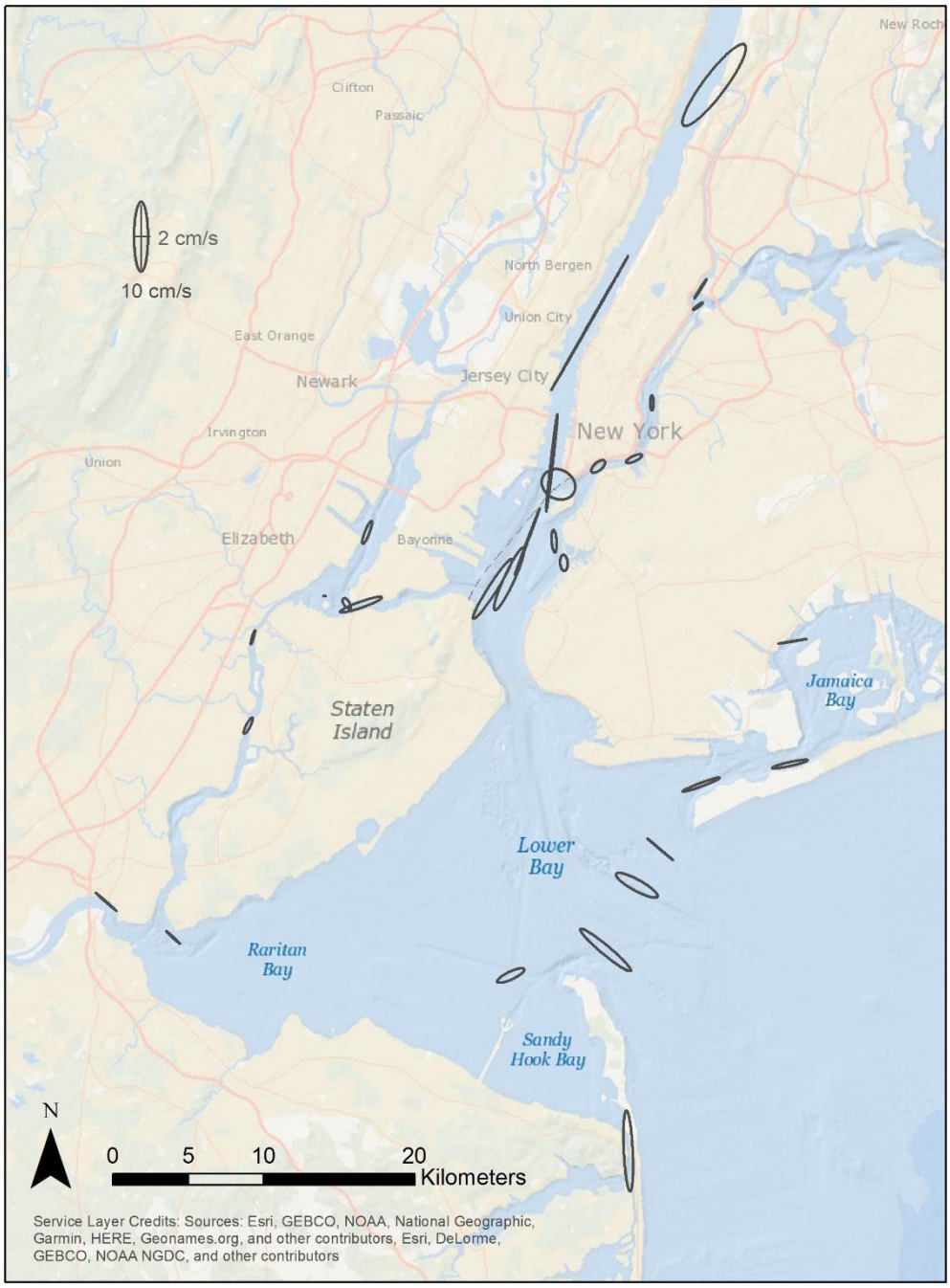

Figure 6-5. K_1 tidal ellipses for the entire study region. Note that these are on a different scale than M_2 in order to see the ellipses. These data are at about 1/8 the scale of the M_2 data.

6.2 Near-surface phases of the tidal current (timing and speed)

Spatial representation of the magnitude and timing of mean ebb and flood currents show the progression of the tides within the estuary and the changes in amplitude due to bathymetry. Figure 6-6 shows the spatial distribution of the mean current magnitude and direction at each station during the maximum flood and ebb currents, and Figure 6-7 shows the corresponding GI timing of ebb and flood. These data are from the near-surface bins found in TCP.

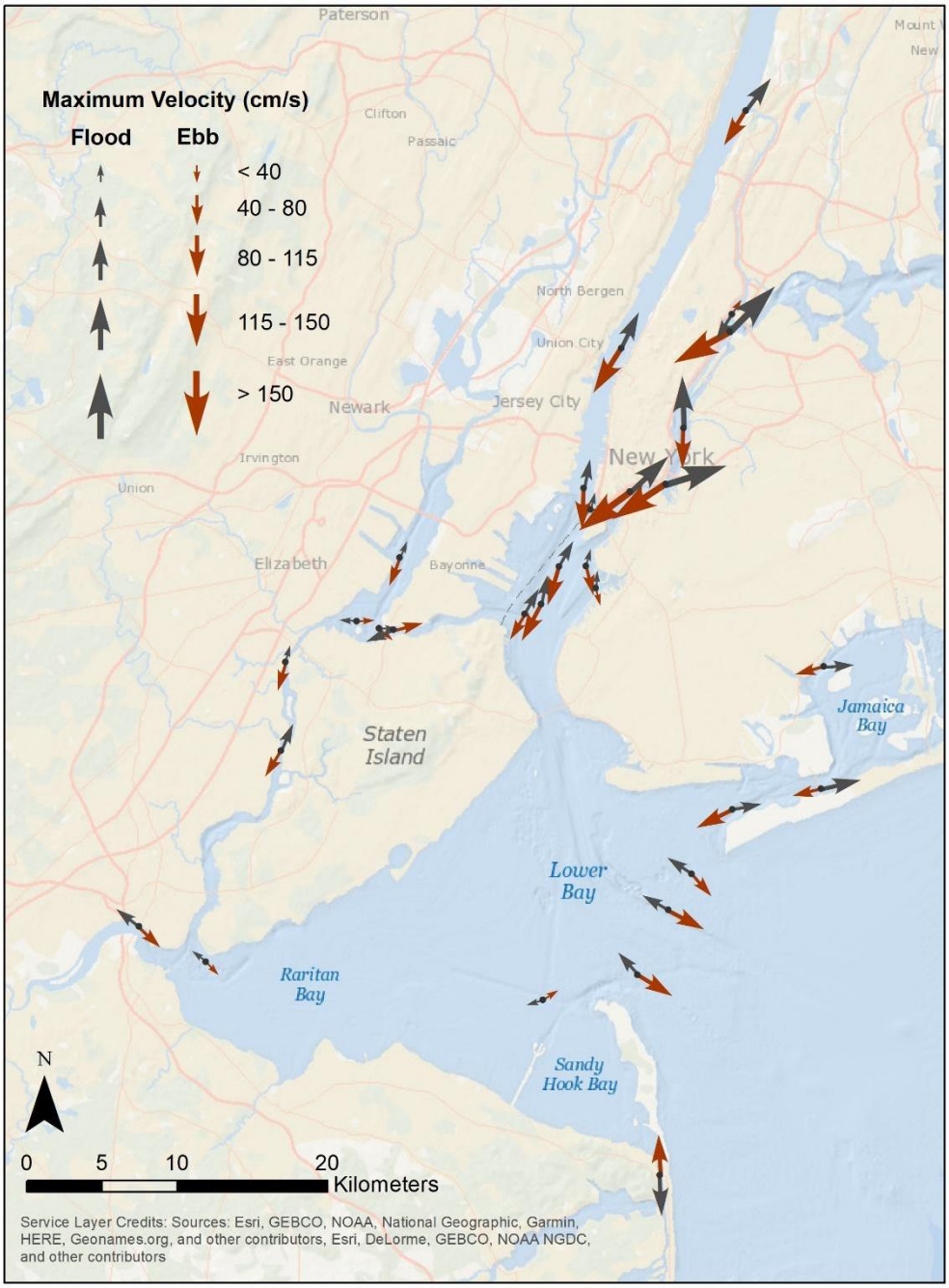

Figure 6-6. Mean values for the tidal currents during maximum flood and ebb for near-surface bins at all stations in the survey.

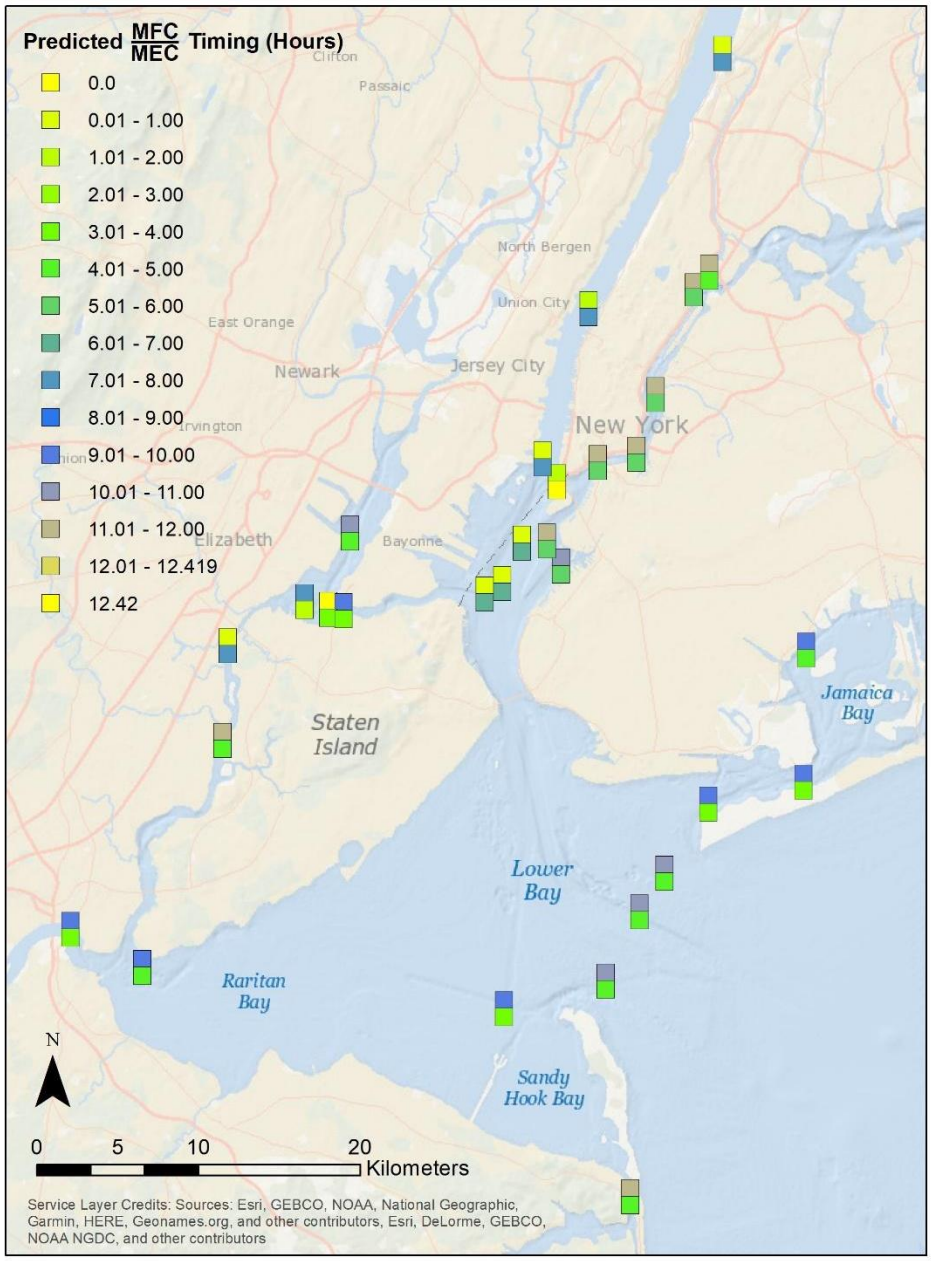

Figure 6-7 GI timing of maximum flood (top) and ebb (bottom) at all stations in the survey. Note that the colors represent hours from 0 to 12.42 with the end interval limits having the same colors to represent the cyclical tides.

7. SUMMARY

CO-OPS occupied 33 stations in 2019 throughout the greater New York Harbor region of New York and New Jersey. In addition to the current data obtained by the ADCPs, CTD profiles were collected during deployment and recovery of the ADCP at each station.

This current survey resulted in a set of measured currents, water temperature, salinity, and pressure observations. The analysis showed that most stations in the region are semidiurnal, with the exception of the Hudson River and Battery stations, which were somewhat mixed, mostly semidiurnal. The tidal currents data were used to update NOAA tidal current predictions and inform future enhancements to a regional hydrodynamic model in New York Harbor, which will support safe and efficient navigation by improving the accuracy of the model predictions and providing a higher density of observations to validate these predictions in the region.

All analyses and plots for the entire time series at all depths are available in detailed station reports (Contact Information). Updated tidal current predictions for each station are also available online via the CO-OPS Tides and Currents website (NOAA Current Predictions). This data set is available to the public and research community by contacting CO-OPS' Stakeholder Services Branch at tide.predictions@noaa.gov to further investigate the circulation of this region and support safe and efficient navigation operations.

ACKNOWLEDGMENTS

We would like to thank Eddie Roggenstein, who was the CO-OPS Field Lead throughout this project, as well as the Atlantic Operations Branch, who supported field operations; Katerina Glebushko for her oversight in the processing of data; and all the CO-OPS technicians, engineers, physical scientists, analysts, and oceanographers who assisted in station planning, the preparation of equipment, in field operations, and in the processing and dissemination of the data. We would also like to thank the captain and crew from Godwin Marine Services, who provided vessel support, and the U.S. Army Corps of Engineers' Caven Point Marine Terminal, who provided use of their facilities and logistical support. Special thanks to Helen Worthington for manuscript editing and Virginia Dentler for final publishing.

REFERENCES

Bosley KT, McGrath CR, Dussault JP, Bushnell M, Evans MJ, French GW, Earwaker KL. 2005. Test, evaluation, and implementation of current measurement systems on aids-to-navigation. Silver Spring (MD): US Dept Commer NOAA NOS CO-OPS. Technical Report No. 043. Accessible at: https://repository.library.noaa.gov/view/noaa/14668

Bowen MM and Geyer WR. 2003. Salt transport and the time-dependent salt balance of a partially stratified estuary. J Geophys Res Oceans. 108(C5): 3158. Accessible at: doi:10.1029/2001JC001231

Browne DR and Dingle G. 1983. New York Harbor circulation survey: 1980-81. US Dept Commer NOS Oceanographic Circulation Survey (Report No. 5) [PDF]. Accessible at: https://tidesandcurrents.noaa.gov/publications/NOS_Oceanographic_Circulation_Survey_Report_No_05.pdf

Charts and publications, 33 C.F.R. Sect. 164.33 (2022). Surveys and other activities, 33 U.S.C. 883a (2012).

Contact Information. NOAA Tides & Currents; [accessed xx]. Accessible at: https://tidesandcurrents.noaa.gov/contact.html

Defant A. 1958. Ebb and flow: the tides of Eearth, air, and water. Ann Arbor (MI): University of Michigan Press. Ann Arbor Paperbacks Series, vol. 506.

Dissemination of data; further activities, 33 U.S.C. 883b (2021).

Fanelli, P, C. Paternostro, G. Dusek, C. Kammerer, J. Park, and A. Carisio (2014). Potential Location Assessment of Coastal and Estuarine Surveys (PLACES). NOAA CO-OPS-NCOP.

[IHO] International Hydrographic Organization. 2008. IHO standards for hydrographic surveys (5th ed., Special Publication No. 44) [PDF]. International Hydrographic Bureau. Accessible at: https://iho.int/uploads/user/pubs/standards/s-44/S-44_5E.pdf

[IOOS] Integrated Ocean Observing System. 2019. Manual for real-time quality control of in-situ current observations: a guide to quality control and quality assurance of acoustic doppler current profiler observations. Version 2.1. Quality Assurance/Quality Control of Real-Time Oceanographic Data (QARTOD). Accessible at: https://doi.org/10.25923/sqe9-e310

[IOOS] Integrated Ocean Observing System. 2020. Manual for real-time oceanographic data quality control flags. Version 1.2. Quality Assurance/Quality Control of Real-Time Oceanographic Data (QARTOD) [PDF]. Accessible at: https://cdn.ioos.noaa.gov/media/2020/07/QARTOD-Data-Flags-Manual_version1.2final.pdf

Lanerolle LWJ, Patchen RC, Aikman F. 2011. The second-generation Chesapeake Bay Operational Forecast System ($CBOFS_2$) model development and skill assessment. Silver

Spring (MD): US Dept Commer NOAA NOS CS. Technical Report No. 29. Accessible at: https://repository.library.noaa.gov/view/noaa/2589

Metropolitan and Micropolitan Statistical Areas Population Totals and Components of Change: 2010-2019. U.S. Census Bureau; [updated 2021 Oct 8; accessed xx]. Accessible at: https://www.census.gov/data/tables/time-series/demo/popest/2010s-total-metro-and-micro-statistical-areas.html

New York/ New Jersey Harbor PORTS®. NOAA Tides & Currents; [accessed xx]. Accessible at: https://tidesandcurrents.noaa.gov/ports/index.html?port=ny

New York and New Jersey Operational Forecast System (NYOFS). NOAA Tides & Currents; [accessed xx]. Accessible at: https://tidesandcurrents.noaa.gov/ofs/nyofs/nyofs.html

NOAA (2018). NOAA's Contribution to the Economy; Powering America's Economy and Protecting Americans. http://performance.noaa.gov/economics

NOAA Current Predictions. NOAA Tides & Currents; [accessed xx]. Accessible at: https://tidesandcurrents.noaa.gov/noaacurrents/Regions

Oey LY, Mellor GL, Hires RI. 1985. A three-dimensional simulation of the Hudson-Raritan Estuary. Part I: Description of the model and model simulations. J Phys Oceanogr. 15(12): 1676-1692. Accessible at: doi:10.1175/1520-0485(1985)015<1676:ATDSOT>2.0.CO

Parker BB. 2007. Tidal analysis and prediction. US Dept Commer NOAA Special Report (NOS CO-OPS 3) [PDF]. Accessible at: https://tidesandcurrents.noaa.gov/publications/Tidal_Analysis_and_Predictions.pdf

Paternostro CL, Pruessner A, Semkiw R. 2005. Designing a quality oceanographic data processing environment. Proceedings of OCEANS 2005 MTS/IEEE; 2005 Sept 17-23; Washington (DC).

Ralston DK, Talke S, Geyer WR, Al-Zubaidi HAM, Sommerfield CK. 2018. Bigger tides, less flooding: effects of dredging on barotropic dynamics in a highly modified estuary. J Geophys Res Oceans. 124(1): 196-211. Accessible at: doi.org/10.1029/2018JC014313

Restoring New York-New Jersey Harbor. NOAA Office of Response and Restoration; [updated 2019 Feb 26; accessed xx]. Accessible at: https://response.restoration.noaa.gov/restoring-new-york-new-jersey-harbor

Swanson RL. 1974. Variability of tidal datums and accuracy in determining datums from short series of observations. Rockville (MD): US Dept Commer NOAA NOS. Technical Report No. 64. Accessible at: https://repository.library.noaa.gov/view/noaa/2944

Vessel traffic data. MarineCadastre.gov; [accessed xx]. Accessible at: https://marinecadastre.gov/ais/

Zervas C. (1999). Tidal current analysis procedures and associated computer programs. Silver Spring (MD): US Dept Commer NOAA NOS CO-OPS. Technical Memorandum No. 0021. [PDF] Accessible at: https://repository.oceanbestpractices.org/bitstream/handle/11329/634/techrpt21.pdf?sequence=1&isAllowed=y

APPENDIX A. STATION LISTING

Table A-1. Station location and deployment information. Station not recovered (italicized) has date of first recovery attempt.

ID	Name	Latitude	Longitude	Depth	Deployment	Recovery
NYH1901	Sandy Hook Channel, Front Range Light	40.4874	-73.9933	11.8	6/26/2019	8/8/2019
NYH1902	Chapel Hill Channel, South End	40.4758	-74.0497	11.1	6/29/2019	8/8/2019
NYH1903	Ambrose Channel	40.5167	-73.9747	9.6	8/12/2019	10/20/2019
NYH1904	Rockaway Inlet Jetty, 1 nm SW of	40.5330	-73.9608	14.0	6/28/2019	8/8/2019
NYH1905	Rockaway Inlet	40.5622	-73.9365	8.4	8/14/2019	10/19/2019
NYH1906	Ward Point Bend	40.4931	-74.2507	10.5	6/28/2019	8/8/2019
NYH1907	Arthur Kill Port Socony	40.5511	-74.2484	10.2	6/30/2019	8/8/2019
NYH1908	Arthur Kill, Tremley Point	40.5889	-74.2060	10.9	8/13/2019	10/18/2019
NYH1909	Arthur Kill Gulfport	40.6289	-74.2032	13.3	8/13/2019	10/18/2019
NYH1910	North of Shooters Island	40.6475	-74.1606	16.0	8/12/2019	10/21/2019
NYH1911	Bergen Point	40.6442	-74.1474	15.8	6/29/2019	8/8/2019
NYH1912	Port Richmond	40.6437	-74.1391	16.0	6/29/2019	8/8/2019
NYH1913	Middle Reach Newark Bay	40.6763	-74.1352	14.5	6/29/2019	8/9/2019
NYH1914	Constable Hook Approach	40.6507	-74.0606	14.5	8/12/2019	10/20/2019
NYH1915	Robbins Reef Light, 0.6 nautical miles E of	40.6552	-74.0507	14.7	8/13/2019	10/19/2019
NYH1916	Claremont Terminal Channel ent.	40.6705	-74.0517	10.1	8/15/2019	10/19/2019
NYH1917	Gowanus Bay Entrance	40.6625	-74.0181	9.5	8/12/2019	10/20/2019
NYH1918	Red Hook	40.6723	-74.0239	13.8	8/14/2019	10/19/2019
NYH1919	Dimond Reef	40.6979	-74.0213	13.3	8/15/2019	10/19/2019
NYH1920	Brooklyn Bridge	40.7060	-73.9977	17.6	8/12/2019	10/20/2019
NYH1921	Corlears Hook	40.7095	-73.9764	13.7	8/12/2019	10/20/2019
NYH1922	Newtown Creek	40.7347	-73.9657	10.0	6/27/2019	8/6/2019
NYH1923	East River 'B' Buoy	40.7421	-73.9676	12.9	8/13/2019	10/18/2019
NYH1924	Hell Gate	40.7783	-73.9383	13.4	8/13/2019	10/20/2019
NYH1926	Harlem River, south end	40.7861	-73.9369	4.0	6/27/2019	8/6/2019
NYH1927	Hudson River Entrance	40.7076	-74.0253	17.3	8/12/2019	10/20/2019
NYH1928	Hudson River, Pier 92	40.7707	-74.0028	17.0	8/12/2019	10/20/2019
NYH1929	*Hudson River, Grant's Tomb*	*40.8137*	*-73.9683*	*20.0*	*8/12/2019*	*10/21/2019*
NYH1930	Spuyten Duyvil	40.8779	-73.9287	20.0	8/12/2019	10/21/2019
NYH1931	Marine Parkway Bridge	40.5715	-73.8837	13.1	8/14/2019	10/18/2019
NYH1932	Raritan River Entrance	40.5092	-74.2906	9.9	6/26/2019	8/8/2019
NYH1933	Highlands Bridge, Shrewsbury River	40.3964	-73.9798	6.2	6/26/2019	8/8/2019
NYH1934	Jamaica Bay - Canarsie (mid-channel)	40.6270	-73.8820	10.2	8/14/2019	10/19/2019

APPENDIX B. STATION PLATFORM TYPES

Table B-1. Platform and sensor information. Stations not used for predictions are italicized, and the unrecovered station is in bold.

Station ID	Mount Class	Orientation	Mount Type	ADCP Make	ADCP Freq. (Hz)	Height Above Bottom (m)	MLLW (m)	Total Bins	Bin Size (m)
NYH1901	Bottom	Up	Tripod	TRDI WH	1200	0.5	11.6	20	1.0
NYH1902	ATON	Down	ATON	Nortek AqD	600	10.1	11.1	20	1.0
NYH1903	Bottom	Up	TRBM	TRDI WH	1200	0.5	10.1	30	0.5
NYH1904	Bottom	Up	MTRBM	TRDI WH	600	0.5	14.8	25	1.0
NYH1905	Bottom	Up	MTRBM	TRDI WH	1200	0.5	8.5	30	0.5
NYH1906	ATON	Down	ATON	Nortek AqD	1000	9.5	10.5	20	1.0
NYH1907	ATON	Down	ATON	Nortek AqD	1000	9.2	10.2	20	1.0
NYH1908	Bottom	Up	Tripod	TRDI WH	600	0.5	11.8	20	1.0
NYH1909	Bottom	Up	MTRBM	TRDI WH	600	0.5	14.1	25	1.0
NYH1910	Bottom	Up	ES-2	TRDI WH	600	0.8	16.0	25	1.0
NYH1911	ATON	Down	ATON	Nortek AqD	600	14.8	15.8	20	1.0
NYH1912	ATON	Down	ATON	Nortek AqD	600	15.0	16.0	20	1.0
NYH1913	Bottom	Up	H-TRBM	TRDI WH	600	0.5	14.6	25	1.0
NYH1914	Bottom	Up	ES-2	TRDI WH	600	0.8	13.6	25	1.0
NYH1915	ATON	Down	ATON	Nortek AqD	1000	13.7	14.7	25	1.0
NYH1916	*ATON*	*Down*	*ATON*	Nortek AqD	*600*	*6.1*	*8.1*	*15*	*1.0*
NYH1917	Bottom	Up	ES-2	TRDI WH	600	0.8	11.5	20	1.0
NYH1918	ATON	Down	ATON	Nortek AqD	600	12.8	13.8	20	1.0
NYH1919	ATON	Down	ATON	Nortek AqD	1000	12.3	13.3	17	1.0
NYH1920	Bottom	Up	TRBM	TRDI WH	600	0.5	16.1	25	1.0
NYH1921	Bottom	Up	TRBM	TRDI WH	600	0.5	14.6	25	1.0
NYH1922	Bottom	Up	MTRBM	TRDI WH	600	0.5	10.7	20	1.0
NYH1923	ATON	Down	ATON	Nortek AqD	1000	11.9	12.9	20	1.0
NYH1924	Bottom	Up	TRBM	TRDI WH	600	0.5	12.4	20	1.0
NYH1926	Bottom	Up	Grate	TRDI WH	2000	0.1	4.5	20	0.5
NYH1927	Bottom	Up	ES-2	TRDI WH	600	0.8	16.9	25	1.0
NYH1928	Bottom	Up	ES-2	TRDI WH	600	0.8	15.7	25	1.0
NYH1929	**Bottom**	**Up**	**ES-2**	TRDI WH	**600**	**0.8**	**21.0**	**25**	**1.0**
NYH1930	Bottom	Up	ES-2	TRDI WH	600	0.8	18.7	0	0.0
NYH1931	Bottom	Up	H-TRBM	TRDI WH	1200	0.5	13.3	25	1.0
NYH1932	Bottom	Up	H-TRBM	TRDI WH	1200	0.5	9.8	30	0.5
NYH1933	Side	Side	Pipe clamp	Nortek AqD 2D	600	3.1	4.9	30	0.5
NYH1934	Bottom	Up	H-TRBM	TRDI WH	1200	0.5	10.0	10	4.0

ACRONYMS

ADCP	acoustic Doppler current profiler
AIS	Automatic identification system
AqD	Nortek Aquadopp current meter
ATON	Aids to Navigation
C	Celsius
cm/s	Centimeters per second
CO-OPS	Center for Operational Oceanographic Products and Services
CTD	conductivity, temperature, and depth
CFR	Code of Federal Regulations
DWB	Deepwater Buoyancy
ENU	Earth-oriented (East-North-Up) coordinates.
ES-2	Bottom mount named for its designer Eddie Shih.
ft	feet
GI	Greenwich Interval
GP35	General Purpose 35-inch bottom mount platform from Mooring Systems, Inc. This platform has been renamed as H-TRBM-35 by the manufacturer.
GT	Great diurnal range. The difference between mean higher high water and mean lower low water.
H-TRBM	hemispheric trawl-resistant bottom mount
IHO	International Hydrographic Organization
kg	kilogram
kHz	kilohertz
km	kilometer
kn	knots
LSQHA	Least squares harmonic analysis
m	meter
MEC	maximum ebb current
MFC	maximum flood current
MHHW	mean higher high water
MLLW	mean lower low water
MSI	Mooring Systems, Inc.
MTRBM	miniature trawl-resistant bottom mount
NCOP	National Current Observation Program
NOAA	National Oceanic and Atmospheric Administration
NOS	National Ocean Service
NYH	New York Harbor
NYOFS	New York Operational Forecast System
PORTS®	Physical Oceanographic Real-Time System
QARTOD	Quality Assurance/Quality Control of Real-Time Oceanographic Data
R/V	Research Vessel

s	second
TCP	NOAA tidal current predictions
TRBM	trawl-resistant bottom mount
TRDI	Teledyne RD Instruments
USACE	U. S. Army Corps of Engineers
XYZ	Orientation based along an instrument’s X-Axis,Y-Axis, and Z-Axis